12-1-2012

Role of cytochrome P4501A1 in vasoreactivity and blood pressure regulation mediated by omega-3 polyunsaturated fatty acids

Njotu Agbor

NJOTU LARRY AGBOR

Candidate

BIOMEDICAL SCIENCES

Department

This dissertation is approved, and it is acceptable in quality and form for publication:

Approved by the Dissertation Committee:

Prof. Mary K. Walker, Chairperson

Dr. Nancy L. Kanagy

Dr. Laura Gonzalez Bosc

Dr. Matthew J. Campen

ROLE OF CYTOCHROME P4501A1 IN VASOREACTIVITY AND BLOOD PRESSURE REGULATION MEDIATED BY OMEGA-3 POLYUNSATURATED FATTY ACIDS

BY

NJOTU LARRY AGBOR

BS, BIOCHEMISTRY, UNIVERSITY OF BUEA, 2001
MS, BIOLOGY, NEW MEXICO HIGHLANDS UNIVERSITY, 2006

DISSERTATION

Submitted in Partial Fulfillment of the
Requirements for the Degree of

DOCTOR OF PHILOSOPHY
BIOMEDICAL SCIENCES

The University of New Mexico
Albuquerque, New Mexico

DECEMBER 2012

DEDICATION

I dedicate this dissertation to my mother, Elisabeth Agbor who instilled in me the sense of hard work, sacrifice, perseverance, humility, respect and most of all love. Thank you for believing in me and supporting me through College. I also dedicate this dissertation to my younger sister and only sibling, Colette Agbor for her encouragement and believing in me, even when she could not understand what kind of research I do.

I equally dedicate this dissertation to my beautiful and loving wife, Angelina Rose Agbor. Your support and interest in my research really gave me all the strength I needed, and catapulted me towards the completion of this dissertation. Thank you for taking the time to come out to the laboratory and see the animals that survived my surgeries, taking the time to come and check out my new wire myograph instrument, bringing me lunches when I was stuck in the lab during long hours,……etc. Thank you for asking me each day after long laboratory hours how my day and research went. Even during the writing of this dissertation, all the inspiration you gave me was much appreciated. You, Angelina Rose Agbor, are a blessing to me and I will always continue to love and cherish you in my life.

I equally dedicate this dissertation to Prof. Mary k. Walker for giving me the opportunity and providing me with the resources in every possible way, to earn it.

ACKNOWLEDGEMENTS

I would like to acknowledge and thank my dissertation committee chairperson, Prof. Mary K. Walker, who first of all, gave me the opportunity to join her laboratory as a research technician. Thank you for believing in me and accepting me back into your laboratory as a Ph.D student. Words could never express the impact you have made in my life as a whole. Your mentorship, one-on-one meetings, advice, directions, encouragement, reviews, support, have all been the best and the finest. As I continue to explore new opportunities in the field of scientific research, I will always look back and remember the good times I had in your laboratory.

I would also like to thank the other members of my committee, Dr. Nancy L. Kanagy, Dr. Laura Gonzalez-Bosc, and Dr. Mathew J. Campen for their contributions, great ideas, and recommendations to all the studies I have conducted. To have a committee made up of the brightest minds has been a privilege for me. Thank you all for attending my committee meetings, even during snow in days when the University of New Mexico was closed.

Special acknowledgement goes to Mary T. Walsh for her help in most of the studies I carried out. To you Jason Boberg, I say thank for your help. I do hereby also acknowledge all members of Prof. Mary Walker's Laboratory, past and present, for being part of a wonderful family in and outside of the laboratory. Finally, I do acknowledge the University of New Mexico, School of Medicine, for accepting me into the Ph.D program, and the UNM College of Pharmacy for contributing to my stipend over the years. I also acknowledge support from Mary Walker's grant [R01 HL078914 to M.K.W.].

Role of Cytochrome P4501A1 in Vasoreactivity and Blood Pressure Regulation Mediated by Omega-3 Polyunsaturated Fatty Acids.

BY

NJOTU LARRY AGBOR

BS, Biochemistry, University of Buea, 2001
MS, Biology, New Mexico Highlands University, 2006
Ph.D, Biomedical Sciences, University of New Mexico, 2012

ABSTRACT

The aryl hydrocarbon receptor (AHR) is a ligand-activated transcription factor involved in the metabolism of environmental pollutants including halogenated aromatic hydrocarbons, for example, 2,3,7,8-tetrachlorodibenzo-ρ-dioxin (TCDD). The AHR and its downstream target gene cytochrome P4501A1 (CYP1A1) are also involved in cardiovascular development. AHR knockout (KO) mice are hypotensive, with cardiac hypertrophy. Additionally, CYP1A1 is involved in the production of potent vasodilator metabolites from omega-3 polyunsaturated fatty acids (n-3 PUFAs) metabolism. Thus, we hypothesize that the AHR and its downstream target gene, CYP1A1, both contribute to normal vascular reactivity of blood vessels and to blood pressure (BP) regulation.

We generated mice with conditional deletion of the AHR from the endothelium (*ECahr*$^{-/-}$), to elucidate the degree to which loss of AHR contributes to vasoreactivity and BP regulation *in vivo*. BP and heart rate (HR) was assessed prior to and following angiotensin (Ang) II injection, or chronic treatment with an angiotensin converting enzyme inhibitor, captopril. Vasoreactivity was assessed in aorta in presence of perivascular adipose tissue. Immunoblot was used to assess Ang 1 receptor A (AT1R) protein expression in the aorta.

We used CYP1A1 KO mice to determine the degree to which global deletion of CYP1A1 contributes to vasoreactivity in the aorta and mesenteric arterioles, and to BP regulation. BP and HR was measured ± nitric oxide synthase (NOS) inhibitor, LNNA. Vasoreactivity to eicosapentaenoic acids (EPA) and docosahexaenoic acids (DHA) were conducted in aorta and mesenteric arterioles. CYP1A1 WT and KO mice were provided n-3 or n-6 PUFA-enriched diets for 2 months, and BP and HR measured ± LNNA. Endothelial NOS (eNOS) and phospho-eNOS protein were measured in the aorta of all diet treated mice.

Our data showed that *ECahr*$^{-/-}$ mice are hypotensive, associated with reduced responses to Ang II, and reduced aortic AT1R expression. Moreover, CYP1A1 KO mice exhibited elevated BP compared to WT mice, with attenuated vasodilation to EPA and DHA. Further, supplementation with an n-3 PUFA-enriched diet normalizes BP in CYP1A1 KO mice to WT levels. In contrast, an n-6 PUFA-enriched diet increased BP in WT mice to levels seen in CYP1A1 KO mice on standard chow. Phospho-eNOS protein expression was reduced in aorta of CYP1A1 KO mice fed an n-3 PUFA-enriched diet, compared to WT mice.

Taken together, these data suggest that endothelial AHR and global CYP1A1 have a physiologically important role in the regulation of vascular function and BP, and involve different mechanisms. The clinical implications are that n-3 PUFA-enriched diets could be recommended in the treatment of hypertension in humans. Additionally, AHR antagonists and stable analogues of CYP1A1 n-3 PUFA metabolites could be used in the treatment of long term resistant hypertension.

TABLE OF CONTENTS

LIST OF FIGURES……x

LIST OF TABLES……xiii

CHAPTER 1

Introduction……1

The Aryl Hydrocarbon Receptor……1

AHR Signaling Pathway……1

AHR in Cardiovascular Development and Blood Pressure Control……4

Endogenous Ligands of the AHR……7

Cytochrome P4501A1 (CYP1A1)……8

Regulation and Function of CYP1A1 gene……8

Expression and Localization of CYP1A1……10

CYP1A1 Polymorphisms and Cardiovascular disease……12

Omega-3 Polyunsaturated Fatty Acids (PUFAs)……13

n-3 PUFA Biology and the Cardiovascular System……13

P450s and Omega-3 PUFA Metabolism……18

CYP1A1 and n-3 PUFA Metanolism……18

Cardiovascular function of CYP1A1 Metabolites of n-3 PUFAs……19

Arachidonic acids (AA) as Endogenous Substrates of CYP1A1……20

Nitric Oxide……21

Nitric Oxide Biology, Regulation and the Cardiovascular System…...…….21

Nitric Oxide and n-3 PUFA Crosstalk……24

Rationale for Research 26

AIM 1……...…..……27
AIM 2……...……..27
AIM 3……...……..28

CHAPTER II

Endothelial Cell-Specific Aryl Hydrocarbon Receptor Knockout Mice Exhibit Hypotension Mediated, in part, by an Attenuated Angiotensin II Responsiveness...29

Abstract.....30

Introduction.....31

Methods 34

Results.....40

Discussion 57

Supplement data…….……..…….64

CHAPTER III

Elevated Blood Pressure in Cytochrome P4501A1 (CYP1A1) Knockout Mice is Associated with Reduced Vasodilatation to Omega-3 Polyunsaturated fatty acids..71

Abstract 72

Introduction 74

Methods 77

Results 82

Discussion 97

CHAPTER IV

Cytochrome P4501A1 Contributes to Nitric Oxide-Dependent Vasodilation and Blood Pressure Lowering on an Omega-3 Polyunsaturated Fatty acid-Enriched Diet 103

Abstract 104

Introduction 106

Methods 109

Results 116

Discussion 135

CHAPTER V

Conclusion and Future Directions 140

Endothelial cell-specific aryl hydrocarbon receptor knockout mice 140

Cytochrome P4501A1 knockout mice 143

REFERENCES 150

LIST OF FIGURES

CHAPTER 1

Figure 1.1: Schematic of the AHR signaling pathway……..…….....3

Figure 1.2: Structures of arachidonic acid (AA), eicosapentaenoic acid (EPA), and docosahexaenoic acid (DHA)…….....17

Figure 1.3: Mechannism of nitric oxide (NO) production by endothelial cells……..23

CHAPTER 2

Figure 2.1: Cre^{Tek}-mediated excision of the *ahr* floxed allele (*ahr*$^{fx/fx}$)…….…….....41

Figure 2.2: Loss of *ahr* alleles in endothelial cells (EC) decreases systolic and diastolic blood pressure ……..……42

Figure 2.3: EC*ahr*$^{-/-}$ mice exhibit normal responses to NOS inhibition by LNNA *in vivo*…….……...……46

Figure 2.4: Loss of *ahr* in endothelium attenuates RAS responsiveness *in vivo*.……....48

Figure 2.5: Loss of *ahr* in endothelium attenuates the contribution of Ang II to basal blood pressure……51

Figure 2.6: Loss of *ahr* in endothelium alters mRNA expression of RAS components in adipose……...53

Figure 2.7: Loss of *ahr* in endothelium diminishes AT1R expression in aorta……..…55

Figure 2.8: Loss of *ahr* in endothelium reduces abdominal aortic reactivity to Ang II in the presence of perivascular adipose tissue (PVAT)……..……56

Figure 2.1S: Hypotension in EC*ahr*$^{-/-}$ mice is not associated with increased eNOS expression nor increased NO bioavailability……...…….…..67

Figure 2.2S: Loss of AHR in endothelial cells enhances sympathetic innervation to the vasculature……..……..……68

CHAPTER 3

Figure 3.1: Genetic deletion of CYP1A1 increases systolic and diastolic BP, and reduces HR…….85

Figure 3.2: Loss of CYP1A1 does not affect vascular sensitivity to ACh- or SNAP-mediated dilation, nor PE-mediated contraction in the absence or presence of the NOS inhibitor, LNNA……...88

Figure 3.3: NOS inhibition by LNNA does not normalize BP in CYP1A1 KO mice *in vivo*…..…….89

Figure 3.4: DHA and EPA-mediated vasorelaxation are significantly attenuated in abdominal aorta of CYP1A1 KO mice...…….……91

Figure 3.5: DHA and EPA-mediated vasorelaxation are attenuated in pressurized mesenteric resistance arteries at both 40 and 60 mmHg……92

Figure 3.6: P450 metabolites of EPA and DHA, 17,18-EEQ and 19,20-EDP, respectively, induce an equivalent degree of vasorelaxation in the abdominal aorta and vasodilation in mesenteric arterioles in CYP1A1 WT and KO mice……..……95

Figure 3.7: Kv and BK channels are targets for DHA-mediated vasodilation in mesenteric resistance arteries……..…..……..……96

CHAPTER 4

Figure 4.1: Food consumption in CYP1A1 WT and KO mice fed an n-3 PUFA-enriched diet or an n-6 PUFA-enriched diet ……..……....118

Figure 4.2: Effects of n-3 and n-6 PUFA-enriched diets on mean 24 hr BP and HR in CYP1A1 WT and KO mice.....121

Figure 4.3: Effects of n-3 PUFA-enriched diet ± LNNA on mean hourly BP and HR in CYP1A1 WT and KO mice.....123

Figure 4.4: Effects of NOS inhibition on MAP in CYP1A1 WT and KO mice fed standard chow and an n-3 PUFA-enriched diet.....124

Figure 4.5: Effects of n-6 PUFA-enriched diet ± LNNA on mean hourly BP and HR in CYP1A1 WT and KO mice.....126

Figure 4.6: Effects of n-3 PUFA-enriched diet on acute Ang II responsiveness in CYP1A1 WT and KO mice *in vivo*……..127

Figure 4.7: Effects of n-3 and n-6 PUFA-enriched diets on aortic eNOS protein expression in CYP1A1 WT and KO mice.....129

Figure 4.8: Effects of n-3 PUFA-enriched diet on aortic phospho-eNOS protein expression in CYP1A1 WT and KO mice.....130

Figure 4.9: Effects of n-3 and n-6 PUFA-enriched diets on ACh-mediated vasodilation and U46619-dependent vasoconstriction in mesenteric arterioles of CYP1A1 WT and KO mice.....132

Figure 4.10: Effects of n-3 and n-6 PUFA-enriched diets on plasma NOx levels.....133

Figure 4.11: Effects of standard chow, n-3 PUFA-enriched diet, and n-6 PUFA-enriched diet on cardiac TBARS levels.....134

LIST OF TABLES

CHAPTER 2

Table 2.1: Body and organ weights of 4 month old male EC*ahr*$^{+/+}$ and EC*ahr*$^{-/-}$ mice…..43

Table 2.2: Indices of the renin-angiotensin system (RAS) in EC*ahr*$^{+/+}$ and EC*ahr*$^{-/-}$ mice ……...……....52

Table 2.1S: Real time PCR primer sequences……...69

Table 2.2S: Adipose weights of 2-month-old male EC*ahr*$^{+/+}$ and EC*ahr*$^{-/-}$ mice…….....70

CHAPTER 3

Table 3.1: Real-time PCR primer sequences……..…….....83

Table 3.2: Gross tissue weights in 4 month-old CYP1A1 WT and KO mice…..…….....84

CHAPTER 4

Table 4.1: Diet composition: Standard chow, n-3 PUFA-enriched diet, and n-6 PUFA-enriched diet……..…...111

Table 4.2: Body and organ weights in 8 month-old CYP1A1 WT and KO mice on n-3 and n-6 PUFA-enriched diets ……..……..……..119

Table 4.3: Lipid profile measurements in CYP1A1 WT and KO mice fed standard chow, an n-3 and an n-6 PUFA-enriched diet…..……...…….…..120

I. CHAPTER 1

Introduction

The aryl hydrocarbon receptor (AHR)

AHR signaling pathway

The aryl hydrocarbon receptor (AHR) is a ligand-activated, basic helix-loop-helix/Per-ARNT-Sim transcription factor involved in the adaptive and toxic responses of xenobiotics (Mimura and Fujii-Kuriyama, Feb 17). The AHR evolved about 500 million years ago and is evolutionarily conserved from invertebrates to vertebrates (Hahn, Nov; Hahn, Sep 20). Several studies have demonstrated that the AHR exists in an inactive cytosolic complex sequestered to two molecules of the chaperone heat shock protein 90 (HSP90), the co-chaperone aryl hydrocarbon receptor-associated protein 9 (ARA9), and p23. Binding of HSP90 to AHR is thought to mask the AHR-nuclear localization signal, and this interaction is necessary for cytoplasmic retention of the AHR (Kazlauskas *et al*., 2001). Therefore, the ARA9 maintains the AHR in a cytosolic localization, decreases AHR degradation, and increases its ligand binding capacity (LaPres *et al*., 2000). AHR mRNA is constitutively expressed in a large number of mammalian tissues, with the highest amounts of expression found in the liver, lung, kidney, heart, and placenta (Dohr *et al*., 1996).

In response to agonist binding, the AHR undergoes a conformational change, translocates to the nucleus, dissociates from the HSP90, and dimerizes with its nuclear partner, the aryl hydrocarbon receptor nuclear translocator (ARNT). The formation of the heterodimeric complex leads to its interaction with dioxin-response elements (DREs) upstream of target genes, inducing their activation and transcription (Fig. 1.1). Once

transcriptional activation has occurred, the AHR is exported to the cytosol where it is degraded by the ubiquitin-proteosome pathway (Davarinos and Pollenz, 1999). DREs are located upstream of both Phase I metabolizing enzymes (e.g., cytochromes P450 (P450s) 1A1, 1A2, 1B1), and Phase II metabolizing enzymes (e.g., glutathione S-transferase and UDP glucuronosyltransferase). The AHR is activated by halogenated aromatic hydrocarbons (HAH), including 2,3,7,8-tetrachlorodibenzo-*p*-dioxin (TCDD), and the sustained activation of AHR, has been proposed to account for its toxicity (Fernandez-Salguero *et al*., 1996). The AHR has been shown to mediate the toxic endpoints of HAH exposure, including teratogenicity. For example, in pregnant mice treated with dioxin at a dose of 40 μg/kg body weight at gestation day 12.5, fetuses that were AHR-null were insensitive to the teratogenic effects of TCDD. In contrast, all wildtype fetuses suffered from cleft palate and hydronephrosis, suggesting that the AHR is involved in teratogenicity (Mimura *et al.*, 1997).

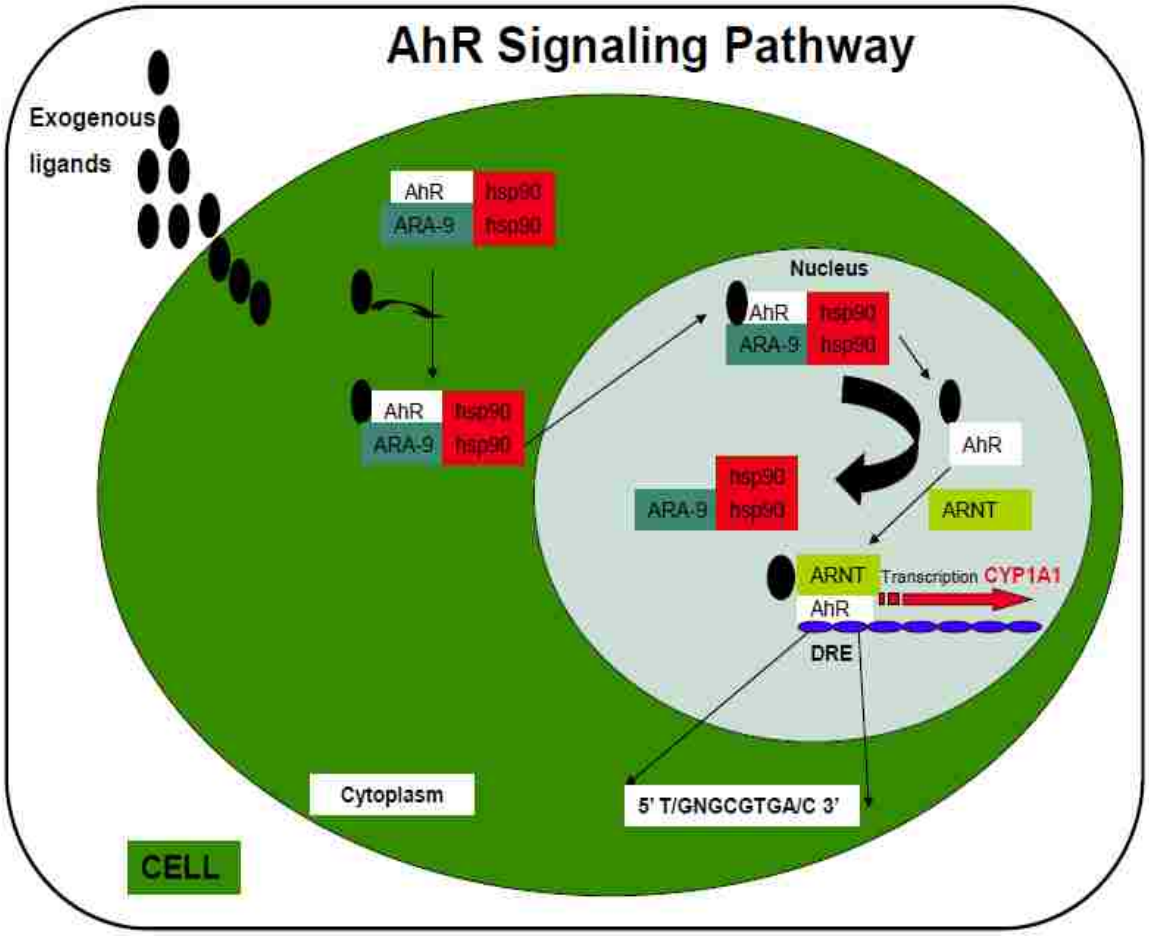

Figure 1.1. Schematic of the AHR signaling pathway. Exogenous ligands bind to the AHR in the cytoplasm and induce a conformational change exposing the nuclear localization signals, which facilitates nuclear translocation. Once in the nucleus, the aryl hydrocarbon receptor nuclear translocator (ARNT) binds to the AHR and a transcriptionally active heterodimer is formed that can bind to consensus regulatory dioxin response elements (DREs) located in the promoter upstream of target genes, such as cytochrome P4501A1 (CYP1A1). After transcriptional activation has occurred, the AHR dissociates from ARNT and is targeted back to the cytoplasm where it is degraded by the proteasomal system. (Abbreviations; ARA9: aryl hydrocarbon receptor-associated protein 9; hsp90: heat shock protein 90; AHR: aryl hydrocarbon receptor)

AHR in cardiovascular development and blood pressure control

The AHR is necessary for cardiovascular development. In addition to its orthodox role in the metabolism of xenobiotics, recent studies demonstrate a functional role for AHR in vascular development and homeostasis, in the absence of exogenous ligands. In patients with cardiomyopathy, the expression of the AHR mRNA and protein levels were highly upregulated in the left ventricle, suggesting a potential pathological role for the AHR in heart disease (Mehrabi *et al*., 2002). Moreover, the generation and investigation of the aryl hydrocarbon receptor knockout (*ahr*$^{-/-}$) mouse by several laboratories has shed more light in this area (Fernandez-Salguero *et al.*, 1995; Schmidt *et al.*, 1996). The *ahr*$^{-/-}$ mice exhibit a reduction in liver size due to smaller hepatocytes, which results from the persistence of the fetal ductus venosus (DV) after birth. The DV shunts blood from the umbilical vein to the inferior vena cava in the fetus, and rapidly closes after birth. The patency of the DV greatly reduces the portal blood supply in the *ahr*$^{-/-}$ mice, and the failure of this vessel to close is dependent on AHR expression. Further, studies in which the AHR is genetically deleted solely from endothelial cells (ECs), versus deletion solely from hepatocytes or KÜpfer cells, demonstrate that AHR expression in ECs is required for closure of the DV after birth (Lahvis *et al*., 2005; Walisser *et al*., 2005). It has been suggested that the failure of the DV to close in the *ahr*$^{-/-}$ mice may result from the failure of this blood vessel to adequately constrict (Fugelseth et al., 1998; Lahvis *et al*., 2005). In addition, the *ahr*$^{-/-}$ mice also develop cardiac hypertrophy and fibrosis, correlated with an increase in size of cardiomyocytes (Thackaberry *et al*., 2002; Vasquez *et al*., 2003). These studies highlight the role of AHR in cardiovascular development and homeostasis.

Studies show that the AHR also contributes to BP regulation in addition to cardiovascular development. Eight month old *ahr*$^{-/-}$ mice were demonstrated to be hypotensive using invasive catherization of the carotid artery with a 1.4F Millar micromanometer (Miller instruments, Inc, TX) connected to a heart performance analyzer (MicroMed, Louisville, KY). The hypotension was associated with a decreased cardiac output caused by diminished stroke volume (Vasquez *et al*., 2003), suggesting a role for AHR in cardiac function. In another study, three month old *ahr*$^{-/-}$ mice were also shown to be hypotensive (Zhang *et al*., 2010). Mean arterial pressure (MAP), systolic and diastolic BP were significantly lower during both light and dark cycles in *ahr*$^{-/-}$ mice, with no difference in heart rate (HR). Interestingly, endothelial nitric oxide synthase (eNOS) protein was upregulated in the aorta, but increased NO bioavailabilty did not mediate the resultant hypotension in the *ahr*$^{-/-}$ mice as demonstrated by the inability of pharmacological NOS inhibition to normalized BP (Zhang *et al*., 2010). In contrast, inhibition of the renin angiotensin system (RAS) by the angiotensin converting enzyme (ACE) inhibitor, captopril, produced a less significant decrease in MAP in the *ahr*$^{-/-}$ mice, suggesting that the RAS contributed significantly less to maintaining basal BP in the *ahr*$^{-/-}$ mice as compared to *ahr*$^{+/+}$ mice. Nonetheless, indices of RAS activity, including plasma renin activity, ACE activity, and plasma Ang II levels were normal, suggesting that hypotension in *ahr*$^{-/-}$ mice may be due to an attenuation of Ang II downstream signaling.

Additionally, the AHR is activated by shear stress (SS). SS is the frictional force exerted on the vascular endothelium due to blood flow, and is necessary in regulating vascular tone and BP. Laminar SS (10-30 dynes/cm^2) occurs in linear regions of the vasculature and elicits a response in vascular ECs that is predominantly considered to be

anti-atherogenic and anti-proliferative (Traub and Berk, 1998). The vasoprotective effect of laminar SS is mediated, in part, by an upregulation and activation of the endothelial NOS (eNOS), and a subsequent increase in NO production. Under static conditions, constitutive expression of AHR and its downstream target gene, CYP1A1, have been detected in cultured human ECs, albeit at low levels. However, upon induction of laminar SS (25 dynes/cm^2), mRNA and protein levels of AHR and CYP1A1 were significantly upregulated after 24 h of SS. Additionally, CYP1A1 activity levels were up seven fold after 48 h of laminar SS. Interestingly, the modest inducible expression was attenuated by turbulent SS (Eskin *et al.*, 2004; Conway *et al.*, 2009). In support of this, Han and coworkers demonstrated that laminar fluid SS-induced CYP1A1 activation in vascular ECs. Human umbilical vein endothelial cells subjected to 15 dynes/cm^2 showed upregulation of CYP1A1 protein levels at 2 h, and increased activity at 1 h after SS induction (Han *et al*., 2008). Interestingly, in bovine aortic endothelial cells subjected to SS (15 dyne/cm^2), eNOS was phosphorylated at serine 1179 (Ser 1179) as early as 2 min, while phosphorylation at serine 635 (Ser 635) was detected at 15 min (Boo *et al.*, 2002a; Boo *et al.*, 2002b). The phosphorylation of eNOS at these specific sites increases its activity, hence NO bioavailability (Dimmeler *et al*., 1999; Iwakiri *et al*., 2002). Taken together, these studies clearly suggest that the activation of AHR and its responsive gene, CYP1A1 by SS might contribute to EC regulation, NO production, and overall vascular function.

Endogenous ligands of the AHR

The physiological function of AHR as identified from the *ahr*$^{-/-}$ mice, suggests that there is an endogenous mechanism leading to AHR activation, such as the presence of an endogenous ligand. In fact, several endogenous compounds have been shown to transactivate the AHR into the nucleus in the absence of xenobiotics, although the physiological relevance of these compounds remains unclear. Some of the compounds proposed to activate the AHR include cyclic adenosine monophosphate (cAMP), modified low density lipoproteins (LDL), indigo and indirubin, and lipoxinA4. The second messenger cAMP has been shown to transactivate the AHR (Oesch-Bartlomowicz and Oesch, 2009). However, this activation did not result in subsequent dimerization with ARNT, a mechanism distinct from that observed with xenobiotic AHR activation. Further, modified LDL have also been shown to act as endogenous ligands for the AHR (McMillan and Bradfield, 2007a). Purified LDL from sheared sera was shown to induce AHR-signaling by up to six fold compared to static sera. Induction of AHR signaling was also shown with modified LDL after preincubation with sodium hypochloride and in the *ahr*$^{-/-}$ mice, increased accumulation of the AHR-activating LDL was evident. Indigo and indirubin, isolated from human urine and from bovine serum, have also been suggested to be endogenous ligands for the AHR. These compounds bind and activate the AHR although activation was about a hundred fold less than dioxin (Adachi *et al.*, 2001; Peter Guengerich *et al.*, 2004). Although the levels of these compounds are low in the picomolar range in human urine, it is possible that they may reach physiological nanomolar range in certain body compartments required to activate DREs of target genes. Therefore, their physiological relevance cannot be completely disregarded. Other suggested

endogenous ligands include a key metabolite of arachidonic acid, Lipoxin A4 which has been demonstrated to induce CYP1A1 and CYP1A2, and in addition, can also serve as their substrates (Schaldach *et al.*, 1999). Chang and colleagues showed using gel shift assay that CYP1A1-deficient mouse hepatoma cell lines (*c*37 cells) contain a transcriptionally active AHR-ARNT complex in the absence of an exogenous ligand. This was also detected when wildtype Hepa-1 cells were treated with the CYP1A1 inhibitor, ellipticine, suggesting that an unknown CYP1A1 substrate is a possible AHR endogenous ligand (Chang and Puga, 1998). Moreover, derivatives of tryptophan as well as biliverdin have been suggested to activate the AHR. Thus, the translocation of the AHR into the nucleus independent of exogenous ligands suggests a biologically relevant role for the AHR.

Cytochrome P4501A1 (CYP1A1)

Regulation and function of CYP1A1 gene

As mentioned above, CYP1A1 is a xenobiotic metabolic enzyme induced by the activation of the AHR, and two regulatory regions of the CYP1A1 gene are responsible for its constitutive and inducible expression. The first region is the DRE which serves as the binding site for the AHR/ARNT complex in response to xenobiotics, depicted by the sequences 5'-TNGCGTG-3. In the rat, the DRE has been demonstrated to be positioned upstream of the CYP1A1 gene promoter (Fujisawa-Sehara *et al*., 1987; Neuhold *et al*., 1989). The DRE also serve as a binding site for several transcription factors (Jones and Whitlock, 1990). Nonetheless, in the mouse, six DRE sites have been identified for the binding of the AHR/ARNT complex (Denison *et al.*, 1989). The second regulatory region

of the CYP1A1 gene is known as the basal transcription element (BTE) and is involved in the constitutive expression of CYP1A1. Most importantly, these two regulatory regions of the human CYP1A1 gene were also shown to be conserved in the mouse (Yanagida *et al.*, 1990).

Chromatin structural analysis of the CYP1A1 gene reveals the presence of a nucleosome at the promoter/enhancer region in the absence of an AHR agonist (Morgan and Whitlock, 1992). Activation of the AHR by TCDD led to a conformational change in the promoter/enhancer region of the CYP1A1 gene, and the resultant disruption of the occupied nucleosome, turning on the CYP1A1 gene. Additionally, chromatin immunoprecipitation experiments have revealed that the CYP1A1 enhancer region is hypermethylated in prostate cancer cells, creating an inaccessible chromatin structure, thereby preventing xenobiotic responsiveness in these cells (Okino *et al.*, 2006).

A positive correlation has also been shown between CYP1A1 expression and protein kinase C (PKC) signaling. It was demonstrated that PKC inhibition blocked ligand activation of the AHR/ARNT complex and inhibited CYP1A1 induction by TCDD (Carrier *et al.*, 1992). Further analysis revealed that the ligand-dependent nuclear translocation of AHR is inhibited by phosphorylation of the amino acid, serine, at position 12 (Ser12), or Ser36 by PKC. In contrast, the phosphorylation of the Ser 68 has been demonstrated to target the AHR from the nucleus back to the cytoplasm thereby attenuating CYP1A1 induction (Ikuta *et al.*, 2004). Thus, the activity and phosphorylation target of PKC directly impacts CYP1A1 expression. In a 2011 study, it was shown that the CYP1A1 promoter harbored a β-catenin binding site. Signaling

through β-catenin contributed to basal expression of CYP1A1 and also, in part, to CYP1A1 induction by xenobiotics (Braeuning *et al.*, 2011).

The best studied function of the CYP1A1 enzyme is the transformation of xenobiotics, thereby facilitating their clearance. The mechanism of action of CYP1A1 has been studied extensively, using benzo (a) pyrene (BaP) as substrate. CYP1A1 metabolizes BaP into reactive epoxide intermediates which are then converted to water soluble diol epoxides for elimination. BaP is oxidized by CYP1A1 to BaP-7,8-oxide, which is further hydrolyzed by the enzyme epoxide hydrolase to B(a)P-7,8-diol and the two enantiomers (+)-BaP-7,8-diol, and (-)-BaP-7,8-diol (Shimada and Fujii-Kuriyama, 2004). Further oxidation of these metabolites produces four diol epoxides that are very reactive (Tang *et al.*, 2000). In rats treated with BaP (10 mg/Kg), CYP1A1 induction was increased after 24 to 48 h in the lung and liver, and this increased was associated with the presence of carcinogenic DNA-adducts (Harrigan *et al.*, 2004; Harrigan *et al.*, 2006).

Expression and localization of CYP1A1

Constitutive levels of CYP1A1 are non-detectable in the liver. Nonetheless, one primary location where CYP1A1 is constitutively expressed is in vascular endothelial cells (ECs). Several *in vitro* studies have demonstrated the constitutive expression of CYP1A1. In human umbilical vein endothelial cells (HUVECs), CYP1A1 protein was detected by western blot. Using immunohistochemical staining of mouse aorta, CYP1A1 was shown to be localized to the endothelial layer, and in addition, immunostaining of CYP1A1 protein was also localized specifically to the endothelium of cross-sections of human coronary artery (Conway *et al.*, 2009). In addition to its constitutive expression,

CYP1A1 mRNA and protein have also been shown to be induced by physiological level of SS in the endothelium (Eskin *et al.*, 2004; Han *et al.*, 2008; Conway *et al.*, 2009). Further, several studies have demonstrated the expression of CYP1A1 in the endothelium following its induction after treatment with AHR agonists. Annas and coworkers, demonstrated that CYP1A1 was present in blood vessels of the heart, kidneys, and liver as detected using substrates for CYP1A1 following induction with AHR agonists, beta-naphthoflavone (BNF). Autoradiography was used to localize sites of metabolic activation of ^{3}H-labeled Trp-P-1 (3-amino-1, 4-dimethyl-5H-pyrido [4, 3-b] indole), a heterocyclic amine shown to be metabolized by CYP1A1 (Annas and Brittebo, 1998; Annas *et al*., 2000). Further evidence comes from detecting the induction of CYP1A1 after treatment with BNF in the coronary arteries, capillaries, and veins of the heart; portal veins of the liver; and afferent and efferent arteries, and glomerular and peritubular capillaries in the kidneys (Annas *et al*., 2000; Granberg *et al*., 2000). More evidence has been shown with polychlorinated biphenyl (PCB)-mediated induction of CYP1A1 mRNA predominantly in vascular endothelium (Farin *et al*., 1994; Stegeman *et al*., 1995). Other studies have shown that CYP1A1 mRNA is not constitutively expressed in the mouse vascular smooth muscle cells (vsmc), and upon treatment with the AHR agonist, BaP (3 μmol/L), CYP1A1 protein levels remained uninducible even though mRNA levels were upregulated (Kerzee and Ramos, 2001). Nonetheless, in a 2007 study, Wilson and colleagues showed that CYP1A1 mRNA was highly induced in vascular endothelial cells, vascular smooth muscle, and nerve cells in the dermis of the bottlenose dolphins, suggestive of PCB contamination (Wilson *et al*., 2007). In a recent study, C57BL/6 wildtype mice were treated with the AHR agonist TCDD and CYP1A1 protein induction

detected by immunohistochemistry was predominantly localized in the endothelial layer of the mesenteric artery and the aorta (Kopf *et al.*, 2010). Given the importance of the endothelium in vascular development and function, it is relevant to consider the role of CYP1A1 in the cardiovascular system.

Additional extrahepatic tissues in which CYP1A1 has been established to be present include the intestine, skin and the lung. In mice treated intraperitoneally with 3-methylcholanthrene (3MC) (200 mg/kg body weight) for 10 h, CYP1A1 mRNA was detected in the villous epithelium and cells around the lamina propria in duodenum, the jejunum (Dey *et al.*, 1999), as well as at low levels in the epidermis in normal human keratinocytes (Pavek and Dvorak, 2008). Lastly, CYP1A1 enzyme activity and mRNA levels have also been detected in the microsomal fractions of human lung (Smith *et al.*, 2001; Bernauer *et al.*, 2006).

CYP1A1 polymorphisms and cardiovascular disease

A plethora of mutations in the CYP1A1 gene have been identified. The first of these polymorphisms denoted *CYP1A1*1* occurs at position 3801 whereby thymidine is substituted by cytosine. This polymorphism does not result in differential CYP1A1 expression. Another polymorphism involves adenine to guanine substitution at position 2455 of codon 462 at exon 7. This polymorphism is known as *CYP1A1*2B* or *Ile462Val* polymorphism (Hayashi *et al.*, 1991). Additionally, the *msp1* polymorphism whereby thymidine is substituted by cytosine at position 3798 (3798T>C), and the *Ile462Val* polymorphisms of CYP1A1 both have been associated with smoking-induced squamous cell carcinoma in the lung, and smoking related coronary artery disease (Nakachi *et al.*,

1993; Wang *et al.*, 2002). Recently, another *CYP1A1 msp1* gene polymorphism was also shown to be associated with greater mortality in patients with acute coronary syndrome (ACS) with a history of smoking. When patients with ACS were genotyped for the T6235C polymorphism and the survival rate was stratified by smoking history, the *CYP1A1* T6235C polymorphism was particularly correlated with mortality of smokers whether past or current (Jarvis *et al.*, 2009). In contrast, the *CYP1A1*2C* (A4889G) polymorphism was shown to be protective against coronary artery disease in the Taiwanese population particularly among non-smokers (Yeh *et al.*, 2009). Lastly, an interaction between human polymorphisms of CYP1A1 and AHR was implicated in determining blood pressure (BP) among smokers, non-smokers, and ex-smokers (Gambier *et al.*, 2006). Thus, CYP1A1 expression and polymorphisms may play a role in the development or pathogenesis of cardiovascular diseases.

Omega-3 Polyunsaturated Fatty Acids (n-3 PUFA)

n-3 PUFA Biology and the Cardiovascular System

Epidemiological evidence shows that fish-eating Greenland Inuits exhibit significantly lower risk of death from acute myocardial infarction when compared to those from the Danish population which consumed less fish. The Inuit diet provides several grams of n-3 PUFAs per day from fish (Blanchet *et al.*, 2000). More evidence has also been seen in the Japanese population with higher fish consumption compared to the United States. A lower rate of acute myocardial infarction and overall death from cardiovascular disease is significantly lower in the Japanese population (Menotti *et al.*, 1999). These

observations were some of the first studies to raise the potential of the beneficial and cardiovascular protective effects of fish oil.

Randomized clinical trials in humans have also revealed some benefits of n-3 PUFA supplementation. In the Gruppo Italiano per lo Studio della Sopravvivenza nell'Infarto Miocardico (GISSI)-Prevenzione (GISSI-Prevenzione) clinical trials, 11,324 patients surviving recent myocardial infarction were randomly assigned supplements of n-3 PUFA (1 g/day), vitamin E (300 mg/day), or both for three and a half years. Treatment with n-3 PUFA only, reduces the risk of cardiovascular deaths, myocardial infarction and stroke by 15% (1999; Marchioli *et al.*, 2002). The second large scale clinical trial conducted was the Japan EPA lipid intervention study (JELIS). In 18,645 patients with hypercholesterolemia, 1.8 g/day of EPA with statin, or statin only, were assigned for a period of 5 years. In patients with a history of coronary artery disease supplemented with EPA, major coronary events and deaths were reduced by 19% (Yokoyama *et al*., 2007). Moreover, in the Diet and Reinfarction Trial (DART), 2,033 Welsh men following myocardial infarction were randomly assigned two servings of fish per week for over two years. Cardiovascular deaths were reduced by 29% in patients who consumed fish, compared to patients with no fish in their diets (Burr *et al.*, 1989). Further, in the Study on Prevention of Coronary Atherosclerosis by Intervention with Marine Omega-3 fatty acids (SCIMO), 223 patients with coronary artery disease were assigned fish oil, at 6 g/day for 3 months and then 3 g/day for 21 months, or placebo. The fish oil group had significantly more regression of coronary atherosclerotic lesions compared to control group (Von Schacky *et al.*, 1999). Taken together, these clinical trials reveal the cardiovascular benefits of n-3 PUFAs.

The cardiovascular benefits of n-3 PUFAs are likely mediated through multiple mechanisms including anti-hypertensive, anti-arrhythmic, anti-inflammatory, vasoprotective, and anti-lipidemic, among others. In a 1996 study, Chen and colleagues showed that the BP-lowering effect of fish oil was independent of thromboxane A2 levels in the spontaneously hypertensive rats (Chen *et al*., 1996). Further, Engler and colleagues followed up with young spontaneously hypertensive rats treated with a DHA-enriched diet for 6 weeks. Systolic BP was reduced by 34 mmHg compared to controls (Engler *et al*., 1999). In addition, in a meta regression analysis of randomized trials in humans, fish oil was shown to reduce systolic BP by 2.1 mmHg and diastolic BP by 1.6 mmHg with greater effects in hypertensive patients (Geleijnse *et al*., 2002). Furthermore, in a population-based randomized 10 week long study, 6 g per day of 85 percent EPA and DHA were fed to 156 men and women with essential hypertension. The mean systolic BP was reduced by 4.6 mmHg while the diastolic BP by 3 mmHg. Interestingly, there was no change in BP in the control group on corn oil (BÃ¸naa *et al*., 1990). Additionally, in a meta-analysis of 31 placebo-controlled trials on 1356 subjects, there was a dose response effect of n-3 PUFAs on BP with strong association in patients with hypertension and atherosclerosis (Morris *et al*., 1993). Taken together, these studies provided compelling evidence of anti-hypertensive benefits of n-3 PUFAs.

The majority of studies done so far have been focused on the effects of n-3 PUFAs on serum cholesterol levels as well as their role in inflammation and lipoprotein metabolism (Bronsgeest-Schoute *et al.*, 1981; Hudert *et al.*, 2006). Nonetheless, few studies have investigated the vascular function of n-3 PUFAs. n-3 fatty acids are essential fatty acids for vertebrates because they cannot be synthesized de novo, but rather must be

obtained from the diet. Marine phytoplankton and other aquatic invertebrates can synthesize these fatty acids (Yazawa, 1996; Wen and Chen, 2003) and thus, these fatty acids biomagnify in fish. n-3 PUFAs are comprised principally of two key constituents; eicosapentaenoic acids (EPA) and docosahexaenoic acids (DHA). EPA consists of twenty carbon atoms with five double bonds (C20:5), whereas DHA is comprised of twenty two carbon atoms with six double bonds (C22:6). In contrast, n-6 fatty acids are more saturated (i.e. fewer double bonds) and these include the precursors linoleic acid (LA) and arachidonic acid (Fig. 1.2).

Figure 1.2. Structure of arachidonic acid, eicosapentaenoic acid (EPA), and docosahexaenoic acid (DHA). Arachidonic acid consists of 20 carbon atoms with 4 double bonds and the last double bond is sixth from the omega end (n-6), EPA consists of 20 carbons with 5 double bonds, and the last unsaturated carbon is located third from the omega end (n-3). Docosahexaenoic acid consists of 22 carbons with 6 double bonds, and also with the last unsaturated carbon located third from the omega end (n-3).

Cytochrome P450s (P450s) and n-3 PUFA metabolism

P450s display different regioselectivities for n-3 PUFA hydroxylation and epoxidation. Several P450 family members metabolize EPA and DHA as preferred substrates. Recombinant human CYP2J2 has been shown to metabolize EPA and DHA into 17,18-epoxyeicosatetraenoic acid (17,18-EEQ), and 19,20- epoxydocosapentaenoic acid (19,20-EDP), respectively (Fer *et al.*, 2008). In addition, all members of the CYP2C epoxygenase family, including 2C8, 2C9 and 2C19, metabolized both DHA and EPA, resulting in a large mixture of products including 10,11-, 13,14-, 16,17-, and 19,20-EDP from DHA, and 11,12-, 14,15-, and 17,18-EEQ from EPA (Barbosa-Sicard *et al.*, 2005). Further, members of the CYP4A family have also been shown to metabolized EPA and DHA. Mouse CYP4a12a metabolizes EPA producing 56% of metabolites as 17,18-EEQ (Muller *et al.*, 2007). Further, human CYP4F2 hydrolyses DHA with higher rates, compared to EPA as a substrate (Fer *et al.*, 2008). Recently, recombinant human CYP1A2 and 2D6 were also shown to metabolize EPA and DHA in a stereospecific manner to 17(R),18(S)-EEQ, and 19(R),20(S)–EDP, respectively (Lucas *et al.*, 2010). Taken together, these results suggest that a large number of P450 families are capable of metabolizing n-3 PUFAs.

CYP1A1 and n-3 PUFA metabolism

CYP1A1 in particular, acts primarily as an epoxygenase toward EPA as substrate (Schwarz *et al.*, 2004). Human CYP1A1 has been shown to epoxidized the 17,18-olefinic bond of EPA in a stereospecific manner to form mainly 17(R),18(S)-EEQ, as 70% of its metabolites. CYP1A1 also hydroxylated EPA in a highly regioselective manner to

produce 19-OH-epoxypentaenoic acid. Interestingly, the human *CYP1A1 Ile462Val* polymorphism has been shown to metabolize EPA as substrate with twice higher rates than wildtype CYP1A1 (Schwarz *et al.*, 2005). This suggests that CYP1A1 metabolism of EPA may contribute to differences between individuals in the production of physiologically active PUFA metabolites. CYP1A1 has also been demonstrated to metabolize DHA into stereospecific products. In an *in vitro* study, recombinant human CYP1A1 was shown to convert DHA 100 % to 19(R),20(S)-EDP (Fer *et al.*, 2008). Furthermore, the degree of epoxidation for EPA and DHA by CYP1A1 was markedly greater compared to arachidonic acid (AA). CYP1A1 also produced 14,15-epoxyeicosatrienoic acid (EET) from AA. Nonetheless, this accounted for a very small percentage of the total epoxides produced.

Cardiovascular function of CYP1A1 metabolites of n-3 PUFAs

Metabolites of n-3 PUFA metabolism have been shown to exhibit vasoactive properties. In fact, 17,18-EEQ, the product of EPA metabolism by CYP1A1 has been reported to induce vasorelaxation in porcine and canine coronary microcirculatory vessels (Zhang *et al.*, 2001). Further, 17,18-EEQ has also been reported to be metabolized to novel prostaglandins that are physiologically relevant (Oliw, 1991). In a recent study, 17,18-EEQ was shown to relax and hyperpolarize both pulmonary artery and bronchial smooth muscle cells in the human lung (Morin *et al.*, 2009). In the spontaneously hypertensive rats, EPA concentration response in aortic rings was shown to elicit significantly greater relaxation at all doses compared to the normotensive Wistar-Kyoto rats (Engler *et al.*, 1994). Interesting, in another study, 19,20-EDP, the product of DHA

metabolism by CYP1A1 was shown to induce up to 70 % relaxation in porcine coronary microvessels, and the mechanism of dilation was shown to be mediated by large conductance calcium-activated potassium channels (Ye *et al.*, 2002). Taken together, CYP1A1 metabolizes DHA and EPA as substrates into vasoactive metabolites.

Arachidonic acid (AA) as endogenous substrate of CYP1A1

The cyclooxygenase and lipoxygenase enzymes have been known to metabolize AA into 5-, 12-, and 15-hydroxyeicosatetraenoic acid (HETE), prostaglandins, 14,15 EET, prostacyclins, and thromboxanes (Miller and Vanhoutte, 1985; Churchill *et al.*, 1989; Escalante *et al.*, 1989; Brock *et al.*, 1999). Additionally, P450 enzymes, including CYP1A1, also use AA as a substrate (Roman, 2002). CYP1A1 has been shown to act mainly as a hydroxylase toward AA metabolism. Recombinant human CYP1A1 was shown to produce 14,15-EET from AA. Nonetheless, the amount of 14,15 EET produced was less than 60% relative to the total epoxides produced from AA, suggesting that AA metabolism by CYP1A1 is of less importance compared to EPA and DHA (Fer *et al.*, 2008; Lucas *et al.*, 2010). In fact, EETs were shown to be 1000 fold less potent that DHA-derived epoxides (Ye *et al.*, 2002). Regardless, 14,15-EET has been demonstrated to relax precontracted coronary microvessels (Campbell *et al.*, 1996), to induce NO-dependent relaxation in pressurized arterioles in the mouse (Hercule *et al.*, 2009), and to dilate the renal microcirculation of rats *ex vivo* (Imig *et al.*, 1996). Taken together, these studies suggest that CYP1A1-generated EETs have vasodilatory properties, even though their potency is less, compared to n-3 PUFA metabolites.

Nitric oxide

Nitric oxide biology, regulation, and the cardiovascular system

NO is a potent vasodilator that is produced by three unique forms of NOS, including eNOS, neuronal NOS (nNOS) and inducible NOS (iNOS). In the endothelium, NO is produced in a reaction catalyzed by eNOS, transforming L-arginine to L-citrulline, in the presence of molecular oxygen with several cofactors including NADPH, flavin adenine dinucleotide (FAD), flavin mononucleotide (FMN), tetrahydrobiopterin (BH_4) and Ca^{2+}/calmodulin (Ignarro *et al*., 1987; Palmer *et al*., 1988). The primary stimulus that increases eNOS activity is a transient increase in intracellular calcium concentration (Busse and Mulsch, 1990; Busse and Fleming, 1995). The availability of both the substrate, L-arginine, and the co-factor, BH_4, also regulates NO production. BH_4, in particular is important because in its deficiency, electron transport through eNOS can become uncoupled, leading to accumulation of reactive oxygen species as superoxide anions (Cosentino *et al.*, 1998; Cherng *et al.*, 2009). The regulation of NO production has also been demonstrated to be affected by the phosphorylation status of eNOS at different serine residues, the most important being ser1177 phosphorylation (Fulton *et al*., 1999).

Basal NO levels play an important role in regulating vascular tone and BP. NO produced from the endothelium, diffuses across the plasma membrane mediated by aquaporin-1, to the underlying vascular smooth muscle cells, and binds to soluble guanylate cyclase to produce cyclic guanosine monophosphate (cGMP). cGMP activates protein kinases, resulting in vasodilation by decreasing smooth muscle intracellular Ca^{2+} (Fig. 1.3). This NO-mediated vasodilation contributes to basal BP regulation. In fact, mice that overexpress the eNOS enzyme are hypotensive (Ohashi *et al*., 1998).

Conversely, eNOS null mice or mice treated with a NOS antagonist are hypertensive (Shesely *et al.*, 1996; Yang *et al.*, 1999). The dysregulation of NO signaling has been implicated in many cardiovascular diseases. In particular, pathological increases in reactive oxygen species have been demonstrated to scavenge NO, leading to loss of NO-mediated relaxation as one common contributor to endothelial dysfunction (Fresquet *et al.*, 2006).

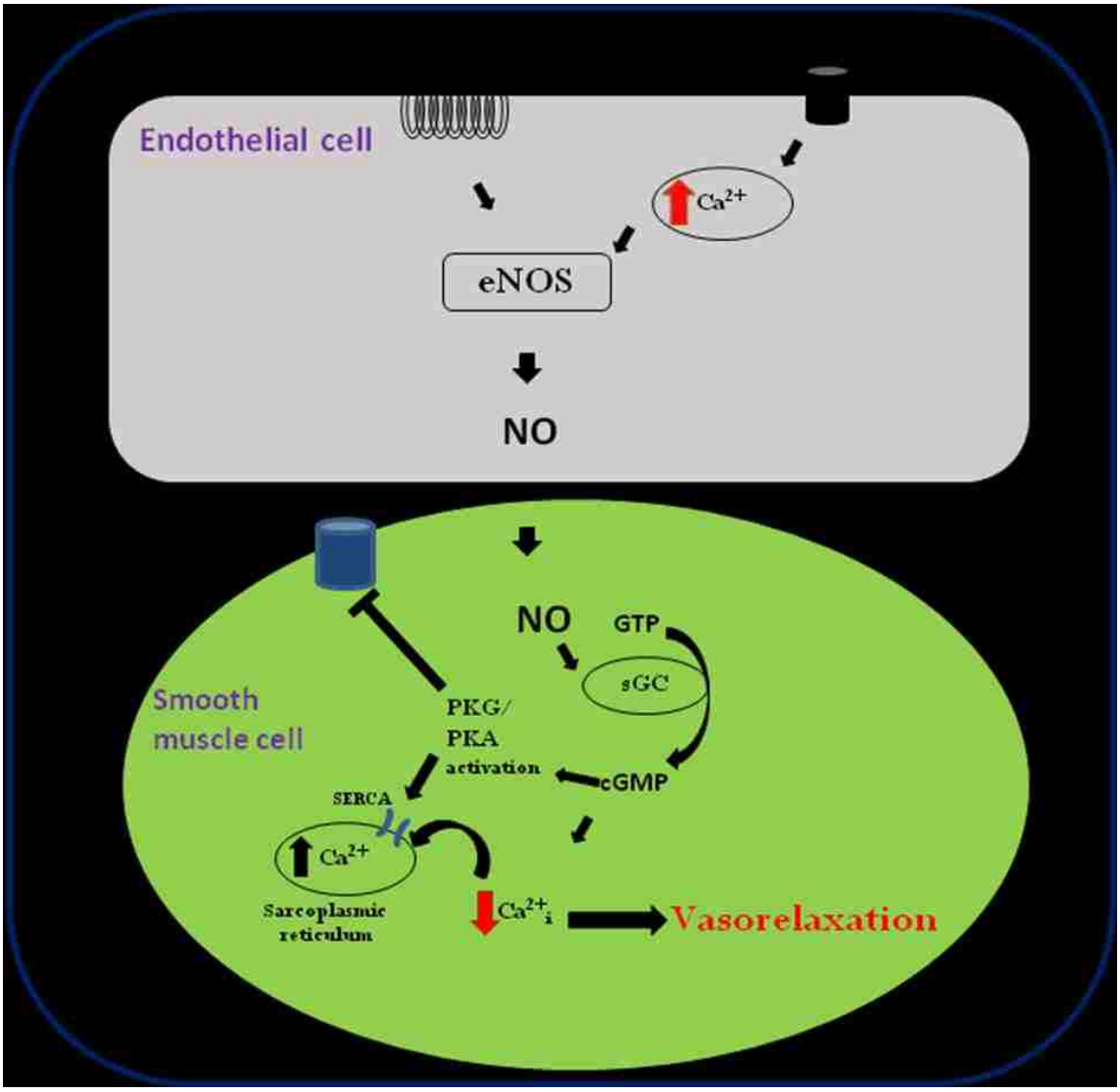

Figure 1.3. Mechanism of endothelial cell production of NO leading to vascular smooth muscle relaxation. Various stimuli, such as acetylcholine, bradykinin, and SS increase intracellular calcium levels in endothelial cells which stimulates the production of NO by eNOS. NO diffuses to the underlying smooth muscle cell and activates soluble guanylate cyclase (sGC) resulting in the accumulation of cGMP. An increase in cGMP activates protein kinase G (PKG) and protein kinase A (PKA). Activation of PKA and PKG inhibits L-type Ca^{2+} channels, activates sarcoplasmic endoplasmic reticulum Ca^{2+} ATPases (SERCA) thereby pumping Ca^{2+} back into the sarcoplasmic reticulum. This leads to a reduction in intracellular calcium in the smooth muscle resulting in vasorelaxation.

Nitric oxide and n-3 PUFA crosstalk

Several studies have investigated potential crosstalk between n-3 PUFAs and NOS expression, particularly eNOS. Treatment of human coronary artery endothelial cells with DHA for 7 days tended to increase both total and phospho-eNOS, and upregulated the expression of phospho-AKT and HSP90, two proteins involved in the activation of eNOS. In addition, nitrate and nitrite (NOx) levels were increased in the media of DHA-treated cells, suggesting an increase in NO production (Stebbins *et al*., 2008).

In another study, using human cultured umbilical vein endothelial cells, EPA stimulated the translocation of eNOS from caveolae to the cytosol, a step required for activation. Interestingly, EPA upregulation of eNOS was not accompanied with a robust increase in intracellular calcium (Omura *et al*., 2001). Li and colleagues also confirmed that EPA stimulated the translocation of eNOS from caveolae (Li *et al*., 2007a; Li *et al*., 2007b). Additionally, in EA hy 926 endothelial cells, both DHA and EPA significantly increased expression of phospho-eNOS, with no change in total eNOS expression (Gousset-Dupont *et al*., 2007).

Animal studies have also demonstrated a possible crosstalk between eNOS expression in caveolae and n-3 PUFAs. In rats treated with n-3 or n-6 diets, phospholipid n-3 fatty acyl content was increased, while caveolin-1 and cholesterol were significantly reduced in the colon of n-3 PUFA fed rats compared to n-6. Moreover, caveolae-resident proteins, eNOS and H-Ras were reduced by 45 and 56%, respectively, in rats fed the n-3 diet, while non-caveolae proteins, K-Ras and clathrin, were not affected (Ma *et al*., 2004). Further evidence also comes from young pigs treated with DHA. DHA significantly

increased BH_4 and NADPH levels in the brain, muscle and liver, and increased NOS activity by 45-48% in the muscle and brain (Li *et al.*, 2008). These data further suggest that n-3 PUFAs can remodel the microdomain of membranes *in vivo*, thereby altering the localization of proteins, including eNOS. Taken together, these data suggest that n-3 PUFAs could lead to increases in NOS activity and potentially in NO bioavailability.

Rationale for Research

Cardiovascular diseases are the leading cause of death in the United States (Roger *et al*., 2011) and high BP is a major independent risk factor, including stroke, myocardial infarction, and coronary artery disease (Stokes *et al*., 1989). The AHR has been implicated in the regulation of vascular function and BP. AHR null mice were demonstrated to exhibit altitude-induced hypertension with low BP at sea level (Lund *et al.*, 2003; Lund *et al.*, 2008). In addition, cardiac hypertrophy and portosystemic shunting were hallmarks of the AHR null mice (Lahvis *et al.*, 2000; Thackaberry *et al.*, 2002). Nonetheless, the sustained activation of the AHR results in vascular dysfunction and hypertension, and it has been established that this cardiovascular toxicity requires the sustained induction of CYP1A1, the AHR downstream target gene (Walker and Catron, 2000; Kopf *et al.*, 2010).

However, many questions remain. The endogenous role of the AHR in the vascular endothelium, and its target gene CYP1A1, in the regulation of BP remain to be determined. The AHR and its downstream target gene CYP1A1 have been demonstrated to be modestly induced by physiological level of laminar SS in the vascular endothelial cells, and in addition, CYP1A1 metabolize n-3 PUFAs as substrate in the production of vasodilator metabolites (Schwarz *et al.*, 2004; Schwarz *et al.*, 2005; Han *et al.*, 2008; Conway *et al.*, 2009). These observations strongly suggest that the AHR and its target gene, CYP1A1, might be involved in cardiovascular homeostasis. Thus, the long term objective of this study is to elucidate the contribution of the AHR in the vascular endothelium and of global CYP1A1 to vascular function and BP regulation in the absence of xenobiotics.

Central Hypothesis: The aryl hydrocarbon receptor (AHR) and its downstream target gene, cytochrome P4501A1 (CYP1A1), both contribute to normal vascular reactivity of blood vessels and to BP regulation.

Aim 1: Establish the degree to which loss of AHR in ECs contributes to vascular reactivity and BP regulation *in vivo.*

Rationale: The *ahr*$^{-/-}$ mice are hypotensive and this is mediated, in part, by a decreased contribution of Ang II to maintaining normal basal BP. However, the specific cell type(s) requiring AHR expression for BP regulation is not known, since this phenotype was elucidated in the global AHR knockout mouse. Nonetheless, since it has been shown that AHR expression in vascular endothelial cells is required for normal vascular development, we hypothesized that loss of AHR in EC would attenuate Ang II-dependent signaling resulting in hypotension. To test this hypothesis we generated EC-specific *ahr*$^{-/-}$ mice (*ECahr*$^{-/-}$) and investigated the contribution of Ang II to vascular reactivity and BP regulation.

Aim 2: Establish the degree to which global deletion of CYP1A1 contributes to vascular reactivity in conduit and mesenteric resistance arterioles, and to BP regulation

Rationale: CYP1A1 is constitutively expressed in vascular endothelial cells and metabolizes n-3 PUFAs, producing vasodilator metabolites that contribute in maintaining vascular tone of blood vessels. However, understanding the contribution of CYP1A1 to vasoreactivity and to BP regulation has not been investigated. Thus, our working hypothesis is that global genetic deletion of CYP1A1 will result in reduced vascular vasodilatory responses to n-3 PUFAs and increases in BP. To test this hypothesis we used

CYP1A1 KO mice that were generously provided by Dr Daniel Nebert (University of Cincinnati), to determine the BP phenotype and n-3 PUFA-mediated vasorelaxation in CYP1A1 KO mice.

Aim 3: Determine the degree to which CYP1A1 contributes to changes in vascular function and BP as a result of providing an n-3 versus n-6 PUFA-enriched diet.

Rationale: CYP1A1 stereospecifically metabolizes n-3 PUFAs to potent vasodilatory products. However, numerous studies have demonstrated the involvement of several P450s in n-3 PUFA metabolism, in addition to CYP1A1, including members of the CYP2C and CYP4A families (Barbosa-Sicard *et al.*, 2005; Muller *et al.*, 2007). Thus, it is not known if any specific P450 is required to mediate the vascular benefits of n-3 PUFAs. In addition, n-3 PUFAs have also been shown to upregulate NOS signaling in animal models and in cell culture (Ma *et al.*, 2004; Li *et al.*, 2007a; Li *et al.*, 2007b). Thus, our working hypothesis is that an n-3 PUFA-enriched diet, but not an n-6 PUFA-enriched diet, will reduce BP in CYP1A1 KO mice via a NOS-dependent mechanism. To test this hypothesis we fed CYP1A1 WT and KO mice either a diet enriched in n-3 PUFAs or n-6 PUFAs, and determine the contribution of CYP1A1 to vascular function and BP regulation.

II. CHAPTER 2

Endothelial cell-specific aryl hydrocarbon receptor knockout mice exhibit hypotension mediated, in part, by an attenuated angiotensin II responsiveness.

Larry N. Agbor, Khalid M. Elased, and Mary K. Walker. Biochem Pharmacol 5: 514–523, 2011.

A. ABSTRACT

Hypotension in aryl hydrocarbon receptor knockout mice (*ahr*$^{-/-}$) is mediated, in part, by a reduced contribution of angiotensin (Ang) II to basal blood pressure (BP). Since AHR is highly expressed in endothelial cells (EC), we hypothesized that EC-specific *ahr*$^{-/-}$ (EC*ahr*$^{-/-}$) mice would exhibit a similar phenotype. We generated EC*ahr*$^{-/-}$ mice by crossing AHR floxed mice (*ahr*$^{fx/fx}$) to mice expressing Cre recombinase driven by an EC-specific promoter. BP was assessed by radiotelemetry prior to and following an acute injection of Ang II or chronic treatment with an angiotensin converting enzyme inhibitor (ACEi). EC*ahr*$^{-/-}$ mice were hypotensive (EC*ahr*$^{+/+}$: 116.1 ± 1.4; EC*ahr*$^{-/-}$: 107.4 ± 2.0 mmHg, n=11, $p<0.05$) and exhibited significantly different responses to Ang II and ACEi. While Ang II increased BP in both genotypes, the increase was sustained in EC*ahr*$^{+/+}$, whereas the increase in EC*ahr*$^{-/-}$ mice steadily declined. Area under the curve analysis showed that Ang II-induced increase in diastolic BP (DBP) over 30 min was significantly lower in EC*ahr*$^{-/-}$ mice (EC*ahr*$^{+/+}$ 1297 ± 223 mmHg/30 min; EC*ahr*$^{-/-}{}_{AUC}$: 504 ± 138 mmHg/30 min, $p<0.05$). In contrast, while ACEi decreased BP in both genotypes, the subsequent rise in DBP after treatment was significantly delayed in the EC*ahr*$^{-/-}$ mice. EC*ahr*$^{-/-}$ mice also exhibited reduced vascular and adipose Ang II type 1 receptor (AT1R) expression, and reduced aortic Ang II-dependent vasoconstriction in the presence of vascular adipose. Taken together these data suggest that hypotension in EC*ahr*$^{-/-}$ mice results from reduced vascular responsiveness to Ang II that is influenced by AT1R expression and adipose.

B. INTRODUCTION

The aryl hydrocarbon receptor (AHR) is a ligand-activated, basic helix-loop-helix/Per-ARNT-Sim transcription factor involved in the adaptive and toxic responses of xenobiotics (McMillan and Bradfield, 2007b). The most potent ligand for AHR is the halogenated aromatic hydrocarbon 2, 3, 7, 8-tetrachlorodibenzo-*p*-dioxin (TCDD). In addition to its conventional role in xenobiotic metabolism, recent studies demonstrate a novel role for AHR in vascular development and physiological homeostasis in the absence of exogenous ligands (Thackaberry *et al.*, 2002; Vasquez *et al.*, 2003). AHR knockout mice ($ahr^{-/-}$) exhibit significant reduction in liver size, which results from the persistence of the fetal ductus venosus after birth. The patency of the ductus venosus greatly reduces the portal blood supply, and the failure of this vessel to close is dependent on AHR expression solely in vascular endothelial cells (EC) (Lahvis *et al.*, 2000; Walisser *et al.*, 2004; Lahvis *et al.*, 2005; Walisser *et al.*, 2005). Beyond its role in vascular development, the AHR also is involved in cardiac development and blood pressure regulation. AHR deficient mice develop cardiac hypertrophy and fibrosis, correlated with an increased size of cardiomyocytes (Thackaberry *et al.*, 2002; Vasquez *et al.*, 2003).

Evidence for the role of AHR in blood pressure regulation has been studied by a number of laboratories. In one study, eight-month-old $ahr^{-/-}$ mice are hypotensive, associated with a decreased cardiac output caused by diminished stroke volume (Vasquez *et al.*, 2003). In another study, three-month-old $ahr^{-/-}$ mice are also hypotensive with mean arterial pressure (MAP) and systolic (SBP) and diastolic blood pressures (DBP) significantly lower during the entire 24 hr light/dark cycle (Zhang *et al.*, 2010). Although both endothelial nitric oxide synthase (eNOS) and its product, nitric oxide (NO), a potent

vasodilator, are upregulated in the aorta of *ahr*$^{-/-}$ mice, the increased NO does not mediate the resultant hypotension. Rather, hypotension in *ahr*$^{-/-}$ mice is mediated, in part, by a decrease in the contribution of the vasoconstrictor, angiotensin (Ang) II, to basal vascular tone. The *ahr*$^{-/-}$ mice are significantly less responsive to a decrease in blood pressure when Ang II formation is inhibited, using the angiotensin converting enzyme (ACE) inhibitor, captopril. These data suggest that Ang II contributes significantly less to maintaining basal blood pressure, compared to *ahr*$^{+/+}$ mice. Interestingly, however, indices of renin-angiotensin system (RAS) activity, including plasma renin and ACE activities, and plasma Ang II levels, are normal, suggesting that hypotension in *ahr*$^{-/-}$ mice may be due to an attenuation of Ang II signaling (Zhang *et al.*, 2010).

In addition to the classic circulating components of the RAS, localized tissue RAS also has been identified in numerous tissues, including the heart, brain, blood vessels, and adipose (Stoll *et al.*, 1995; Vaughan *et al.*, 1995). Angiotensinogen, the precursor of Ang II, is secreted by white adipose tissue and all the components of the RAS are localized in rat and human adipose (Engeli *et al.*, 1999; Engeli *et al.*, 2000; Giacchetti *et al.*, 2000). The perivascular adipose tissue (PVAT) is interspersed with vasa vasorum and transmits secreted factors that act in a paracrine manner on the underlying blood vessels to modulate vascular tone and contribute to blood pressure regulation. These secreted factors include vasodilators, such as adipocyte-derived relaxing factor, Ang_{1-7}, hydrogen peroxide, and others (Lohn *et al.*, 2002; Verlohren *et al.*, 2004; Gao *et al.*, 2007), as well as vasoconstrictors, including Ang II and superoxide anion (Massiera, 2001; Gao *et al.*, 2006). Therefore, adipose is a major vasoregulator of blood pressure, in part, by contributing to overall RAS activity in the blood vessels.

Since AHR is highly expressed in the endothelium, and endothelial AHR is required for normal vascular development, it seemed logical to investigate the contribution of endothelial AHR to blood pressure regulation. To this end, we generated EC*ahr*$^{-/-}$ mice using Cre-lox recombination to elucidate the mechanism by which AHR in the endothelium modulates blood pressure. We hypothesized that loss of AHR in EC will attenuate Ang II-dependent signaling resulting in hypotension.

C. METHODS

Mouse models

Mice expressing the *ahr* floxed allele ($ahr^{fx/fx}$) were crossed to mice expressing a Cre transgene driven by the Tie2 kinase promoter enhancer (Tek) (CreTek, strain name: B6.Cg-Tg(Tek-cre)12FlvJ; (The Jackson Laboratory, Bar Harbor, ME) (Postic *et al.*, 1999; Koni *et al.*, 2001). Mice homozygous for the floxed allele and hemizygous for the Cre transgene ($ahr^{fx/fx}Cre^{Tek}$) were obtained by crossing male $ahr^{fx/+}Cre^{Tek}$ mice to female $ahr^{fx/fx}$ mice. Littermates that were Cre negative were used as genetic controls. Because Cre^{Tek} activity results in the deletion of floxed targets in the female germ line, male mice expressing the $ahr^{fx/fx}$ allele and the Cre^{Tek} transgene were used to transmit Cre^{Tek} to the offspring. Only male mice were used in subsequent experiments. All animal protocols were approved by the University of New Mexico Animal Care and Use Committee and the investigation conforms to the Guide for the Care and Use of Laboratory Animals published by the U. S. National Institutes of Health (NIH Publication No. 85-23, revised 1996).

Assessment of ahr excision

PCR analysis was used to genotype for the Cre transgene using DNA isolated from tail snips. The reaction contained 0.6 µM of each primer (Table 2.1) and 0.05 U/µl Tag Polymerase (Promega, Madison, WI, USA), and 1X buffer (Epicentre Biotechnologies, Madison, WI, USA). PCR was carried out for 39 cycles (94°C/1 min; 55°C/1 min; 72°C/2 mins). A 450-bp band confirmed the presence of the Cre transgene. Analysis of $ahr^{fx/fx}$

excision was carried out by multiplex PCR using 1 µM of two forward primers and one reverse primer (Table 2.1S, supplemental data), and 0.025 U/µl Taq Polymerase (Promega), 1X PE Buffer II (Applied Biosystems, Foster City, CA,USA), 2 mM $MgCl_2$, and 0.2 mM dNTPs. PCR was carried out for 29 cycles (95°C/30 s; 60°C/30 s; 72°C/30 s).

Assessment of endothelial AHR expression

Aortas were fixed in 10% neutral-buffered formalin and embedded in paraffin. Five micron sections were immersed in 1X Tris-EDTA buffer at 95°C for 15 min for antigen retrieval. Sections were then treated with 3% hydrogen peroxide to block endogenous peroxidase activity, followed by blocking with 10% goat serum. Mouse monoclonal anti-AHR antibody (Santa Cruz Biotechnology, Santa Cruz, CA, USA) was applied (1:200) overnight at 4°C. After washing, a secondary antibody, goat anti-mouse conjugated to horseradish peroxidase (SouthernBiotech, Birmingham, AL, USA), was applied for 1 h at room temperature (1:200). Slides were washed, stained with 3, 3'-diaminobenzidine tetrahydrochloride solution (Vector Laboratories, Burlingame, CA, USA) for 5 min, and counterstained with methyl green. Sections treated only with second antibody were used as negative controls.

In vivo analysis of blood pressure

Arterial blood pressure and heart rate were measured using radiotelemetry (Data Sciences International, St. Paul, MN, USA) as described (Lund *et al.*, 2008), using PA-C10 telemeters. Mice were allowed to recover from surgery for 7 d prior to data collection. Basal blood pressure, including systolic, diastolic, mean and pulse arterial blood pressure, and heart rate were collected for 7 d before drug treatments began. Blood pressure was recorded for 10 s every 15 min during baseline measurements and chronic drug treatment, or for 10 s every 1 min for 30 min starting 5 min after prazosin, hexamethonium, or Ang II injection.

Drug treatments

To determine the effects of Ang II on blood pressure, mice were treated with 4 mg/kg captopril (angiotensin converting enzyme inhibitor, ACEi) in the drinking water for 5 d followed by a 4 d washout (Lund *et al.*, 2003). To further elucidate the contribution of Ang II to blood pressure, mice were subsequently challenged with an *i.p.* injection of Ang II (30 µg/kg). Prazosin (1 mg/kg) or hexamethonium (30 mg/kg) was injected *i.p.* into conscious animals to assess acute responses in blood pressure and heart rate (Chen *et al.*, 2005), while N^{ω}-nitro-L-arginine (LNNA) was administered in the drinking water (250 mg/L) to assess chronic changes in blood pressure for 2 wk followed by a 1 wk washout (Duling *et al.*, 2006). In all experiments blood pressure was monitored prior to, during and after drug treatments. All drugs were purchased from Sigma-Aldrich (St. Louis, MO, USA).

Urine collection and analysis

EC*ahr*$^{-/-}$ and EC*ahr*$^{+/+}$ mice were placed into metabolic mouse cages, one animal per cage, with access to food and water *ad libitum*. Mice were acclimated to the cage for 24 h and urine generated during this period was discarded. Then, 24 h urine samples were collected twice in the subsequent 48 h and pooled. Urine was analyzed for osmolality using the Vapro™ Vapor Pressure Osmometer, model 5520 (Wescor, Inc Biomedical Division, Logan, UT, USA). Urinary nitrate/nitrite levels (NOx) were measured using the Griess colorimetric assay (Cayman Chemical, MI, USA).

Analysis of plasma ACE, renin activity, and salt balance

Plasma renin activity (PRA) was determined using a commercial kit (GammaCoat® Plasma Renin Activity ^{125}I Kit; DiaSorin, Stillwater, MN) (Senador *et al.*, 2009). The PRA assay is a two-step process, where first angiotensin I is generated and second angiotensin I is detected by a radioimmunoassay. PRA is expressed as ng/ml/hr of generated angiotensin I. Plasma ACE activity was determined using a commercial kit (Alpco Diagnostics, Salem, NH, USA). Plasma samples were incubated with a synthetic ACE substrate, ^{3}H-hippuryl-glycyl-glycine, and the product, ^{3}H- hippuric acid, was extracted and measured in a beta counter. ACE activity was expressed as Units/Liter. One unit of ACE activity was defined as the amount of enzyme required to release 1 µmol of hippuric acid per minute per liter of plasma at 37° C.

mRNA analysis of renin, angiotensinogen, and AT1R from adipose and aorta

Total RNA was isolated from perirenal visceral white adipose, aortic PVAT, and aortas cleaned of adipose tissue, using Trizol reagent (Invitrogen, Carlsbad, CA, USA). cDNA was synthesized using iScript Select cDNA Synthesis Kit (Bio-Rad Laboratories, Hercules, CA) with the supplied random primers and 250 ng RNA. PCR amplification was performed using an iCycler (Bio-Rad Laboratories) with a reaction mixture comprised of iQ SYBR Green Supermix (Bio-Rad Laboratories) with 500 μM of each forward and reverse primer (Table 2.1S, supplemental data). Cycle threshold data for both the target gene of interest and control normalization gene, DNA Polymerase II (POL2) for adipose and glyceraldehyde-3-phosphate dehydrogenase (GAPDH) for aorta, were used to calculate mean normalized expression as previously described (Simon, 2003).

Aortic AT1R protein analysis

Abdominal aortas, free of PVAT were homogenized in RIPA buffer (Santa Cruz Biotechnology), the homogenate frozen at -80 °C, thawed, sonicated and centrifuged at 15,000 x g 4 °C for 10 min. Protein concentration in the supernatant was measured using micro BCA protein assay kit (Thermo Scientific, Rockford, IL, USA). A 30 μg aliquot of protein was analyzed on a 10 % Tris-HCL polyacrylamide gel for AT1R protein, using rabbit anti-AT1R antibody (Santa Cruz Biotechnology), and GAPDH (Millipore, Billerica, MA, USA) as a normalization control.

Ex vivo analysis of abdominal aortic reactivity

The abdominal aorta was removed, placed in ice-cold physiological saline (PSS) containing 130 nM NaCl, 4.7 mM KCl, 1.2 mM KH_2PO_4, 1.2 mM $MgSO_4$, 15 mM $NaHCO_3$, 5.5 mM glucose, 26 µM $CaNa_2EDTA$, 1.8 mM $CaCl_2$, pH 7.4. The abdominal aorta in presence or absence of PVAT was cut into 2 mm segments and individual rings were suspended in an organ bath containing PSS at 37°C bubbled with 21% O_2, 6% CO_2, balanced N_2. The rings were attached to a force transducer (Grass Technologies, West Warwick, RI, USA) with steel hangers and resting tension was increased step wise to 1.5 g over 30 min. After equilibration, rings were treated with KCl (80 mM) for 5 min. Thereafter, rings were treated to 100 nM and 500 nM Ang II. After a final washout, contraction with 10 µM phenylephrine (PE) for 5 min was followed by relaxation with 10 µM acetylcholine (ACh) to determine the viability of the rings. Rings with dilation less than 50% were discarded. All chemicals were purchased from Sigma-Aldrich.

Statistical analysis

Differences among genotypes were analyzed by student's t-test. The treatment-related changes in blood pressure between genotypes were analyzed by repeated measures, two-way analysis of variance with post hoc Holm-Sidak comparisons; $*P < 0.05$ was considered statistically significant in all cases.

D. RESULTS

ahr excision as determined by PCR and endothelial AHR deletion as determined by immunohistochemistry

PCR amplification of the *ahr*$^{fx/fx}$-unexcised allele results in a 140-bp band, while amplification across the *ahr*$^{fx/fx}$-excised allele amplifies a 180-bp band. PCR amplification of the WT allele, when present, generates a 106-bp band (Walisser *et al.*, 2005). Our results demonstrated the successful excision of the *ahr*$^{fx/fx}$ allele in organs that contain EC and specifically in conduit and resistance blood vessels, including the aorta and mesenteric arteries, respectively (Fig. 2.1A). Further, immunohistochemistry confirmed the deletion of AHR protein from the endothelium of the aorta of EC*ahr*$^{-/-}$ mice, compared to EC*ahr*$^{+/+}$ mice (Fig. 2.1B).

Basal blood pressure, activity, and organ weights

Blood pressure of EC*ahr*$^{-/-}$ and EC*ahr*$^{+/+}$ littermates was measured by radiotelemetry. The EC*ahr*$^{-/-}$ mice exhibited significantly lower SBP and DBP, compared to EC*ahr*$^{+/+}$ mice (Fig. 2.2A). Pulse pressure (data not shown) and heart rate were normal (Fig. 2.2B). The decrease in blood pressure in EC*ahr*$^{-/-}$ mice was evident throughout the entire 24 h light/dark cycle, although the circadian pattern of MAP exhibited a normal increase during the night wakeful period (Fig. 2.2C). The level of activity was comparable between EC*ahr*$^{-/-}$ and EC*ahr*$^{+/+}$ mice during the 24 h light/dark cycle (Fig. 2.2D). Finally, EC*ahr*$^{-/-}$ mice exhibited a decreased liver weight and cardiac hypertrophy accompanied by renal enlargement (Table 2.1), but did not exhibit any changes in weight of adipose tissue (Table 2.2S, supplemental data).

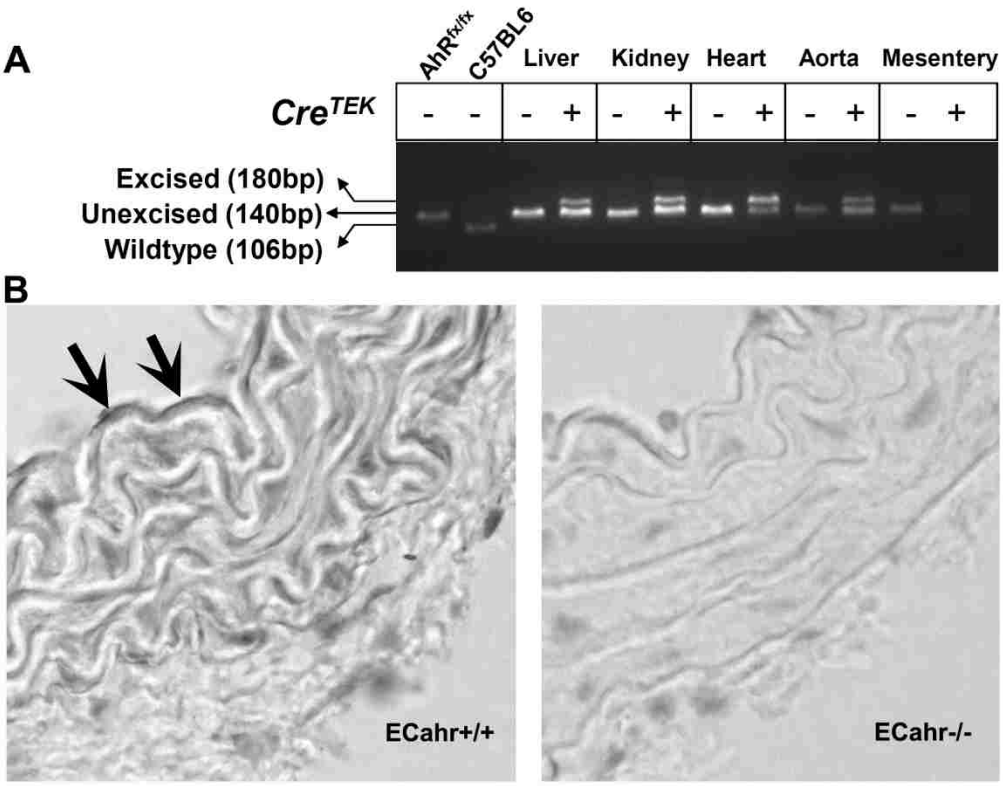

Figure 2.1. Cre^{Tek}-mediated excision of the *ahr* floxed allele (*ahr*$^{fx/fx}$). (A) Excision by Cre^{Tek} was determined by genotyping for both the unexcised (140 bp) and excised (180 bp) alleles of *ahr*$^{fx/fx}$ in genomic DNA isolated from liver, kidney, heart, aorta and mesenteric arterioles obtained from *ahr*$^{fx/fx}$Cre^{-} (EC*ahr*$^{+/+}$) and *ahr*$^{fx/fx}$Cre^{+} (EC*ahr*$^{-/-}$) mice. (B) Representative sections of aorta from EC*ahr*$^{-/-}$ and EC*ahr*$^{+/+}$ mice stained with primary AHR antibody. Positive horseradish peroxidase activity (arrows) can be seen in the endothelium of EC*ahr*$^{+/+}$, but absent in the EC*ahr*$^{-/-}$ mice.

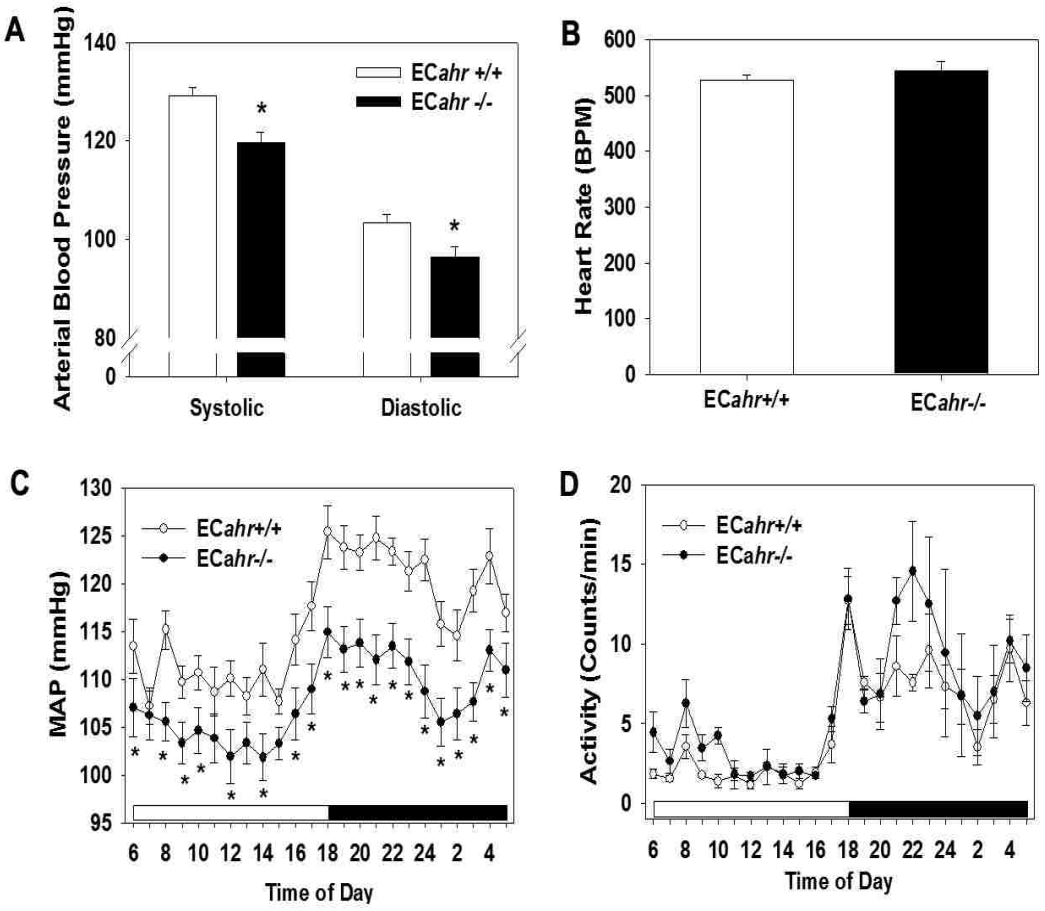

Figure 2.2. Loss of *ahr* alleles in endothelial cells (EC) decreases systolic and diastolic blood pressure. (A) Systolic and diastolic blood pressure, (B) heart rate, (C) hourly mean arterial pressure (MAP) over a 24 hr period (light and dark cycle), and (D) activity of EC*ahr*$^{+/+}$ and EC*ahr*$^{-/-}$ mice, as measured by radiotelemetry (n=12/genotype). Data represent mean ± SEM and were analyzed by Student's t-test; *$p < 0.05$, compared to EC*ahr*$^{+/+}$ (A and B) or by two-way, repeated measures ANOVA, using post hoc Holm-Sidak comparisons; *$p < 0.05$, compared to EC*ahr*$^{+/+}$ mice (C and D).

Table 2.1. Body and organ weights of 4-month-old male EC*ahr*$^{+/+}$ and EC*ahr*$^{-/-}$ mice.

Weight	EC*ahr*$^{+/+}$ (n=10)	EC*ahr*$^{-/-}$ (n=14)
Body (g)	28.8 ± 0.8	28.7 ± 0.8
Heart (mg)	119 ± 4 (0. 412 ± 0. 104)†	130 ± 4 (0. 455 ± 0. 137)*
LV+S (mg)	91.1 ± 3 (0. 320 ± 0. 099)	102 ± 3* (0. 358 ± 0. 087)*
Kidney (mg)	356 ± 17 (0. 616 ± 0. 171)	398 ± 14 (0. 694 ± 0. 162)*
Liver (mg)	1412 ± 52 (0. 049 ± 0. 180)	1110 ± 57* (0. 039 ±0. 168)*

Values are expressed as mean ± SEM
*$P < 0.05$
† (Organ/body weight ratio x 100)
Legend: LV+S, Left ventricle + Septum.

Inhibition of NOS on blood pressure

To determine the potential contribution of NOS and NO to hypotension in EC*ahr*$^{-/-}$ mice, we treated EC*ahr*$^{+/+}$ and EC*ahr*$^{-/-}$ mice chronically with the NOS inhibitor, LNNA (250 mg/L) in drinking water for 2 wk and assessed changes in blood pressure by radiotelemetry. There was an increase in MAP during LNNA treatment in both EC*ahr*$^{-/-}$ and EC*ahr*$^{+/+}$ mice, and the relative change in MAP was similar between the two genotypes (Fig. 2.3A and B). After treatment ended, MAP returned to baseline in both genotypes. To further determine if vascular eNOS or systemic NO levels were altered, we measured aortic eNOS mRNA and protein, and urinary NOx. Aortic eNOS expression and urinary NOx levels did not different between EC*ahr*$^{-/-}$ and EC*ahr*$^{+/+}$ mice (Fig. 2.1S, supplemental data).

Sympathetic nervous system activity and intrinsic heart rate

To determine if a reduction in the sympathetic contribution to vascular tone or a lower intrinsic heart rate drives the hypotension in the EC*ahr*$^{-/-}$ mice, we assessed changes in MAP and heart rate in EC*ahr*$^{-/-}$ and EC*ahr*$^{+/+}$ mice, following an acute exposure to prazosin, an α1 adrenoceptor antagonist, or to hexamethonium, a ganglionic blocker. We found that MAP decreased significantly more in the EC*ahr*$^{-/-}$ mice after prazosin (EC*ahr*$^{+/+}$; -5.3 ± 1.7 mmHg; EC*ahr*$^{-/-}$:-11.7 ± 2.3 mmHg, n=4/genotype, $p<0.05$) and hexamethonium treatment (EC*ahr*$^{+/+}$; -18.2 ± 1.8 mmHg; EC*ahr*$^{-/-}$:-25.8 ± 1.5 mmHg, n=4/genotype, $p<0.05$), compared to EC*ahr*$^{+/+}$ mice, suggesting that sympathetic contribution to vascular tone is increased (Fig. 2.2S, supplemental data). However, the

intrinsic heart rate observed following hexamethonium treatment was similar between genotypes.

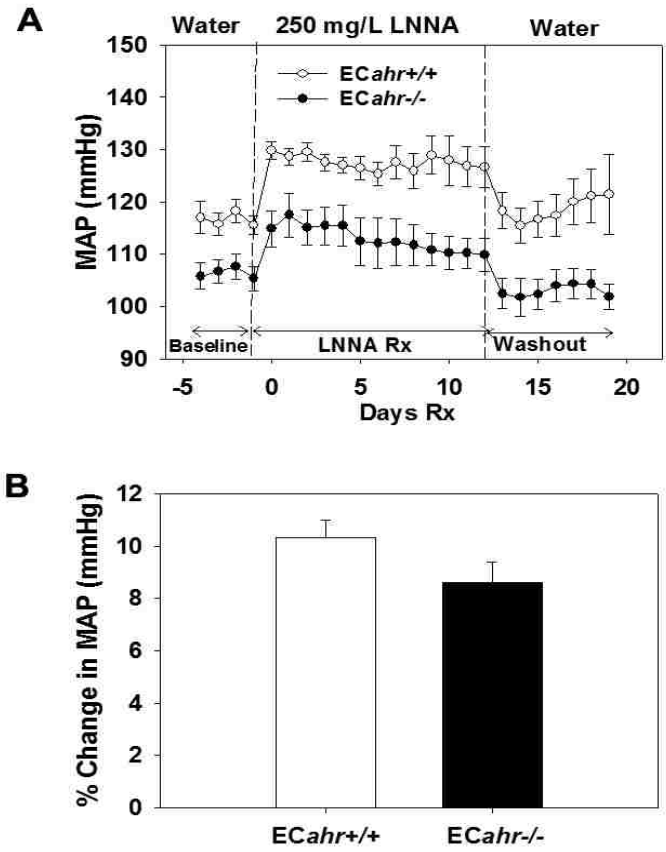

Figure 2.3. EC*ahr*$^{-/-}$ mice exhibit normal responses to NOS inhibition by LNNA *in vivo*. (A) Change in MAP after treatment with 250 mg/L LNNA in drinking water of male EC*ahr*$^{-/-}$ and EC*ahr*$^{+/+}$ mice. (B) Percent change in MAP after treatment with 250 mg/L LNNA. Data represent mean ± SEM and were analyzed by two-way, repeated measures ANOVA, using post hoc Holm-Sidak comparisons; *$p < 0.05$, compared to EC*ahr*$^{+/+}$ (A), and by Student's t-test (B) (n=8/genotype for all experiments).

Functional assessment of Ang II responsiveness in vivo

To determine if hypotension in the EC*ahr*$^{-/-}$ mice was due to reduced responsiveness to Ang II *in vivo*, we challenged EC*ahr*$^{-/-}$ and EC*ahr*$^{+/+}$ mice with a bolus dose of Ang II (30 µg/kg) and recorded the blood pressure response starting 5 min after injection. An immediate, robust response to Ang II was demonstrated by a comparable increase in MAP in both genotypes during the first 2 min (EC*ahr*$^{-/-}$: 150 ± 2 mmHg; EC*ahr*$^{+/+}$ 140 ± 10 mmHg) (Fig. 2.4). However, the subsequent change in blood pressure after the first 5 min differed considerably between genotypes. MAP in EC*ahr*$^{+/+}$ mice remained highly elevated (150 ± 8 mmHg at 5 min) with only a very modest decrease after 30 min (137 ± 3 mmHg). In contrast, the MAP in EC*ahr*$^{-/-}$ mice exhibited a steady decline (138 ± 2 mmHg at 5 min) with significantly lower MAP values being evident as early as 9 min (136 ± 2 mmHg) and dropping further by 30 min (122 ± 4 mmHg) (Fig. 2.4A). Interestingly, the SBP response was similar between EC*ahr*$^{-/-}$ and EC*ahr*$^{+/+}$ mice, although SBP did decrease slightly faster in the EC*ahr*$^{-/-}$ mice reaching significantly lower values by 20 min (Fig. 2.4B). In contrast, the DBP response was significantly diminished in EC*ahr*$^{-/-}$ mice across all time points beginning as early as 3 min (Fig. 2.4C). Area under the curve analysis following Ang II injection showed that the increase in DBP was significantly attenuated in EC*ahr*$^{-/-}$ mice (EC*ahr*$^{-/-}{}_{AUC}$: 504 ± 138 mmHg/30 min; EC*ahr*$^{+/+}{}_{AUC}$: 1297 ± 223 mmHg/30 min, $p<0.05$), while the increase in SBP was not different between genotypes (EC*ahr*$^{-/-}{}_{AUC}$: 702 ± 70 mmHg/30 min; EC*ahr*$^{+/+}{}_{AUC}$: 1106 ± 150 mmHg/30 min, ($p>0.05$)(Fig. 2.4D).

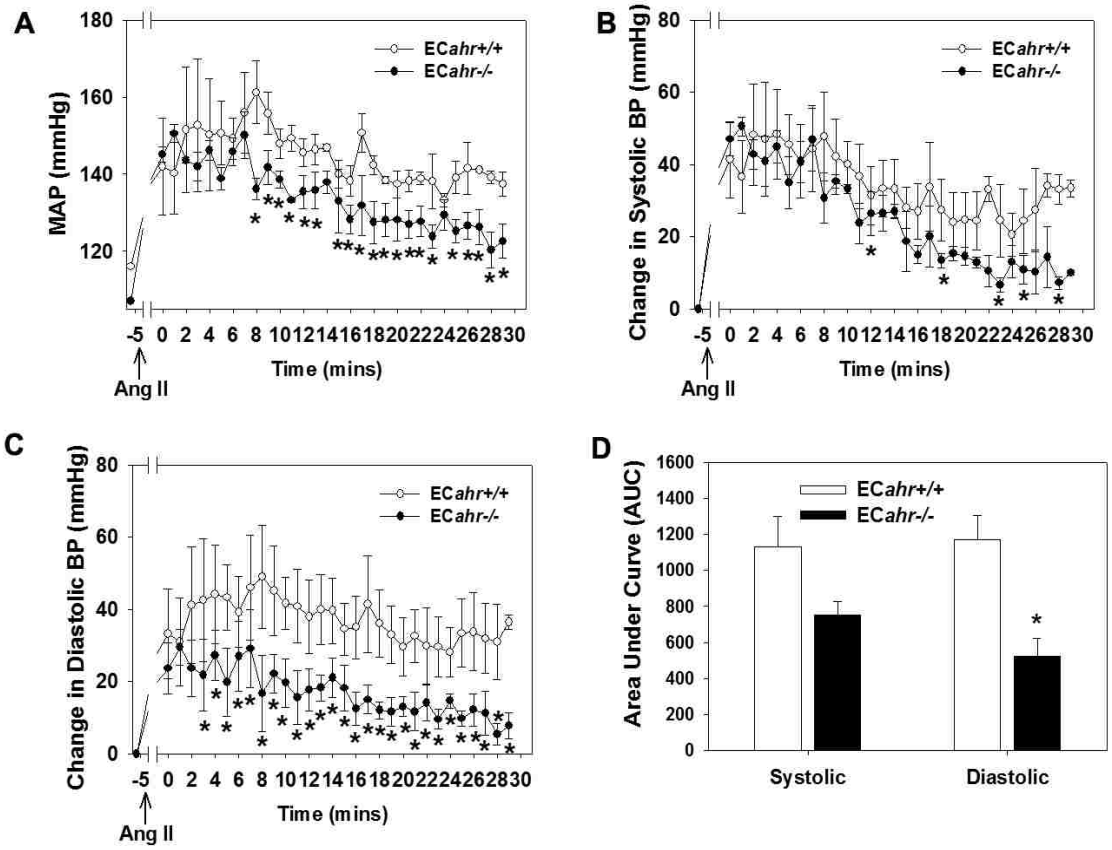

Figure 2.4. Loss of *ahr* in endothelium attenuates RAS responsiveness *in vivo*. (A) MAP response, (B) change in systolic, (C) change in diastolic blood pressure, and (D) area under curve analysis, for 30 min following *i.p.* injection of Ang II (30 µg/kg). Blood pressure was recorded starting after 5 mins of Ang II administration to exclude handling as a confounding factor. Data represent mean ± SEM and were analyzed by two-way, repeated measures ANOVA, using post hoc Holm-Sidak comparisons; *$p < 0.05$ compared to EC*ahr*$^{+/+}$ (Fig. A, B, and C). Data in panel (D) were analyzed by student t-test *$p < 0.05$ compared to EC*ahr*$^{+/+}$ (n=4/genotype).

Inhibition of RAS on blood pressure

To further elucidate the contribution of the RAS to the hypotension in EC*ahr*$^{-/-}$ mice, we investigated the responsiveness of EC*ahr*$^{-/-}$ and EC*ahr*$^{+/+}$ mice to an ACEi. We found that captopril significantly decreased MAP, SBP and DBP in mice of both genotypes after 5 d of treatment. While the decrease tended to be greater in EC*ahr*$^{+/+}$ mice during the first days of treatment, it was not statistically different than the drop seen in EC*ahr*$^{-/-}$ mice (Fig. 2.5A, B and C). Interestingly, during the 4 days of washout after drug treatment stopped, MAP and DBP remained significantly lower and did not return to baseline in EC*ahr*$^{-/-}$ mice, compared to EC*ahr*$^{+/+}$ mice (Fig. 2.5A, C and D). To determine if any components of the systemic RAS or indices of RAS activity, such as salt and water balance were altered, we evaluated PRA, ACE activity, plasma electrolytes and urine osmolality. We found that all, except plasma K, were similar between EC*ahr*$^{-/-}$ and EC*ahr*$^{+/+}$ mice, and although plasma K was slightly reduced in EC*ahr*$^{-/-}$ mice it was still within normal physiological limits (4.0 - 7.0 mM) (Table 2.2).

mRNA analysis of RAS components from adipose and aorta

To determine if tissue RAS components were altered in their expression, we measured mRNA of renin, angiotensinogen (Agt) and AT1R in visceral white adipose, aortic PVAT, and in aortas cleaned of adipose tissue. We found that Agt mRNA was significantly increased in aortic PVAT in EC*ahr*$^{-/-}$ mice, but not altered in either visceral white adipose or the aorta proper, compared to EC*ahr*$^{+/+}$ mice (Fig. 2.6A). In addition, both renin and AT1R mRNA was significantly reduced in visceral adipose from EC*ahr*$^{-/-}$

mice, compared to EC*ahr*$^{+/+}$ mice, but not altered in aortic PVAT or the aorta (Fig. 2.6B and C).

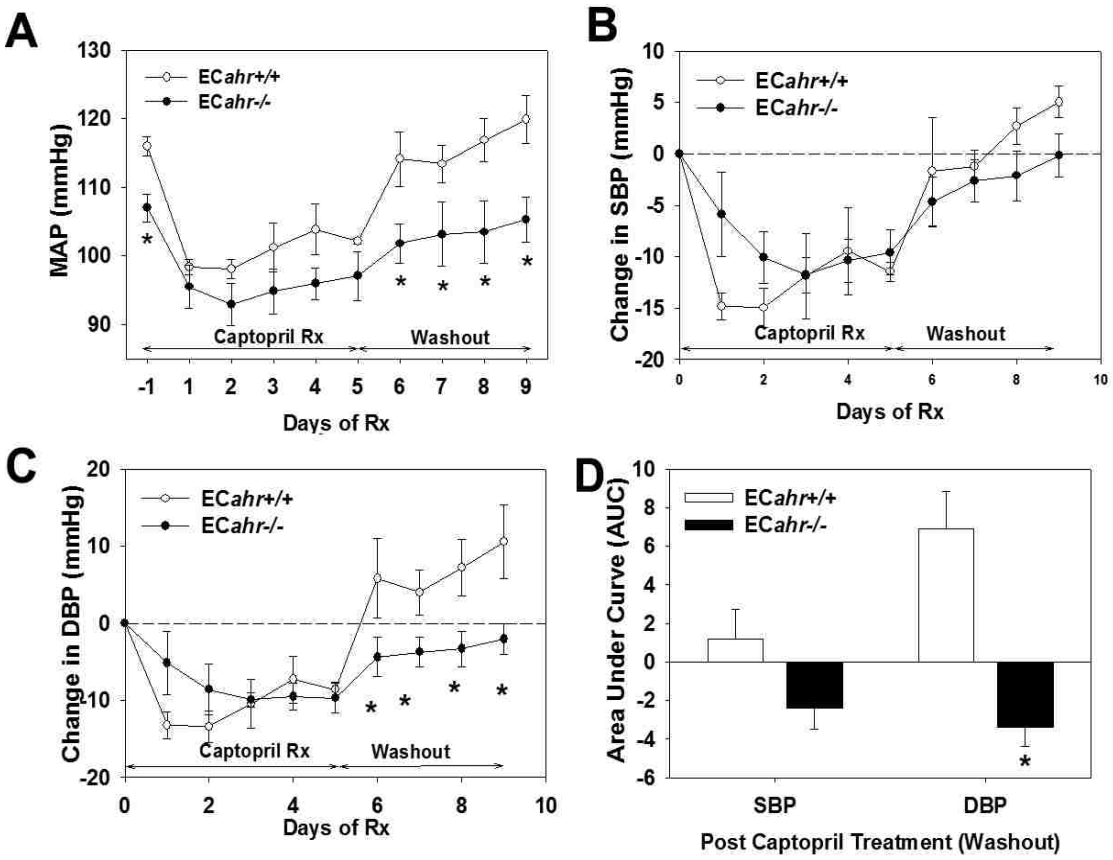

Figure 2.5. Loss of *ahr* in endothelium attenuates the contribution of Ang II to basal blood pressure. (A) MAP response, (B) change in diastolic, and (C) change in systolic blood pressure, following treatment with 4 mg/kg ACEi, captopril, in drinking water for 5 d, followed by a 4 d washout. (D) Area under the curve analysis of systolic and diastolic blood pressure response during washout. Data represent mean ± SEM and were analyzed by repeated measures two-way ANOVA, using post hoc Holm-Sidak comparisons; *$p < 0.05$, compared to EC*ahr*$^{+/+}$ (Fig. A, B and C). Data in panel (D) were analyzed by student's t-test *$p < 0.05$, compared to EC*ahr*$^{+/+}$ (n=4/genotype).

Table 2.2. Indices of the renin-angiotensin system (RAS) in EC*ahr*$^{+/+}$ and EC*ahr*$^{-/-}$ mice.

Parameter	EC*ahr*$^{+/+}$ (n)	EC*ahr*$^{-/-}$ (n)
PRA (ng Ang I/ml/hr)	3.9 ± 0.2 (10)	3.7 ± 0.2 (10)
Plasma ACE (units/L)	196 ± 7 (10)	189 ± 9 (10)
Hematocrit (%)	46. 8 ± 0.6 (9)	44. 9 ± 1.0 (8)
Plasma Na (mM)	148. 4± 0.8 (9)	146. 2 ± 0.9 (8)
Plasma K (mM)	6. 8 ± 0.2 (9)	5. 8 ± 0. 2 (8)*
Plasma Cl (mM)	118. 2 ± 1.2 (9)	115. 4 ± 0.9 (8)
Urine Osmolality (mmol/Kg)	3566.9 ± 216 (9)	3952.1 ± 260 (14)

Values are expressed as mean ± SEM
*$p < 0.05$; n, sample size.

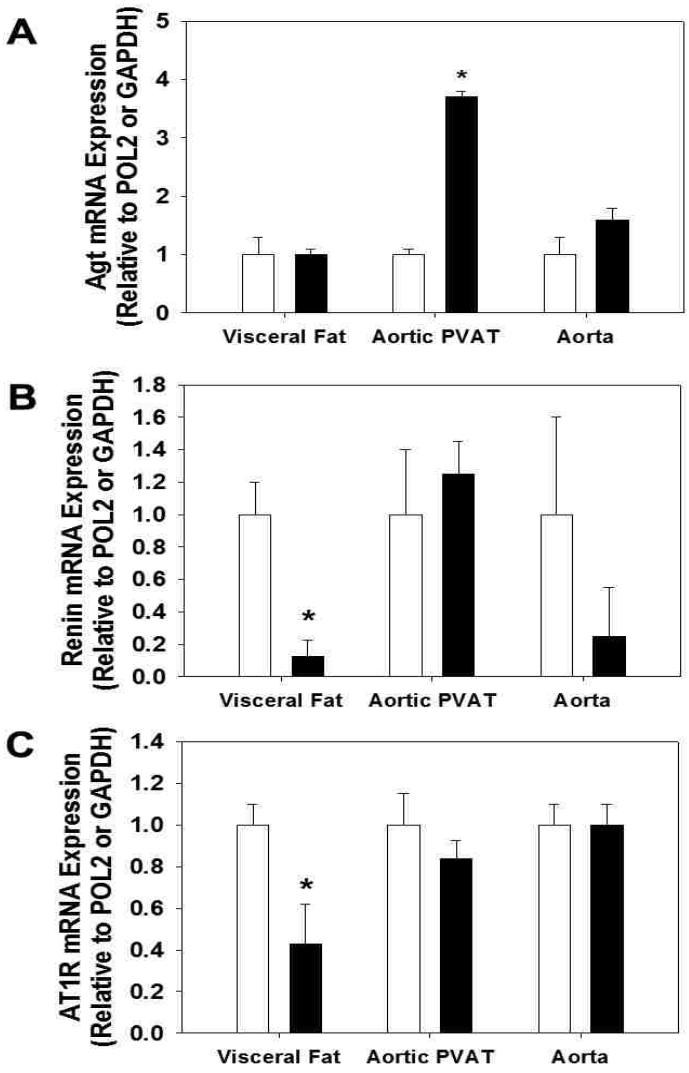

Figure 2.6. Loss of *ahr* in endothelium alters mRNA expression of RAS components in adipose. mRNA quantification of (A) Agt, (B) renin, and (C) AT1R from visceral white adipose, aortic PVAT, and aorta free of PVAT. Data represent mean ± SEM and were analyzed by Student's t-test; $*P < 0.05$, compared to EC*ahr*$^{+/+}$.

AT1R protein expression and aortic reactivity to Ang II

To determine if the decreased responsiveness to Ang II could result from decreased protein expression of the AT1R EC*ahr*$^{-/-}$ mice, we measured AT1R protein expression in aortas cleaned of adipose. We found that AT1R protein expression in the aorta free of adipose was significantly lower in the EC*ahr*$^{-/-}$, compared to EC*ahr*$^{+/+}$ mice (Fig. 2.7A and B). To further determine if vascular reactivity to Ang II was decreased in EC*ahr*$^{-/-}$ mice, and if this was influenced by the presence of PVAT, we examined *ex vivo* abdominal aortic reactivity to two different doses of Ang II in the presence and absence of aortic PVAT. We found that responsiveness of the abdominal aorta to Ang II was completely normal in EC*ahr*$^{-/-}$ mice in the absence of PVAT (Fig. 2.8A). However, we found that the responsiveness of the abdominal aorta to Ang II was significantly attenuated in EC*ahr*$^{-/-}$ mice in the presence of PVAT (EC*ahr*$^{+/+}$; 0.2 ± 0.04 ; EC*ahr*$^{-/-}$: 0.1 ± 0.01, n=11/genotype, $p<0.05$) (Fig. 2.8B).

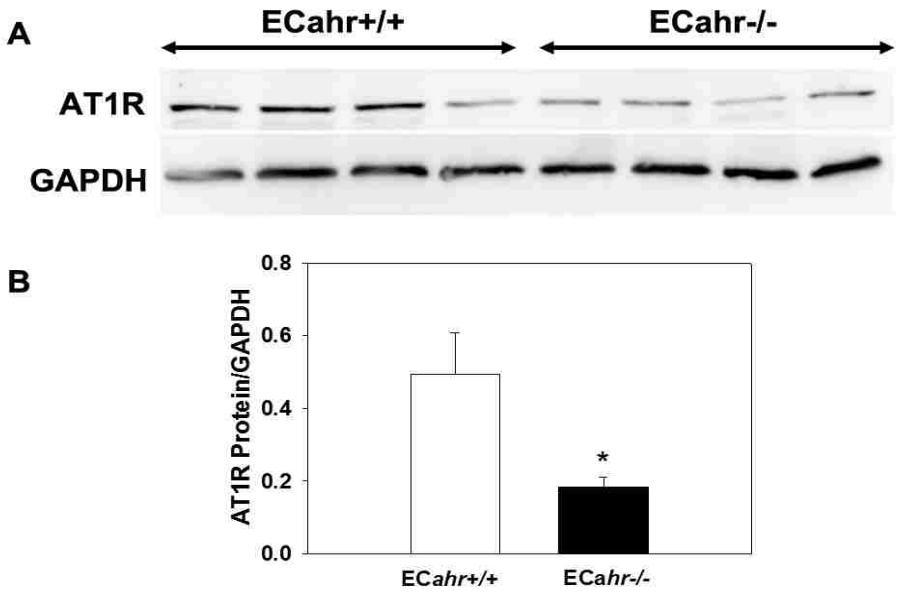

Figure 2.7. Loss of *ahr* in endothelium diminishes AT1R expression in aorta. (A) Representative western blot of abdominal aortic AT1R protein expression. (B) Quantification of AT1R protein expression relative to GAPDH. Data represent mean ± SEM and were analyzed by Student's t-test; $*P < 0.05$, compared to EC*ahr*$^{+/+}$.

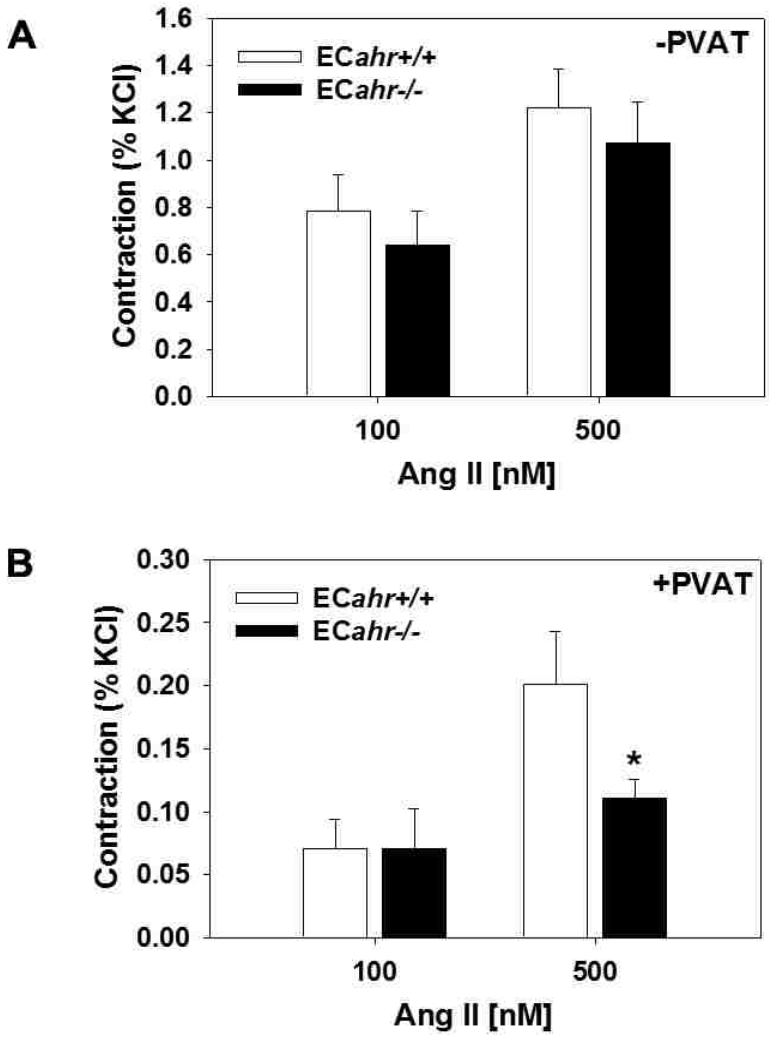

Figure 2.8. Loss of *ahr* in endothelium reduces abdominal aortic reactivity to Ang II in the presence of perivascular adipose tissue (PVAT). (A) Ang II-induced contraction (% KCl) in absence of PVAT. (B) Ang II-induced contraction (% KCl) in the presence of PVAT. (EC*ahr*$^{-/-}$ n=12; and EC*ahr*$^{+/+}$ n=11). Data represent the mean ± SEM and were analyzed by Student's t-test; **P* < 0.05, compared to EC*ahr*$^{+/+}$.

E. DISCUSSION

The findings from our study show for the first time that AHR in the endothelium is critically involved in blood pressure regulation and is required to maintain normal basal levels of blood pressure. Notably, EC*ahr*$^{-/-}$ mice are significantly hypotensive and this phenotype is associated with alter gene expression of tissue RAS components as well as decreased protein expression of vascular AT1R. Further, the hypotension is mediated, in part, by a reduction in vasoconstrictive responsiveness to Ang II, measured both *in vivo* and *ex vivo*. The blood pressure phenotype in EC*ahr*$^{-/-}$ mice is nearly identical to that observed in the global AHR knockout mice, demonstrating that endothelial-expressed AHR is a critical regulator of vascular control of blood pressure and this function cannot be compensated by the normal expression of AHR in other tissues or cell types.

Hypotension can have many physiological etiologies, such as decreases in the contribution of the sympathetic nervous system to vasoconstriction or increases in vascular eNOS expression and NO production. For example, genetic deletion of α1 adrenergic receptors or transgenetic overexpression of vascular eNOS both produces hypotension (Ohashi *et al.*, 1998; van Haperen *et al.*, 2002; Sanbe *et al.*, 2007). However, our data rule out these two possible mechanisms in contributing to the hypotension observed in EC*ahr*$^{-/-}$ mice. Treatment of EC*ahr*$^{-/-}$ mice with the α1 adrenoceptor blocker, prazosin, or the ganglionic blocker, hexamethonium, significantly reduce blood pressure in EC*ahr*$^{-/-}$ mice, suggesting that sympathetic nervous system control of blood pressure is actually enhanced in EC*ahr*$^{-/-}$ mice, rather than reduced. Additionally, neither eNOS expression nor NOx levels are increased in EC*ahr*$^{-/-}$ mice and chronic NOS inhibition increases blood pressure to the same degree in both genotypes.

Taken together these data suggest that increased NO is not responsible for the hypotension in EC*ahr*$^{-/-}$ mice. This observation is consistent with that observed for the global AHR knockout mice (Zhang *et al.*, 2010).

Another mechanism that may mediate hypotension in EC*ahr*$^{-/-}$ mice is a reduction in RAS signaling. Several studies have demonstrated the requirement for the RAS in maintaining basal blood pressure within a normal range. Mice that lack angiotensinogen, ACE, or AT1R, have all been shown to be hypotensive (Kim *et al.*, 1995; Esther *et al.*, 1996; Tsuchida *et al.*, 1998), and our data clearly demonstrate a decrease of Ang II signaling both *in vivo* and *ex vivo*. *In vivo* exposure of EC*ahr*$^{-/-}$ and EC*ahr*$^{+/+}$ mice to an acute dose of Ang II produces an immediate rise in blood pressure in both genotypes; however, this increase is not sustained in the EC*ahr*$^{-/-}$ mice. Further, the steady decline in DBP in EC*ahr*$^{-/-}$ mice after acute Ang II injection suggests a significant reduction in the duration of the vasoconstrictor response. In addition, chronic exposure of EC*ahr*$^{-/-}$ and EC*ahr*$^{+/+}$ mice to an ACEi reduces blood pressure in both genotypes; however, the subsequent increase in DBP after drug treatment is stopped is significantly attenuated in EC*ahr*$^{-/-}$ mice, further suggesting a decrease in response to Ang II-mediated vasoconstriction. These *in vivo* data are further supported by *ex vivo* vasoreactivity data that show abdominal aortas from EC*ahr*$^{-/-}$ mice are significantly less responsive to Ang II-mediated constriction in the presence of PVAT. It is notable that although Ang II responsiveness is reduced, other indices of RAS activity are normal, including PRA and ACE activity, renin, angiotensinogen, and plasma Ang II. Taken together these data suggest that downstream signaling of Ang II is reduced.

One mechanism by which Ang II-mediated vasoconstriction could be reduced is by a reduction in receptor expression. Both pharmacological blockade of AT1R and genetic deletion of AT1R reduce blood pressure (Kim *et al.*, 1995; Iyer *et al.*, 1996; Lu *et al.*, 1997). Our data show that loss of endothelial AHR significantly reduces white adipose expression of AT1R mRNA as well as aortic expression of AT1R protein. The mechanism by which AHR deficiency reduces AT1R expression is not known. The AHR regulates gene expression via binding to dioxin response elements (DRE) containing the core recognition motif 5'-GCGTG-3'(Swanson *et al.*, 1995). Putative DREs are located in the promoter sequence of both the mouse AT1a and AT1b receptors, supporting the plausibility that expression of the mouse AT1R could be directly regulated by AHR. This is further supported by the fact that activation of the AHR by exogenous ligands sensitizes mice to Ang II-mediated hypertension (Aragon *et al.*, 2008), and induces AT1R mRNA expression in mesenteric arteries (unpublished data). Further, physiological shear stress has been shown to activate the AHR (Eskin *et al.*, 2004; Han *et al.*, 2008; Conway *et al.*, 2009), and to increase AT1R expression (Lindstedt *et al.*, 2009), providing indirect evidence that AHR may contribute to the regulation of AT1R expression. Additionally, the AHR interacts with several other transcription factors including E2F1, TFIIE, TFIIB, as well as coactivators like CREB-binding protein, CBP/p300 and nuclear receptor-interacting protein 1 (RIP140) (Swanson and Yang, 1998; Hankinson, 2005) and thus alteration in AT1R expression could result from crosstalk with other signaling pathways.

Despite the observed reduction in vascular AT1R expression, this is unlikely to be the sole explanation for the hypotensive phenotype observed in EC*ahr*$^{-/-}$ mice, since vasoreactivity to Ang II *ex vivo* is not significantly attenuated in the absence of PVAT.

Rather, a significant decrease in vasoconstriction to Ang II is only observed in EC*ahr*$^{-/-}$ mice in the presence of PVAT. It is possible that loss of AHR from the endothelium might alter the paracrine signaling between that occurs between the microcirculation and the adipose, including PVAT. Both renin and AT1R mRNA were significantly decreased in expression in visceral white adipose, which might contribute to a reduction in Ang II release from the adipose and a shift in the balance between vasoconstrictors and vasodilators released from adipose. It has been shown that stimulation of adipose AT1R by Ang II acts in a feedforward mechanism to increase adipocyte release of Ang II (Takemori *et al.*, 2007). It is also possible the loss of AHR from the endothelium increases vasodilators released from adipose. These dilators could include the newly discovered hydrogen sulphide gas (H_2S) generated by cystathionine gamma lyase enzyme (CSE) (Yang *et al.*, 2008; Fang *et al.*, 2009)as well as adipocyte-derived relaxing factor, adiponectin, leptin, omentin, and interleukin-6 (Fesus *et al.*, 2007; Sahin and Bariskaner, 2007; Yamawaki *et al.*, 2010). Taken together, the deregulation of the RAS in adipose associated with diminished AT1R expression in the vasculature might drive the subsequent hypotension observed in the EC*ahr*$^{-/-}$ mice.

The *ahr* floxed mice (*ahr*$^{fx/fx}$), which were our genetic control in these studies, harbor the low affinity, ahr^{d} allele, derived from the DBA-2 strain (Poland and Glover, 1980). In contrast, the *ahr*$^{+/+}$ mice used as a genetic control in previously published studies harbor the high affinity, ahr^{b1} allele. Thus, we cannot directly compare the blood pressure phenotype of the EC*ahr*$^{-/-}$ mice and *ahr*$^{-/-}$ mice. Nevertheless, the blood pressure phenotype of the EC*ahr*$^{-/-}$ and the *ahr*$^{-/-}$ mice, compared to their respective wildtype controls, shares many similarities. First, hypotension is a hallmark of both of these mouse

models (Zhang *et al.*, 2010), where the *ahr*$^{-/-}$ mice exhibit a 14% lower MAP, compared to *ahr*$^{+/+}$mice, while EC*ahr*$^{-/-}$ mice exhibit an 8% lower MAP, compared to EC*ahr*$^{+/+}$ mice. Second, the resultant hypotension in both EC*ahr*$^{-/-}$ and the *ahr*$^{-/-}$ mice is not mediated by an increase in NO production. Third, both EC*ahr*$^{-/-}$ and the *ahr*$^{-/-}$ mice exhibit a reduced responsiveness to the RAS without apparent changes in indices of RAS activation, suggesting that the RAS contributes less in maintaining basal blood pressure in both the EC*ahr*$^{-/-}$ and *ahr*$^{-/-}$ mice (Zhang *et al.*, 2010).

Finally, EC*ahr*$^{-/-}$ and *ahr*$^{-/-}$ mice also share some fundamental similarities related to in changes in organ weight. The *ahr*$^{-/-}$ mice exhibit decreased liver size, as well as increased weight of heart and kidneys (Lund *et al.*, 2006; Zhang *et al.*, 2010). In our study, EC*ahr*$^{-/-}$ mice also exhibit a decreased liver size, as well as increased weight of heart and kidneys. While the reduction in liver weight has been attributed to the persistent ductus venosus and reduced hepatocyte size (Lahvis *et al.*, 2000; Lahvis *et al.*, 2005), the reasons for the increases in heart and kidney weight have not been firmly established. The increased heart weight might reflect a compensatory response to increase cardiac output in an attempt to normalize blood pressure, hence a physiological hypertrophy (Vasquez *et al.*, 2003), while increased kidney weight may result from altered developmental vascularization (Lahvis *et al.*, 2000). Nonetheless, our study demonstrates that these organ weight changes result from loss of AHR solely from the endothelium.

The mechanism by which AHR regulates blood pressure remains to be fully determined; however, our study establishes that AHR expression in the endothelium is particularly critical to normal vascular responsiveness to Ang II and thus basal blood pressure control. Since the RAS is not only essential to the physiological regulation of

basal blood pressure but also a primary pathological mediator of hypertension, the AHR signaling pathway could represent an important novel mechanism to influence RAS activity and to control blood pressure. Future studies are needed, however, to identify the specific AHR genes that mediate these changes in RAS responsiveness and that influence the vascular responsiveness in the context of adipose tissue.

SUPPLEMENT DATA

Endothelial cell-specific aryl hydrocarbon receptor knockout mice exhibit hypotension mediated, in part, by an attenuated angiotensin II responsiveness.

Larry N. Agbor, Khalid M. Elased, and Mary K. Walker. Biochem Pharmacol 5: 514–523, 2011.

RNA isolation and qPCR analysis.

Aortic eNOS mRNA was analyzed from total RNA by quantitative real time PCR using an Icycler (Bio-Rad), with PGK gene as an internal normalization control. Total RNA was isolated from aortas with RNeasy Fibrous Tissue Mini Kit (Qiagen, GmbH, Germany). cDNA was synthesized using iScript Select cDNA Synthesis Kit (Bio-Rad Laboratories,Hercules, CA) with the supplied random primers and 250 ng RNA. PCR amplification was performed using an iCycler (Bio-Rad Laboratories) with a reaction mixture comprised of iQ SYBR Green Supermix (Bio-Rad Laboratories) with 500 µM sense and antisense primers, and 250 pg cDNA. Cycle threshold data for the target gene and reference, PGK, were used to calculate mean normalized expression.

Protein extraction and western blot.

Aortas were homogenized in RIPA buffer (Santa Cruz Biotechnology), homogenate frozen at -80 °C for 15 min, sonicated for 10 s and centrifuged at 15,000 x g 4 °C for 10 min. Protein concentration was measured using Bio-Rad protein assay (Bio-Rad Laboratories). A 20 µg aliquot of protein was mixed with 2× loading buffer (100 mM pH6.8 Tris-HCl, 4% sodium dodecyl sulfate, 0.2% bromophenol blue, 20% glycerol, 200 mM dithiothreitol) and denatured at 95 °C for 5 min. Denatured samples were subjected to electrophoresis on 7.5% Tris-HCL polyacrylamide gel at 150 V for 1 hour in running buffer (25 mM Tris-base, 150 mM glycine, 0.1% sodium dodecyl sulfate) and separated proteins were transferred to polyvinylidene fluoride (PVDF) membrane (Bio-Rad Laboratories) at 100 V for 1 hour in cold transfer buffer (20 mM Tris-base, 150 mM glycine, 20% methanol). The membrane was washed with Tris-buffered saline (TBST,

0.8% NaCl, 0.02% KCl, 0.3% Tris-base, 0.05% Tween-20, pH7.4) and blocked for 1 hour in 5% nonfat dry milk in TBST. The blocked membrane was incubated with mouse anti-eNOS antibody (1:2000, Catalogue No. 610296, BD Transduction Laboratories, San Jose, CA) at 4 °C overnight, washed with TBST, and incubated with horseradish peroxidase (HRP) conjugated goat anti-mouse (Southern Biotech, Birmingham, AL) for 1 hour at room temperature. The membrane was washed with TBST and developed for 10 min with 1 mL chemiluminescence reagent (Perkin-Elmer, Waltham, MA) under KODAK Image Station 4000MM digital imaging system (Perkin-Elmer). The membrane was stripped (7 M guanidine hydrochloride, 0.75% KCl, 0.38% glycine, 50 µM EDTA, 0.14% 2-mercaptoethanol, pH10), washed with TBST, reblocked, and incubated with mouse glyceraldehyde-3-phosphate dehydrogenase (GAPDH) (Millipore, Billerica, MA, USA) overnight, washed with TBST, incubated with HRP-conjugated goat anti-mouse IgG (Southern Biotech), washed and developed as above. Protein quantification was done using Image J software (National institute of Health, USA)

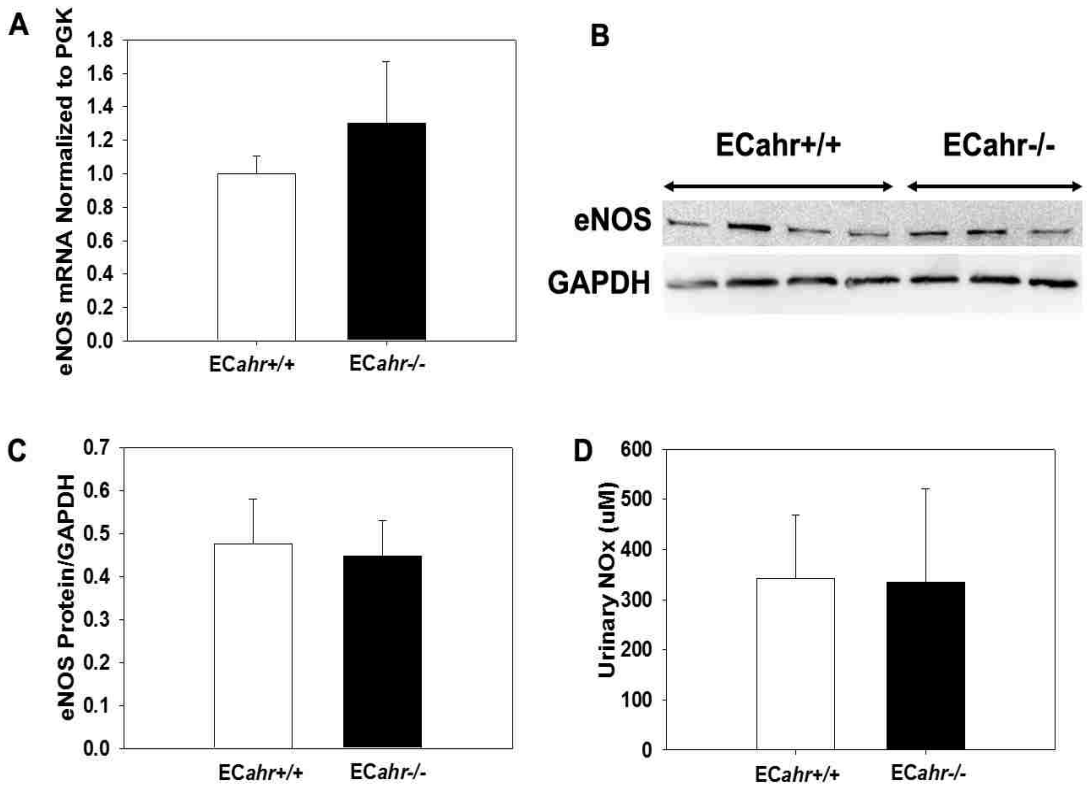

Figure. 2.1S. Hypotension in EC*ahr*$^{-/-}$ mice is not associated with increased eNOS expression nor increased NO bioavailability. (**A**) Aortic eNOS mRNA from EC*ahr*$^{-/-}$ and EC*ahr*$^{+/+}$ mice as measured by qPCR and normalized to PGK. (**B**) Representative western blot of total eNOS protein expression from aorta, (**C**) quantification of total eNOS protein expression relative to GAPDH, and (**D**) urinary NOx of EC*ahr*$^{+/+}$ and EC*ahr*$^{-/-}$ mice (n=5/genotype) . Data represent mean ± SEM and were analyzed by Student's t-test.

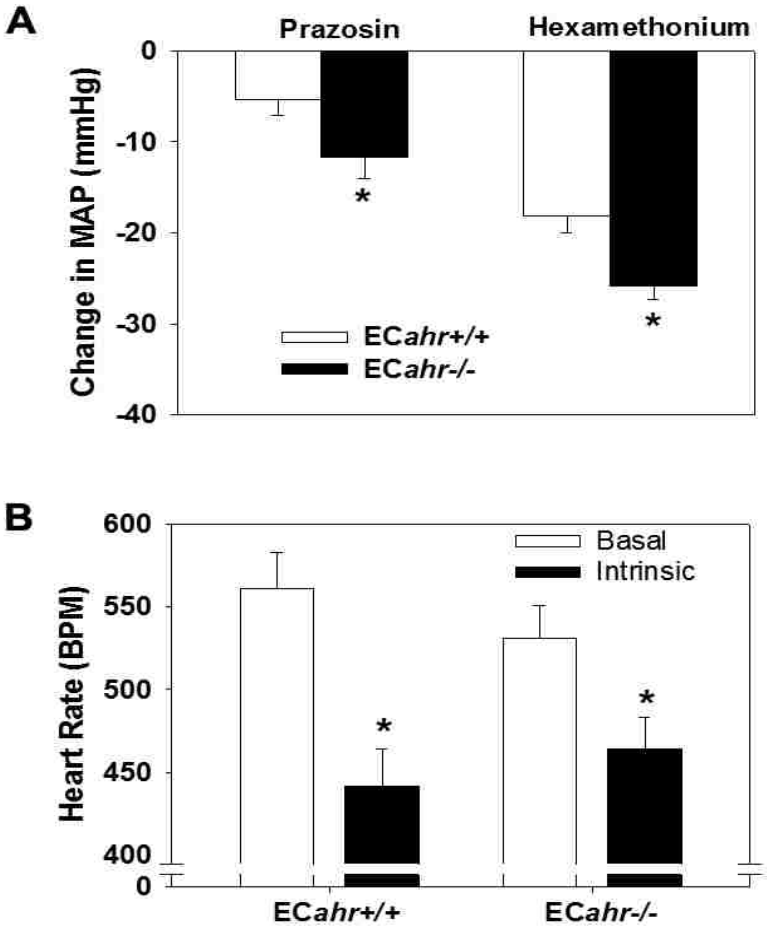

Figure. 2.2S. Loss of AHR in endothelial cells enhances sympathetic innervation to the vasculature. (**A**) Change in blood pressure following prazosin and hexamethonium treatment was calculated by averaging readings for 30 mins after injections, and expressed as change from baseline MAP. (**B**) Basal and intrinsic heart rate following hexamethonium injection. Data represent mean ± SEM and were analyzed by Student's t-test; *$p < 0.05$, compared to EC*ahr*$^{+/+}$, n=5/genotype.

Table 1S: Real Time PCR primer sequences

Gene	Sense primer	Antisense primer (s)
DNA Polymerase 2 (POL2)	TGACTCACAAACTGGCTGACATT	TACATCTTCTGCTATGACATGGGC
AT1R	GGGCGTCATCCATGACTGTAAA	TTCCCCAGAAAGCCGTAAAACA
Glyceraldehyde 3-phosphate dehydrogenase (GAPDH)	CCAATGTGTCCGTCGTGGATC	TGTAGCCCAAGATGCCCTTCA
Renin	ATGAATATGTTGTGAGCTGTAGCC	GTCTCTCCTGTTGGGATACTGTAG
Angiotensinogen	CACTCATTTGTTCAGAGCCTGG	GTTCATCTTCCACCCTGTCACA
Cre recombinase (cre)	TGCCTGCATTACCGGTCGATGC	CCATGAGTGAACGAACCTGGTCG
Aryl hydrocarbon receptor genotyping primers (*ahr*$^{fx/fx}$)	GTCACTCAGCATTACACTTTCTA	CAGTGGGAATAAGGCAAGAGTGA/ /GGTACAAGTGCACATGCCTGC
Endothelial nitric oxide Synthase (eNOS)	GCCAAAGTGACCATAGTGGACC	TTCTGCTCATTTTCCAGGTGCTT

Table 2S: Adipose weights of 2-month-old male EC*ahr*$^{+/+}$ and EC*ahr*$^{-/-}$ mice.

Adipose	EC*ahr*$^{+/+}$ (n=8)	EC*ahr*$^{-/-}$ (n=5)
Mesentery (mg)	65.7 ± 5.9 (0.249 ± 0.02)†	44.1 ± 8.9 (0.177± 0.01)†
Perirennal (mg)	123.6 ± 9.5 (0. 107 ± 0. 008)	91.6 ± 4.3 (0.125 ±0.02) †
PVAT (mg)	28.1 ± 2.1 (0.469 ± 0.03)†	31.0 ± 4.9 (0.369 ± 0.04)†

Values are expressed as mean ± SEM
† (Adipose/body weight ratio x 100)
Legend: PVAT, Perivascular adipose tissue.

III. CHAPTER 3

Elevated blood pressure in cytochrome P4501A1 (CYP1A1) knockout mice is associated with reduced vasodilation to omega-3 polyunsaturated fatty acids.

In preparation for submission to Toxicology and Applied Pharmacology

A. ABTRACT

Cytochrome P4501A1 (CYP1A1) metabolizes omega-3 polyunsaturated fatty acids (n-3 PUFAs); eicosapentaenoic acid (EPA) and docosahexaenoic acid (DHA), to potent vasodilators *in vitro*. Although CYP1A1 is constitutively expressed in the vasculature, its role in regulating vascular tone and blood pressure (BP) has not been investigated. Thus, we tested the hypothesis that global genetic deletion of CYP1A1 will result in reduced vasodilatory responses to n-3 PUFAs and increases in BP. We assessed BP by radiotelemetry in CYP1A1 wild type (WT) and knockout (KO) mice ± nitric oxide synthase (NOS) inhibitor (N^{ω}-nitro-L-arginine). Acetylcholine (ACh), EPA, DHA, 19,20-epoxydocosapentaenoic acid (19,20-EDP), and 17,18-epoxyeicosatetraenoic acid (17,18-EEQ)-mediated vasorelaxation was assessed in the aorta and first order mesenteric arterioles. Further, S-nitroso-N-acetylpenicillamine (SNAP)-mediated relaxation was assessed in endothelium-disrupted aorta and DHA-mediated relaxation was assessed in mesenteric arterioles ± inhibitors of the voltage-gated (Kv), and large conductance, calcium-activated potassium channels (BK). We found that CYP1A1 KO mice were hypertensive, compared to WT mice (mean arterial pressure in mmHg, WT 103±1, KO 116±1; systolic BP: WT 114±1, KO 124±1; diastolic BP: WT 93±1, KO 108±1, n=5/genotype, $p<0.05$), and exhibited a reduced HR (in beats per minute, WT 575±5; KO 530±7; $p<0.05$). Nonetheless, CYP1A1 KO mice exhibited normal responses to NOS inhibition and aortic vasorelaxation to ACh and SNAP, suggesting that hypertension is not associated with loss of NO. Conversely, CYP1A1 KO mice exhibited significant attenuation to EPA and DHA-mediated vasodilation in mesenteric arterioles and aorta, but normal vasodilatory responses to putative CYP1A1 metabolites of EPA and DHA, 17,18-

EEQ and 19,20-EDP . Lastly, inhibition of Kv and BK channels significantly inhibited DHA-mediated vasodilation in mesenteric arterioles. These data suggest that constitutive CYP1A1 expression has a physiologically important role in the regulation of vascular function and blood pressure, which may involve vasodilatory responses to n-3 PUFAs.

B. INTRODUCTION

Omega-3 polyunsaturated fatty acids (n-3 PUFAs) are metabolized by numerous cytochrome P450s into several products that have potent vasodilatory properties (Schwarz *et al.*, 2004; Schwarz *et al.*, 2005). Some of these metabolites have been recognized to play key roles in contributing to underlying vascular tone, BP, and overall cardiovascular health (Billman *et al.*, 1994; Engler *et al.*, 1999; Menotti *et al.*, 1999; Blanchet *et al.*, 2000). Nonetheless, the contribution of specific P450s to the regulation of vascular tone and BP via n-3 PUFA metabolism remains poorly understood.

Cytochrome P4501A1 (CYP1A1) is one P450 shown to metabolize n-3 PUFAs to vasodilatory products. CYP1A1 is constitutively expressed in vascular endothelium with CYP1A1 mRNA and protein levels detected in cultured human umbilical vein endothelial cells as well as in endothelial cells of the mouse descending thoracic aorta, and human coronary arteries (Eskin *et al.*, 2004; Han *et al.*, 2008; Conway *et al.*, 2009). In addition to its basal expression in the endothelium, CYP1A1 is also induced in the endothelium by physiological levels of shear stress (Han *et al.*, 2008; Conway *et al.*, 2009). Physiological laminar shear stress is considered to be anti-atherogenic (Cunningham and Gotlieb, 2004). It significantly induces antioxidants, antithrombotic factors, and vasodilators, such as nitric oxide (NO) and prostacyclin, and suppresses prothrombotic substances and vasoconstrictors. This raises the possibility, as suggested by Conway *et al.* (2009) and De Caterina and Madonna (2009), that physiological induction of CYP1A1 in the endothelium could also contribute to the anti-atherogenic phenotype and that this may be mediated via metabolism of PUFAs. Parallel increases in CYP1A1 and NO have also been observed in

cultured endothelial cells treated with an aryl hydrocarbon receptor agonist (Lim *et al.*, 2007).

As noted above, evidence from several studies show that CYP1A1 metabolizes two major n-3 PUFAs, eicosapentaenoic acid (EPA) and docosahexaenoic acid (DHA), in a stereospecific manner. Human CYP1A1 epoxidizes the 17,18-olefinic bond of EPA in a regiospecific manner to form mainly 17(R),18(S)-epoxyeicosatetraenoic acid [(17(R),18(S) EEQ)] (Schwarz *et al.*, 2004). CYP1A1 also exclusively epoxidizes the 19,20-olefinic bond of DHA, producing 19(R),20(S)-epoxydocosapentaenoic acid [19(R),20(S)-EDP] (Fer *et al.*, 2008; Lucas *et al.*, 2010). Furthermore, both of these metabolites, 17,18-EEQ and 19,20-EDP, are potent vasodilators in the microcirculatory vessels of the pig and/or mouse (Zhang *et al.*, 2001), and 17,18-EEQ causes relaxation and hyperpolarization of pulmonary artery smooth muscle (Morin *et al.*, 2009). Studies have identified a variety of downstream mechanisms that mediate this vasodilation, including increases in NO signaling (Ma *et al.*, 2004; Li *et al.*, 2007a; Stebbins *et al.*, 2008) as well as activation of potassium channels on vascular smooth muscle cells (Lauterbach *et al.*, 2002; Ye *et al.*, 2002; Wang *et al.*, 2011).

Taken together, these data suggest that CYP1A1 could metabolize DHA and EPA as substrates *in vivo* into vasodilatory metabolites that act via NO or potassium channel activation. Thus, we sought to determine the degree and mechanism by which CYP1A1 contributes to vascular responses to n-3 PUFAs and to BP regulation. We used CYP1A1 wild type (WT) and knockout (KO) mice to test the hypothesis that global genetic deletion

of CYP1A1 will result in reduced vasodilatory responses to n-3 PUFAs and increases in BP.

C. METHODS

Chemicals

Acetylcholine (ACh), phenylephine (PE), N^{ω}-nitro-L-arginine (LNNA), S-nitroso-N-acetyl penicillamine (SNAP), 4-aminopyridine, iberiotoxin, and all ingredients of physiological saline solution (PSS) and HEPES-PSS were purchased from Sigma–Aldrich (St. Louis, MO). EPA, DHA, 17,18-EEQ, 19,20-EDP and U46619 were purchased from Cayman Chemical (Ann Arbor, MI). Ionomycin was purchased from EMD Millipore Chemicals (San Diego, CA).

Animals

CYP1A1 KO mice, backcrossed more than eight generations onto the C57BL/6J background, were generously provided by Dr. Daniel Nebert (University of Cincinnati) and were bred at the University of New Mexico (Dalton *et al.*, 2000). Age-matched C57BL/6J mice served as WT controls. Animals were housed in a temperature-controlled environment receiving standard mouse chow and water *ad libitum*. All animal protocols were approved by the University of New Mexico Animal Care and Use Committee and the investigations conform to the Guide for the Care and Use of Laboratory Animals published by the U. S. National Institutes of Health (NIH Publication No. 85-23, revised 1996). When tissues were harvested and organ weight determined, mice were anesthetized with ketamine (80 mg/kg)/xylazine (4 mg/kg). The heart was removed, atria were dissected, and the total ventricle weight measured. The right ventricle was dissected and the left ventricle and ventricular septum measured. Kidneys and liver weights were also measured. All tissues were frozen at −80°C.

In vivo analysis of blood pressure

Arterial BP and heart rate (HR) were measured using radiotelemetry in 4-5 month-old CYP1A1 WT and KO male mice (Data Sciences International, St. Paul, MN, USA) as previously described (Lund *et al.*, 2008), using PA-C10 radiotelemeters. Mice were allowed to recover from surgery for 7 d prior to data collection. BP, including systolic, diastolic, mean and pulse pressures, and HR were collected for 7 d before drug treatments began. BP was recorded for 10 s every 15 min during baseline measurements. After basal BP was measured, all mice were treated with LNNA in the drinking water (250 mg/L) for one week followed by one week of washout (Duling *et al.*, 2006).

Aortic vasoreactivity analysis

Mice were anesthetized with ketamine (80 mg/kg)/xylazine (4 mg/kg) and euthanized by exsanguinations. Either the thoracic or abdominal aorta was removed, depending on the study, and placed in ice-cold physiological saline (PSS) containing 130 mM NaCl, 4.7 mM KCl, 1.2 mM KH_2PO_4, 1.2 mM $MgSO_4$, 15 mM $NaHCO_3$, 5.5 mM glucose, 26 mM $CaNa_2EDTA$, 1.8 mM $CaCl_2$, pH 7.4, and cleaned of connective tissue and adventitial fat. The vessel was cut into 3 mm segments and individual rings were suspended in an organ bath containing PSS at 37 ^{0}C bubbled with 21% O_2, 6% CO_2, balanced N_2. The rings were attached to a force transducer (Grass Technologies, West Warwick, RI) with steel hangers and resting tension was increased stepwise to 1.5 g over 1 h. In thoracic aorta, after an initial contraction with 10 mM PE followed by relaxation with 10 mM ACh, dose-response curves to PE (0.001–10 mM), or PE following a 30 min preincubation with the NOS inhibitor, LNNA (100 µM) was performed. An ACh dose-

response (0.001–10 mM) was also conducted in the thoracic aorta following preconstriction with PE (30 µM). In endothelium-disrupted thoracic aorta, a dose-response to the NO donor, SNAP (0.001–10 mM) was also conducted. In abdominal aorta, DHA and EPA dose-response studies (0.001–10 mM) were conducted following preconstriction with the thromboxane A2 mimetic, U46619. Lastly, dose-response curves to 17,18-EEQ, and 19,20-EDP (10^{-5}-10 nM) were conducted in the abdominal aorta preconstricted with U46619.

Mesenteric vasoreactivity analysis

Mice were administered heparin (10 µl/g of 1000 U/ml) by intraperitoneal injection for 5 min, anesthetized with ketamine (80 mg/kg)/xylazine (4 mg/kg), and euthanized by exsanguination. The intestine together with mesenteric arteries were quickly excised and placed in HEPES-PSS solution (134 mM NaCl, 6.0 mM KCl, 1 mM $MgCl_2$, 2 mM $CaCl_2$, 10 mM HEPES, 0.026 mM EDTA, 10 mM glucose, and buffered to pH 7.4 with NaOH). The tissue was then pinned to the bottom of a petri dish, and a long segment of a first-order branch of the mesenteric artery was cleared from surrounding adipose tissue and dissected. The artery was transferred to the chamber of a pressure myograph system (DMT -110 systems, Danish Myo Technology, Ann Harbor, MI) for cannulation. The chamber was filled with warm PSS at 37 ^{0}C bubbled with 21% O_2, 6% CO_2, balanced N_2 (130 mM NaCl, 4.7 mM KCl, 1.18 mM KH_2PO_4, 1.17 mM $MgSO_4$, 14.9 mM $NaHCO_3$, 5.5 mM glucose, 26 µM $CaNa_2EDTA$, and 1.8 mM $CaCl_2$, pH 7.4). One end of the vessel was cannulated with the outflow pipette and tied securely with 10-0 ethilon surgical silk thread. The other end of the vessel was then cannulated with the inflow pipette. The

pressure was then increased by 10 mmHg increment every 5 mins to a maximum of 40 or 60 mmHg, and the artery allowed to equilibrate for 30 min. After equilibration, baseline internal diameter (WT 167.9 ± 3.3, KO 171.7± 3.1) was measured using edge detection software (MyoView acquisition software, DMTVAS 6.2.0.59 Danish Myo Technology, Ann Harbor, MI). In other vessels, passive internal diameter (WT 178.3 ± 5.1, KO 181.4 ± 2.0) was also determined after preincubation with the calcium ionophore, ionomycin (10 µM) for 15 mins. Viability of the arteries was tested by constriction to 60 mM KCl and vessels that failed to constrict to 30% of baseline internal diameter were discarded. After a PSS wash, the artery was allowed to return to baseline diameter and to rest for at least 15 min. Arteries were then preconstricted to 45% of internal diameter with U46619, and a dose-response to EPA (0.001–100 mM) and DHA (0.001–100 mM) conducted. In other vessels, a DHA dose-response was conducted after preincubation with 100 nM Iberiotoxin (IBTX) ± 4-aminopyridine (4-AP) (5 mM). Further, a dose-response to U46619 (0.01-1 µM) was also conducted. Lastly, we assessed dose-responses to 17,18-EEQ and 19,20-EDP (10^{-5} -10 nM). All experiments were performed without luminal flow.

Plasma NOx analyses

Mice were anesthetized with ketamine (80 mg/kg)/xylazine (4 mg/kg) and euthanized by exsanguination. Plasma was collected from whole blood using heparinized syringes. Plasma nitrate/nitrite levels (NOx) were measured using the Griess colorimetric assay (Cayman Chemical).

mRNA analysis of potassium channel subunits, CYP2C29, CYP2E1, CYP2D6 and COX2

Total RNA was isolated from aorta cleaned of connective tissue and adventitial fat, using Trizol reagent (Invitrogen, Carlsbad, CA, USA). cDNA was synthesized using iScript Select cDNA Synthesis Kit (Bio-Rad Laboratories, Hercules, CA) with the supplied random primers and 250 ng RNA. PCR amplification was performed using an iCycler (Bio-Rad Laboratories) with a reaction mixture comprised of iQ SYBR Green Supermix (Bio-Rad Laboratories) with 500 μM of each forward and reverse primer (Table 3.1). Cycle threshold data for both the target gene of interest and control normalization gene, DNA Polymerase II (POL2) was used to calculate mean normalized expression as previously described (Simon, 2003).

Statistical analysis

Differences between genotypes were analyzed by Student's test. The treatment-related changes in BP and vasoreactivity between genotypes were analyzed by repeated measures, two-way analysis of variance with post hoc Holm-Sidak comparisons; $p < 0.05$ was considered statistically significant.

D. RESULTS

Body and organ weights

We compared body and organ weights of CYP1A1 WT and KO mice. CYP1A1 KO mice exhibited significantly lower body weights, compared with age-matched CYP1A1 WT mice (Table 3.2). All organs weighed from CYP1A1 KO mice, including heart, kidneys and liver, were significantly smaller than WT. When organ weight was normalized to body weight, the liver/body weight and kidney/body weight ratios remained significantly lower in CYP1A1 KO mice, compared to WT mice.

Basal blood pressure, heart rate, and activity

BP of CYP1A1 WT and KO mice was measured by radiotelemetry. The CYP1A1 KO mice exhibited significantly higher systolic and diastolic BPs, compared to WT (Fig. 3.1A). Corresponding HR was significantly lower in CYP1A1 KO mice, compared to WT (Fig. 3.1B). When assessed over a 24 h light/dark cycle, the increase in systolic BP in CYP1A1 KO mice was evident only at nighttime (Fig. 3.1C). In contrast, diastolic BP was significantly increased in CYP1A1 KO mice throughout the entire 24 h light/dark cycle, although the normal circadian pattern of an increased BP during the night wakeful period was preserved (Fig. 3.1D). The level of activity was comparable between CYP1A1 WT and KO mice over the 24 h light/dark cycle (Fig. 3.1E). Finally, the difference between mean nighttime and mean daytime arterial pressure (MAP) was significantly higher in CYP1A1 KO mice, compared to WT (Fig. 3.1F).

Table 3.1. Real-time PCR primer sequences

Gene	Sense Primer	Antisense Primer
BKα subunit	TCACGGAACTCGCTAAGCC	AATGTGCGTCCCACTGTTTTT
BKβ4 subunit	GCGAAGCTCAGGGTGTCTTAC	CCGGAGACGATGAGGAACAA
Kv1.5 subunit	TCCGACGGCTGGACTCAATAA	GCCTCCTCGGTGATGTTTCT
CYP2C29	TGGTCCACCCAAAAGAAATTGA	GCAGAGAGGCAAATCCATTCA
COX2	TGCCTGGTCTGATGATGTATGCCA	AGTATGTCGCACACTCTGTTGTGCT
CYP2E1	TGCGGAGGTTTTCCCTAAGTA	TGTGCCTCTCTTTGGATGCG
CYP2D6	CCGCCTTCGCTGACCATAC	CGATCACGTTACACACTGCTT

Table 3.2. Gross tissue weight measurements in 4 month-old CYP1A1 WT and KO mice

Weight	CYP1A1 WT (n=5)	CYP1A1 KO (n=5)
Body (g)	29.4 ± 0.4	23.6 ± 0.3*
Heart (mg)	129 ± 4 (0. 439 ± 0. 024) †	107 ± 3* (0. 452 ± 0. 029)
LV+S (mg)	101 ± 4 (0. 343 ± 0. 022)	84.5 ± 3* (0. 356 ± 0. 024)
Kidney (mg)	425 ± 11 (2.13 ± 0. 024)	293 ± 10* (1.54 ± 0. 003) *
Liver (mg)	1671 ± 42 (5.6 ± 0. 014)	1215 ± 31* (5.1 ±0. 089)*

Values are expressed as mean ± SEM
* $p < 0.05$
†(Organ/body weight ratio x 100)
Legend: LV+S, Left ventricle + Septum.

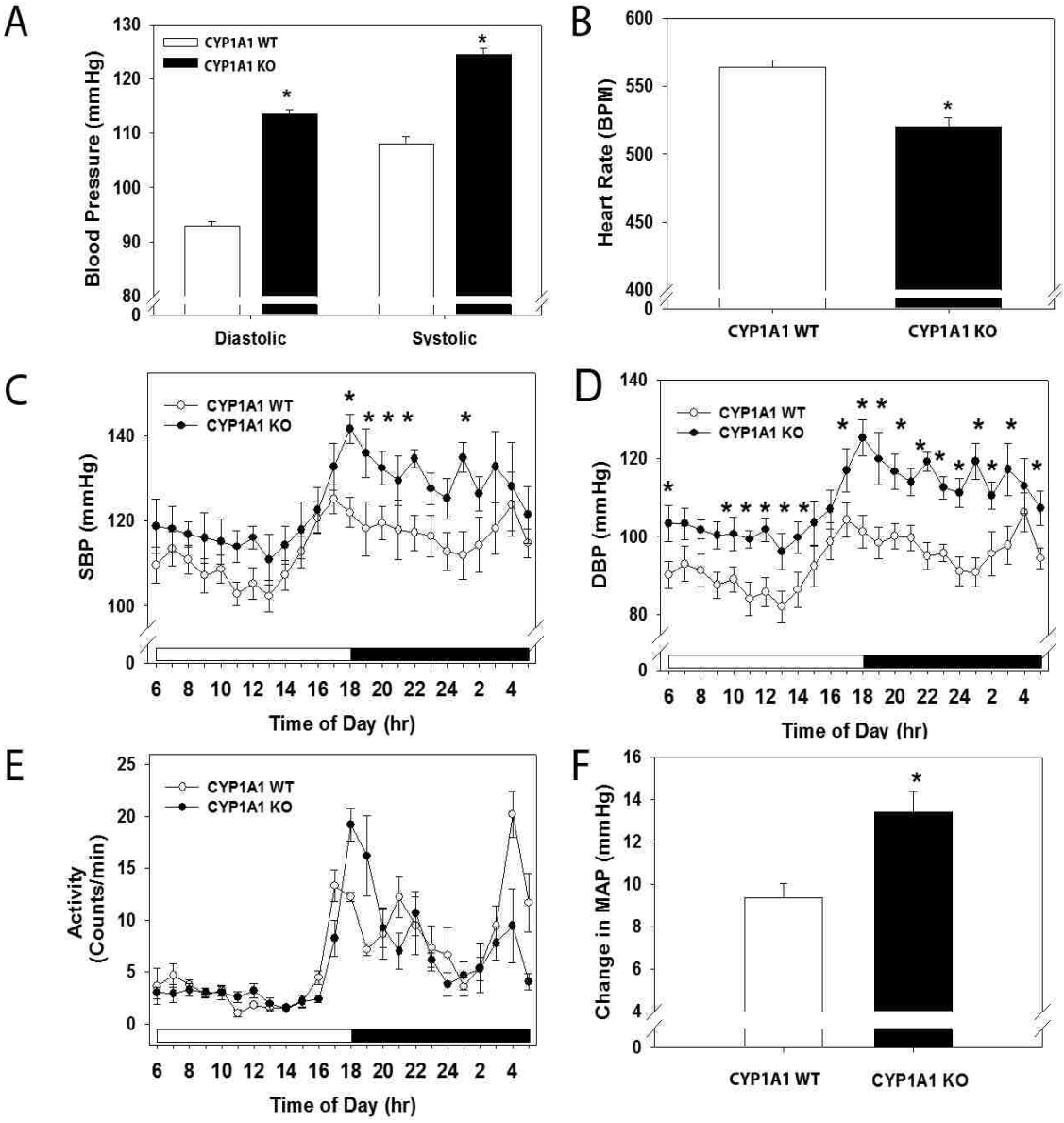

Figure 3.1. Genetic deletion of CYP1A1 increases systolic and diastolic BP, and reduces HR. (A) 24 h mean systolic and diastolic BP, (B) 24 h mean HR, (C) Hourly systolic pressure over a 24 hr period (light and dark cycle), (D) Hourly diastolic pressure over a 24 hr period (light and dark cycle), (E) Activity over a 24 hr period, and (F) Difference in MAP between nighttime and daytime, as measured by radiotelemetry. Data represent mean ± SEM. Data in A, B, and F were analyzed by Student's t-test; *$p < 0.05$, and in C, D and E by two-way, repeated measures ANOVA, using post hoc Holm-Sidak comparisons; *$p < 0.05$ (n=7/genotype)

Vascular reactivity in aorta and mesenteric resistance arterioles

We sought to determine if genetic deletion of CYP1A1 resulted in altered vascular responses indicative of a loss of the endothelial-derived vasodilator, NO. Since ACh-mediated vasorelaxation in the thoracic aorta is dependent solely on NO (Rees *et al.*, 1989), we conducted a dose-response to ACh in aortic segments preconstricted with PE. We found that CYP1A1 KO mice exhibited completely normal vasorelaxation responses to ACh (Fig 3.2A). To confirm that NO-mediated signaling was normal in the vascular smooth muscle, we next conducted a dose-response to the NO donor, SNAP, in endothelium-disrupted aortic segments. Again, CYP1A1 KO mice exhibited completely normal responses to SNAP (Fig. 3.2B). Lastly, if NO was reduced we would expect constrictor responses to be enhanced and the enhancement eliminated by treatment with a NOS inhibitor. We found that CYP1A1 KO mice exhibited normal vasoconstriction responses to PE with and without a NOS inhibitor, LNNA (Fig. 3.2C and D). Since ACh-mediated dilation in resistance vessels also is dependent on NO to a limited degree, we conducted a dose response to ACh in first-order pressurized mesenteric arterioles. Again CYP1A1 KO mice exhibited completely normal vasodilation responses to ACh, suggesting that NO-dependent dilation is also not altered in resistance vessels (Fig. 3.2E).

Plasma NOx and effects of NOS inhibition on blood pressure.

To further confirm whether a reduction in NO bioavailability contributed to the hypertension in CYP1A1 KO mice, we measured plasma NOx as an indicator of systemic NO and we treated CYP1A1 WT and KO mice with a NOS inhibitor and measured their BP responses. We found that CYP1A1 KO mice tended to have reduced plasma NOx

(p=0.07), although it was not statistically different (data not shown). Further, NOS inhibition failed to normalize BP between CYP1A1 WT and KO mice. Hourly MAP over a 24 hr period (light and dark cycle) after NOS inhibition showed that CYP1A1 KO mice remain hypertensive (Fig. 3.3A) and the relative change in MAP was equivalent between CYP1A1 KO and WT (Fig. 3.3B).

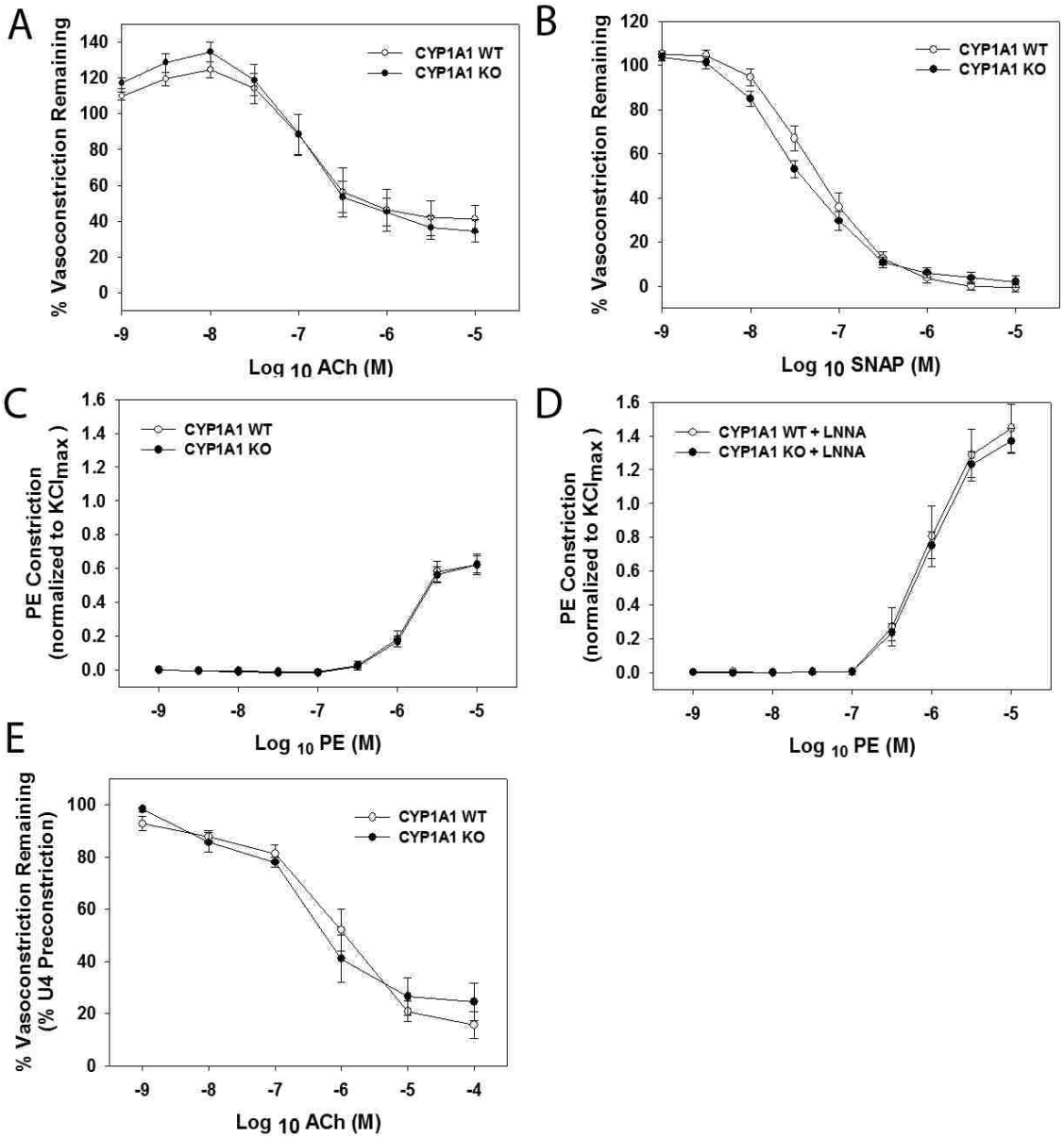

Figure 3.2. Loss of CYP1A1 does not affect vascular sensitivity to ACh- or SNAP-mediated dilation, nor PE-mediated contraction in the absence or presence of the NOS inhibitor, LNNA (A)-(D) thoracic aorta, (E) mesenteric arterioles. (A) ACh-mediated dilation (% PE preconstriction), (B) SNAP-mediated dilation in endothelium denuded aorta (% PE preconstruction), (C) PE-mediated constriction (% KCl), and (D) PE-mediated constriction in the presence of LNNA, (E) ACh-mediated relaxation (% U46619 preconstriction). Data represent mean ± SEM and were analyzed by two-way, repeated measures ANOVA, using post hoc Holm-Sidak comparisons (n=7-8/genotype).

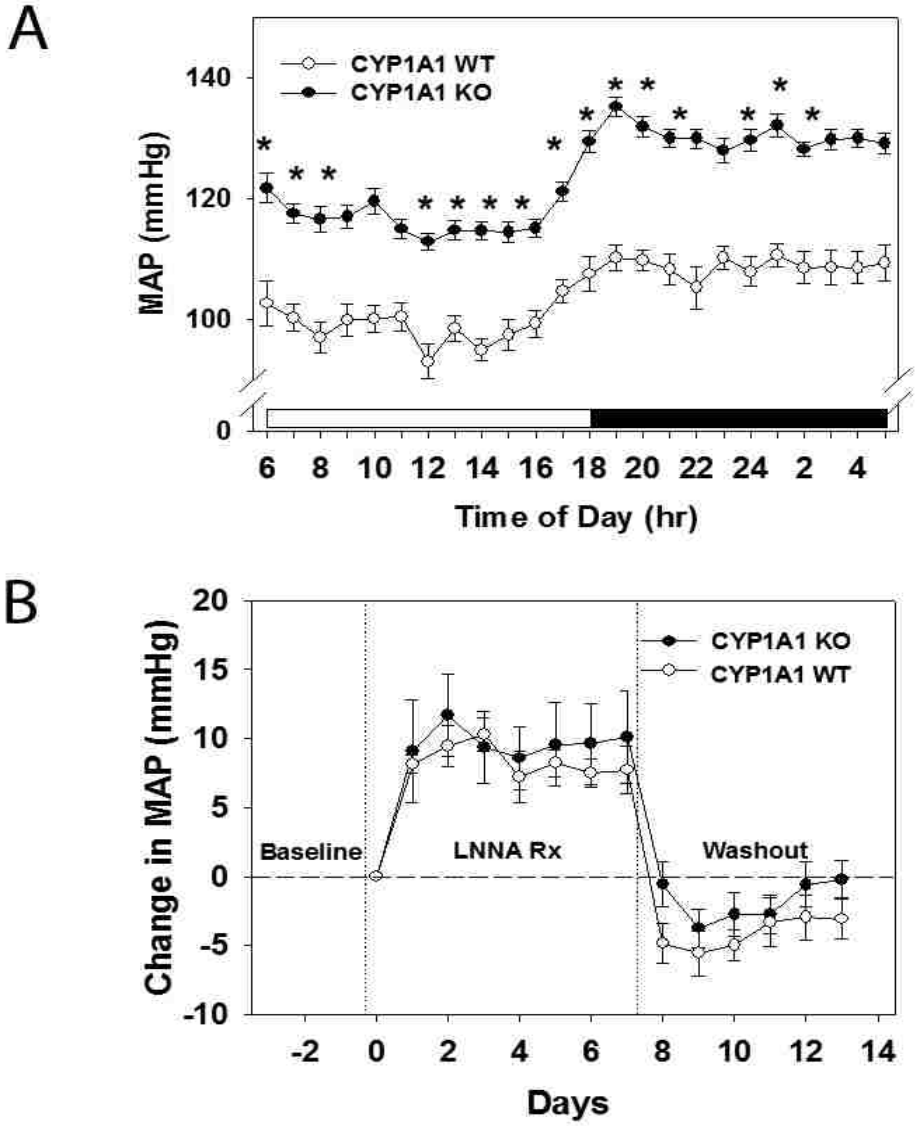

Figure 3.3. NOS inhibition by LNNA does not normalize BP in CYP1A1 KO mice *in vivo*. (A) MAP over a 24 hr period (light and dark cycle) after NOS inhibition. (B) Change in MAP from baseline after treatment with 250 mg/L LNNA in drinking water of male CYP1A1 KO and wildtype mice. Data represent mean ± SEM and were analyzed by two-way, repeated measures ANOVA, using post hoc Holm-Sidak comparisons; *$p < 0.05$, compared to wildtype (A), and by Student's t-test (B) (n=5/genotype).

DHA- and EPA-mediated vasorelaxation and vasodilation are attenuated in abdominal aorta and mesentery arteries, respectively, of CYP1A1 KO mice

Given that our previous results ruled out a loss of NO bioavailability as a contributor to hypertension in CYP1A1 KO mice, we next sought to determine if vascular reactivity to n-3 PUFAs; DHA and EPA, was altered. We assessed the vasodilation responses in abdominal aorta and pressurized mesenteric arterioles to DHA and EPA. CYP1A1 KO mice exhibited significantly attenuated dose-dependent vasorelaxation to both DHA and EPA in the aorta (Fig. 3.4A and B). Similarly, CYP1A1 KO mice exhibited significantly reduced dose-dependent vasodilation to DHA and EPA in mesenteric arterioles when pressurized at 40 (Fig. 3.5A and B) or 60 mmHg (Fig. 3.5C and D).

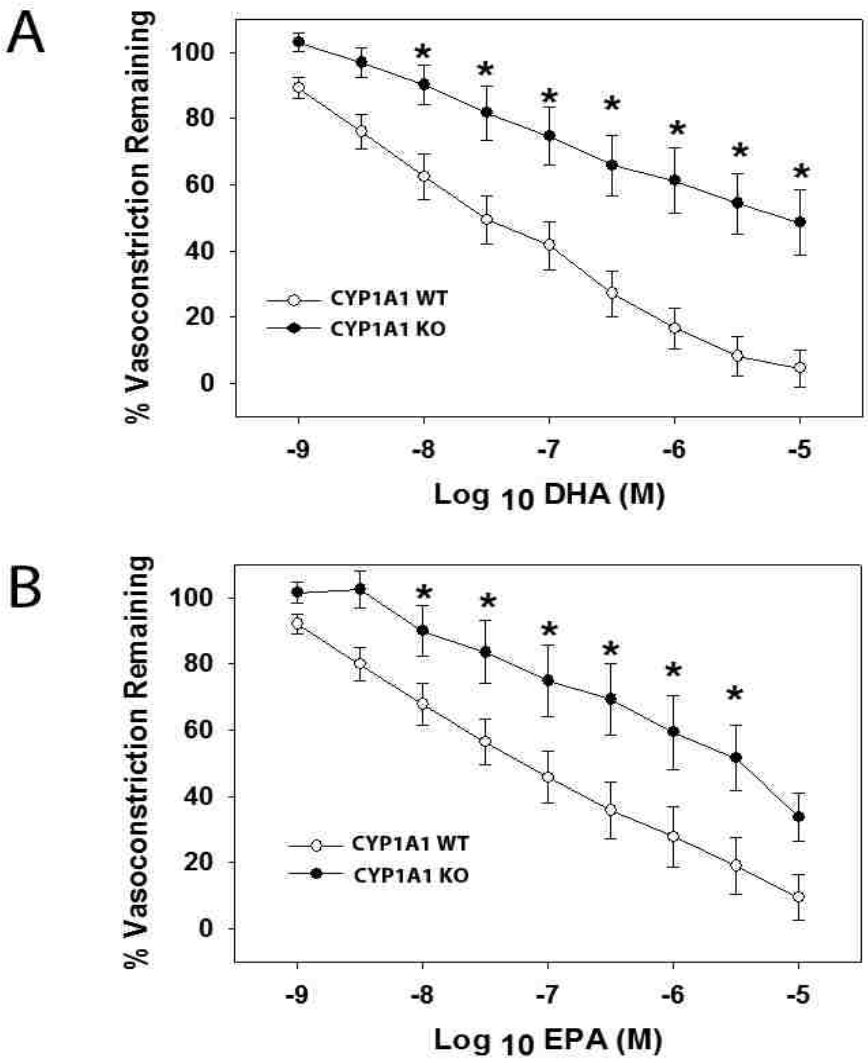

Figure 3.4. DHA and EPA-mediated vasorelaxation are significantly attenuated in abdominal aorta of CYP1A1 KO mice. (A) DHA-mediated relaxation (% U46619 preconstriction), (B) EPA-mediated relaxation (% U46619 preconstriction), in abdominal aorta from CYP1A1 WT and KO and wildtype mice. Data represent mean ± SEM and were analyzed by two-way, repeated measures ANOVA, using post hoc Holm-Sidak comparisons; *$p < 0.05$, compared to wildtype ((n=6/genotype).

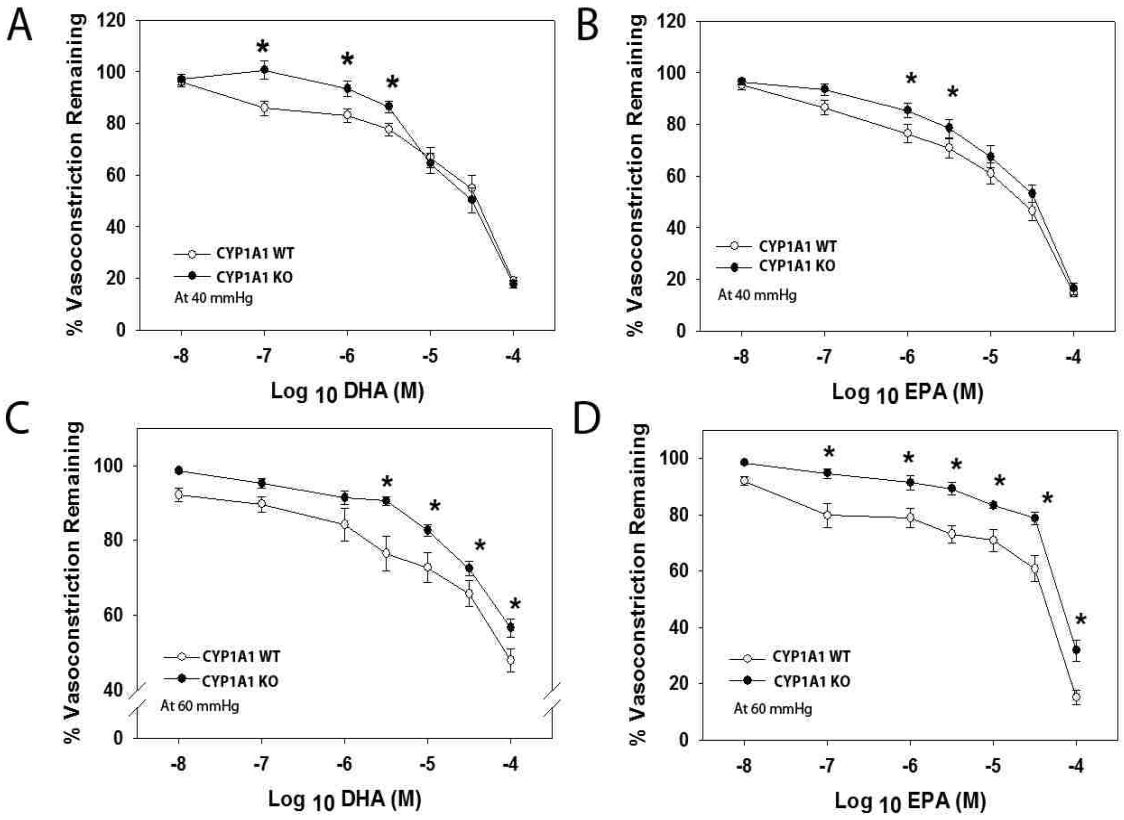

Figure 3.5. DHA and EPA-mediated vasorelaxation are attenuated in pressurized mesenteric resistance arteries at both 40 and 60 mmHg. (A) DHA-mediated relaxation at 40 mmHg, (B) EPA-mediated relaxation at 40 mmHg, (C) DHA-mediated relaxation at 60 mmHg, and (D) EPA-mediated relaxation at 60 mmHg. All relaxation experiments were subjected to U46619 preconstriction. Data represent mean ± SEM and were analyzed by two-way, repeated measures ANOVA, using post hoc Holm-Sidak comparisons; *$p < 0.05$, compared to wildtype (n=8-14/genotype).

CYP1A1metabolites of EPA and DHA (17,18-EEQ and 19,20-EDP, respectively) are potent vasodilators in the abdominal aorta and mesenteric arterioles.

If CYP1A1 mediates n-3 PUFA vasodilation by generating the 17,18-EEQ and 19,20-EDP metabolites as has been demonstrated *in vitro*, then we would expect that the ability of these metabolites to produce vasodilation when applied directly to the vessel would not differ between genotypes. Thus, we assessed vasorelaxation of the abdominal aorta and vasodilation of mesenteric arterioles to 17,18-EEQ and 19,20-EDP. We found that 17,18-EEQ and 19,20-EDP elicited potent and highly efficacious vasorelaxation responses in the aorta of both CYP1A1 WT and KO mice at nanomolar concentrations (Fig. 3.6A and B). In mesenteric arterioles, both metabolites were less potent in inducing vasodilation compared to the aorta, and 17,18-EEQ was significantly less efficacious. Nonetheless, the responses elicited in both CYP1A1 WT and KO mesenteric arterioles were equivalent (Fig. 3.6C and D).

Voltage-gated (Kv) and large conductance, calcium-activated potassium (BK) channels are targets for DHA-mediated vasodilation

Since previous studies have implicated the activation of potassium ion channels in mediating vasodilation to n-3 PUFA, we investigated the contribution of two of these channels to vasodilation in CYP1A1 WT and KO mice. We preincubated mesenteric arterioles with a blocker of the BK channel, IBTX, in the absence or presence of an inhibitor of the Kv channel, 4-AP, and then conducted a dose-response with DHA. We found that both CYP1A1 WT and KO mesenteric arterioles elicited vasodilation to DHA in the presence of the BK channel blocker (Fig. 3.7A and B). Nonetheless, blockade of

both BK and Kv channels significantly inhibited DHA-mediated vasodilation in both CYP1A1 WT and KO mice (Fig. 3.7C and D).

mRNA analysis of Kv and BK channel subunits, CYP2C29, CYP2E1, CYP2D6 and COX2

To determine if aortic expression of BK and Kv channel subunits, as well as several vascular P450s involved in n-3 PUFA metabolism, CYP2C29, CYP2E1, CYP2D6, and COX2 were altered in their expression, we measured mRNA of BKα, BKβ4, Kv1.5, CYP2C29, CYP2E1, CYP2D6 and COX2 in aortas of CYP1A1 KO and WT mice cleaned of adipose tissue. We did not find any differences in the mRNA expression of these potassium channel subunits or P450 (data not shown). In contrast, COX2 mRNA expression was significantly lower by two fold in the aorta of CYP1A1 KO mice, compared to WT mice (data not shown).

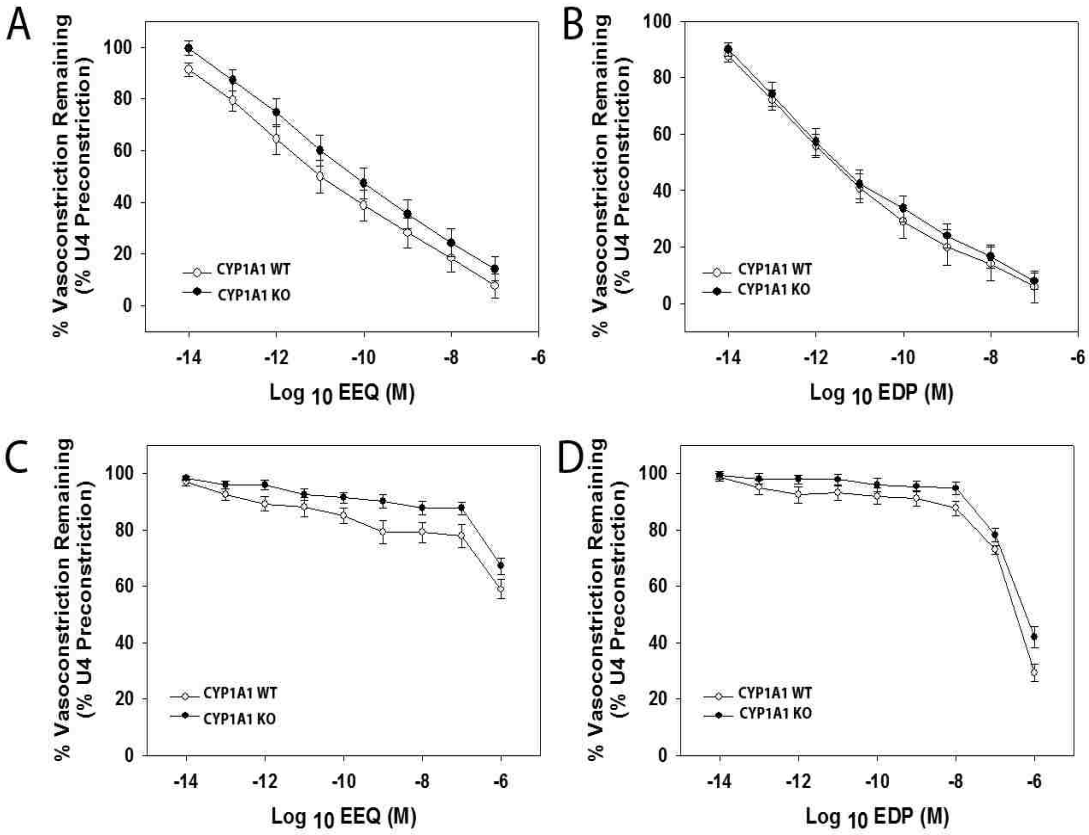

Figure 3.6. P450 metabolites of EPA and DHA, 17,18-EEQ and 19,20-EDP, respectively, induce an equivalent degree of vasorelaxation in the abdominal aorta and vasodilation in mesenteric arterioles in CYP1A1 WT and KO mice. Vasorelaxation in abdominal aorta to 17,18-EEQ (A) and to 19,20-EDP (B). Vasodilation in mesenteric resistance arterioles to 17,18-EEQ (C), and 19,20-EDP (D). Data represent mean ± SEM and were analyzed by two-way, repeated measures ANOVA, using post hoc Holm-Sidak comparisons; *$p < 0.05$, compared to WT (n=6-8/genotype).

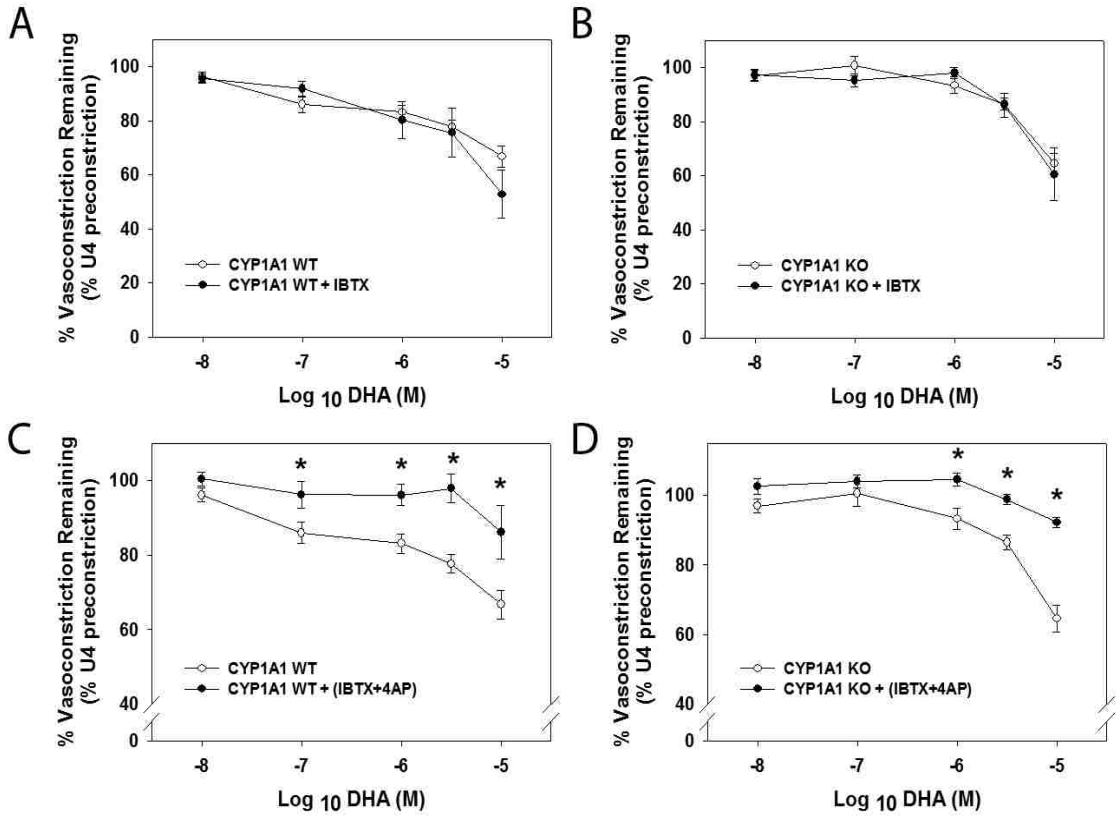

Figure 3.7. Voltage-gated (Kv) and large conductance calcium-activated potassium (BK) channels are targets for DHA-mediated vasodilation in mesenteric resistance arteries in both CYP1A1 WT and KO mice. DHA-mediated vasodilation after pre-incubation with the BK channel blocker, iberiotoxin (IBTX) in CYP1A1 WT (A), and KO mice (B). DHA-mediated relaxation after pre-incubation with both IBTX and the voltage gated potassium blocker, 4-aminopyridine (4-AP) in CYP1A1 WT (C) and KO mice (D). Data represent mean ± SEM and were analyzed by two-way, repeated measures ANOVA, using post hoc Holm-Sidak comparisons; *$p < 0.05$, compared to wildtype (n=4-6/genotype).

E. DISCUSSION

Our study shows for the first time that constitutive expression of CYP1A1 is required to maintain normal levels of BP and to mediate vasodilation responses to n-3 PUFAs *ex vivo*. CYP1A1 KO mice are hypertensive with a reduced HR. Additionally, they exhibit attenuated vasodilation to the n-3 PUFAs, EPA and DHA, in both conduit arteries as well as resistance arterioles. Notably, the putative CYP1A1 metabolites of EPA and DHA, 17,18-EEQ and 19,20-EDP, respectively, exhibit equivalent vasodilatory effects in CYP1A1 WT and KO mice, demonstrating that downstream signaling pathways are not altered by loss of CYP1A1. Finally, although DHA-induced vasodilation was attenuated in CYP1A1 KO mice, compared to WT, our results suggest that this vasodilation is mediated by activation of potassium channels in both genotypes, further suggesting that the loss of n-3 PUFA-mediated vasodilation in CYP1A1 KO mice is not a result of changes in the downstream signaling pathways.

Despite evidence that CYP1A1 is expressed in the vascular endothelium and highly induced by physiological shear stress (Han *et al.*, 2008; Conway *et al.*, 2009), the role of CYP1A1 in the regulation of blood pressure has never been investigated previously. We found that CYP1A1 KO mice exhibit significantly elevated systolic and diastolic blood pressure. Interestingly, systolic blood pressure is significantly increased only at night when the mice are active. Since physical activity is associated with increased levels of physiological shear stress, this would suggest that CYP1A1 plays a role in the blood pressure responses to activity and physiological shear stress. In addition, we found that CYP1A1 KO mice exhibit significantly elevated diastolic blood pressure throughout the entire 24 h light/dark cycle. This would suggest that CYP1A1 also plays a role in the

overall regulation of peripheral vascular resistance, which would be consistent with a decrease in HR as a compensatory response. Nonetheless, future studies that assess cardiac output and stroke volume, or use of flow probes would be needed to confirm if, in fact, peripheral vascular resistance is increased.

Despite evidence that CYP1A1 and NO are induced simultaneously by physiological shear stress in the endothelium (Malek *et al.*, 1999; Boo *et al.*, 2002a; Boo *et al.*, 2002b; Eskin *et al.*, 2004; Han *et al.*, 2008; Conway *et al.*, 2009) and that n-3 PUFAs mediate vasodilation, in part, via increases in NO (Ma *et al.*, 2004; Li *et al.*, 2007a; Stebbins *et al.*, 2008), the increase in BP in CYP1A1 KO mice is not a result of a loss of NO. In fact, multiple lines of evidence demonstrate that NO bioavailability and signaling are normal in CYP1A1 KO mice. We found that ACh-mediated dilation in the thoracic aorta, which is exclusively NO-dependent (Rees *et al.*, 1989), is normal in CYP1A1 KO mice as is the dilation response to a NO donor. Most convincingly, treatment of CYP1A1 WT and KO mice with a NOS inhibitor does not normalize BP between the two genotypes, demonstrating that NO contributes equally to BP regulation.

Since constitutive expression of CYP1A1 is regulated by the AHR as is shown in the AHR KO mice, it might be expected that AHR KO and CYP1A1 KO mice would exhibit similar BP phenotypes. However, this is not the case. Our data show that genetic deletion of CYP1A1 is associated with elevated BP, in contrast to reduced blood pressure (i.e. hypotension) observed for global AHR KO mice (Zhang *et al.*, 2010) as well as the endothelial cell-specific AHR conditional KO mice (Agbor *et al.*, 2011). This suggests that multiple downstream targets regulated by the AHR are involved in BP regulation. One of these targets, in addition to CYP1A1, could be CYP1B1. CYP1B1 is

constitutively expressed in vascular smooth muscle, and although CYP1B1 KO mice have normal blood pressure, they show a significantly attenuated response to angiotensin II-induced hypertension (Jennings *et al.*, 2010). Thus, constitutive expression of CYP1B1 may be pro-hypertensive, while that of CYP1A1 is pro-hypotensive.

The involvement of P450s in blood pressure regulation is not unique to CYP1A1. Genetic deletion of CYP2J5 is associated with increased BP and overt afferent arteriolar responses to angiotensin II and endothelin I (Athirakul *et al.*, 2008). In addition, loss of CYP4A10 in mice is associated with a hypertensive phenotype which is salt-sensitive (Nakagawa *et al.*, 2006). Further, mice in which CYP4A14 is deleted are also hypertensive (Holla *et al.*, 2001), associated with an increase in renal CYP4A12 expression and an increase in the production of the potent vasoconstrictor, 20-hydroxyeicosatetraenoic acid (Carroll *et al.*, 1996). Nonetheless, to the best of our knowledge, other P450s that have been shown to metabolize n-3 PUFAs in a stereospecific manner *in vitro* have not been investigated for their contribution to BP regulation *in vivo* (Lucas *et al.*, 2010; Westphal *et al.*, 2011).

Our study also provides the first *in vivo* evidence that constitutive expression of CYP1A1 mediates, in part, the vasodilatory properties of n-3 PUFAs, EPA and DHA, in both conduit arteries and resistance arterioles. This result is highly consistent with the *in vitro* studies demonstrating that recombinant human CYP1A1 metabolizes EPA and DHA stereospecifically into products with vasodilatory properties (Fer *et al.*, 2008; Lucas *et al.*, 2010). Schwarz *et al.* (2004) show that 17(R),18(S)-EEQ represents 70% of the products produced by human CYP1A1 metabolism of EPA, while 19(R),20(S)-EDP is the only product produced by human CYP1A1 metabolism of DHA (Fer *et al.*, 2008). While

it is not known if mouse CYP1A1 also shows this same degree of specificity in EPA and DHA metabolism, our results strongly suggest that mouse CYP1A1 mediates the production of vasodilatory products from EPA and DHA *in vivo*.

Our data also suggest that the attenuation of vasodilation to EPA and DHA in arteries of CYP1A1 KO mice is not likely a result of altered downstream signaling. There are no differences in the vasodilation responses between CYP1A1 WT and KO mice when the two putative CYP1A1-metabolites, 17,18-EEQ and 19,20-EDP, are applied directly to the arteries. Further, DHA-mediated vasodilation is attenuated by two potassium channel inhibitors in both genotypes, again suggesting that downstream signaling that results in vasodilation is not different between genotypes.

Irrespective of the P450 involved, our data also confirm that 17,18-EEQ and 19,20-EDP are potent and efficacious vasodilators. We found that 17,18-EEQ and 19,20-EDP induce ~50% relaxation of the aorta at sub-nM concentrations and >90% relaxation at nM concentrations. In general, the mesenteric arterioles are less responsive and require nM to μM concentrations to induce vasodilation. The potency and efficacy of 17,18-EEQ and 19,20-EDP in vasorelaxation of the mouse aorta is similar to the vasodilatory responses observed in porcine coronary microvessels (Zhang *et al.*, 2001; Ye *et al.*, 2002). However, the vasodilation responses to 17,18-EEQ in the mouse mesenteric arterioles is more similar to that observed in human pulmonary arteries with ~ 80% relaxation occurring at μM concentrations (Morin *et al.*, 2009). Thus, the vasodilatory responses to these n-3 PUFA metabolites are likely to be both species- and vascular bed-specific.

Studies suggest that there are various downstream mechanisms by which EPA and DHA mediate their vasodilatory responses. Wang *et al*. (2011) showed that the

vasodilatory actions of DHA are mediated by P450 metabolism and downstream activation of Kv and BK channels in rat coronary arteries, while Lauterback *et al*. (2002) showed that 17,18-EEQ hyperpolarizes vascular smooth muscles from rat cerebral arteries exclusively by BK channel activation. Our data show blockade of BK channels alone does not attenuate DHA-mediated dilation in mouse mesenteric arteries; however, the simultaneous inhibition of Kv channels does significantly attenuate the dilation response, suggesting that BK channels may not play a role in DHA dilation in this microvascular bed.

Finally, CYP1A1 KO mice exhibit key phenotypic characteristics that are distinct from age-matched CYP1A1 WT mice. Body weights in CYP1A1 KO mice are significantly lower as are kidney and liver weights when normalized to body weight. The decrease in liver weight is similar to the AHR KO mice which exhibit decreased liver size resulting from a persistent ductus venosus and reduced hepatocyte size (Lahvis *et al.*, 2000; Lahvis *et al.*, 2005). Further studies are needed to determine the underlying reasons for the differences in body and organ weights between CYP1A1 WT and KO mice. Since the WT and KO mice used in this study are not littermates, it is possible that maternal factors could contribute to these differences.

In summary, our study suggests for the first time that constitutive CYP1A1 expression has a physiologically important role in the regulation of vascular function and blood pressure, which may involve vasodilatory responses to n-3 PUFAs. Since CYP1A1 is constitutively expressed in the vascular endothelium and physiological levels of shear stress can induce its expression, CYP1A1 metabolism of n-3 PUFAs could represent a novel pathway contributing to an anti-atherogenic phenotype. Future studies will need to

determine whether the loss of n-3 PUFA vasodilation and potential increase in peripheral vascular resistance are the proximal mediators of the increase in blood pressure in CYP1A1 KO mice.

IV. CHAPTER 4

Cytochrome P4501A1 contributes to nitric oxide-dependent vasodilation and blood pressure lowering on an omega-3 polyunsaturated fatty acid-enriched diet.

In preparation for submission to Hypertension.

A. ABSTRACT

Elevated blood pressure (BP) in cytochrome P4501A1 knockout (CYP1A1 KO) mice is associated with attenuated vasodilation to omega-3 polyunsaturated fatty acids (n-3 PUFAs); eicosapentaenoic acids (EPA) and docosahexaenoic acids (DHA) *ex vivo*. We tested the hypothesis that dietary supplementation of n-3 PUFAs rather than n-6 PUFAs will reduce BP in CYP1A1 KO mice via a nitric oxide synthase (NOS) dependent pathway. Diets enriched in n-3 or n-6 PUFAs were fed to CYP1A1 WT and KO mice for 2 months. BP and heart rate (HR) was assessed by radiotelemetry in CYP1A1 WT and KO mice ± NOS inhibitor (N^{ω}-nitro-L-arginine, LNNA), and following an acute Ang II challenge *in vivo* (30 µg/kg). We measured endothelial NOS (eNOS) and phospho-eNOS protein expression in aorta, and also assessed mesenteric dose-responses to acetylcholine (ACh), and to the thromboxane A2 mimetic, U46619. We found that an n-3 PUFA-enriched diet significantly reduced mean arterial pressure (MAP) in CYP1A1 KO mice (Chow, 116.0 ± 1.2, n-3: 107.6 ± 1.5, $p<0.005$), with no effect in CYP1A1 WT mice (Chow, 103.0 ± 0.9, n-3: 105.0 ± 2.5). In contrast, MAP in CYP1A1 WT mice fed an n-6 PUFA-enriched diet was significantly increased (Chow, 103.0 ± 0.9, n-6: 118.2 ± 4.1, $p<0.005$), with no effect in CYP1A1 KO mice (Chow, 116.0 ± 1.2, n-6: 115.3 ± 1.5). Interestingly, NOS inhibition increased BP significantly more in the CYP1A1 WT mice (+16 ± 0.5 mmHg) than CYP1A1 KO mice (+11 ± 0.6, $p<0.002$) on an n-3 PUFA-enriched diet, but resulted in similar increases in BP in CYP1A1 WT and KO mice on an n-6 PUFA-enriched diet (WT: +11 ± 1.8; KO: +11 ± 0.8). Area under the curve analysis showed that Ang II significantly increased systolic BP in CYP1A1 KO mice fed an n-3 PUFA-enriched diet, compared to CYP1A1 WT mice (WT_{n-3}, 938 ± 90; KO_{n-3}, 1250 ± 51,

$p<0.05$). Additionally, CYP1A1KO mice on an n-3 PUFA-enriched diet exhibited significantly attenuated ACh-dependent vasodilation in mesenteric arterioles, and reduced expression of aortic phospho-eNOS protein, compared to CYP1A1 WT mice. However, neither of the endpoints was altered in CYP1A1 KO mice on an n-6 diet, compared to CYP1A1 WT mice. Taken together, these data suggest that CYP1A1 contributes to NO-mediated vasodilation and BP lowering benefits derived from dietary n-3 PUFAs.

B. INTRODUCTION

Although cardiovascular (CV) disease is a leading cause of death in the developed countries, studies have shown that there are considerable differences in the incidence and death rates among different cultures. One of the contributing factors is dietary patterns, and numerous studies have shown that diets high in marine fish and mammals, which contain high levels of omega-3 polyunsaturated fatty acids (n-3 PUFAs), are inversely correlated with CV mortality. For example, Greenland Eskimos, who consume diets highly enriched in n-3 PUFAs, show significantly lower rates of coronary heart disease and CV mortality than Western European countries (Bang *et al.*, 1980; Kromann and Green, 1980). These benefits are observed even among Western countries. The Seven Countries Study of dietary eating patterns of more than 12,000 men shows that consumption of a diet high in fish significantly reduces the risk of death from acute myocardial infarction (Menotti *et al.*, 1999). The CV benefits of n-3PUFAs have been further confirmed by clinical trials. Randomized human clinical trials show that n-3 PUFAs reduce the risk of cardiovascular death, myocardial infarction, and stroke by up to 20% (Marchioli *et al.*, 2002; Yokoyama *et al.*, 2007).

The mechanisms by which n-3 PUFAs mediate their cardioprotective benefits are multifactorial and include anti-hypertensive, anti-hyperlipidemic, anti-arrhythmic, and anti-inflammatory effects. For example, a meta-analysis of randomized human clinical trials found that n-3 PUFAs systematically reduce systolic and diastolic blood pressure (BP) (Morris *et al.*, 1993; Geleijnse *et al.*, 2002). Additionally, n-3 PUFAs have been shown to significantly reduce triglyceride levels by up to 30% (Harris, 1997) and reduce plasma

levels of soluble adhesion molecules associated with the inflammatory disease process as shown in a meta-analysis of 18 separate studies (Yang *et al.*, 2012).

The mechanisms that mediate the anti-hypertensive effects of n-3 PUFAs have not been fully elucidated, but likely result from pro-vasodilatory effects. n-3 PUFAs are metabolized to vasodilatory products via cytochrome P450s (Schwarz *et al.*, 2004; Schwarz *et al.*, 2005; Fer *et al.*, 2008; Lucas *et al.*, 2010) and lead to increases in nitric oxide (NO) bioavailability, a potent vasodilator (Rees *et al.*, 1989). Using a broad spectrum P450 inhibitor in rat coronary arteries, Wang *et al.*, (2011) show that the vasodilatory actions of docosapentaenoic acid (DHA), an n-3 PUFA, require P450 metabolism. Further, multiple studies show that n-3 PUFAs increase the activation of endothelial nitric oxide synthase (eNOS) in cultured endothelial cells (Omura *et al.*, 2001; Gousset-Dupont *et al.*, 2007; Li *et al.*, 2007a; Stebbins *et al.*, 2008) and increase eNOS and NO production in rats and mice *in vivo* (Nishimura *et al.*, 2000; Lopez *et al.*, 2004; Ma *et al.*, 2004). Lastly, dietary n-3 PUFA supplementation in humans enhances NO-dependent forearm vasodilation (Tagawa *et al.*, 1999). Nonetheless, it is not clear if P450-generated metabolites are responsible for the increases in NO production or if the increases in NO result from an independent mechanism.

n-3 PUFAs are efficient and, in some cases, the preferred endogenous substrates for members of the CYP1A, CYP2D and CYP2E families of P450s,which metabolize n-3 PUFAs in a stereospecific manner, generating potent and efficacious vasodilators (Barbosa-Sicard *et al.*, 2005; Muller *et al.*, 2007; Westphal *et al.*, 2011). For example, CYP1A1 metabolizes the principal n-3 PUFAs, DHA and eicosapentaenoic acids (EPA), to the stereospecific products 19(R),20(S)-epoxydocosapentaenoic acid (19(R),20(S)-

EDP) and 17(R),18(S)-epoxyeicosatetraenoic acid (17(R),18(S)-EEQ), respectively (Schwarz *et al.*, 2004; Lucas *et al.*, 2010). Both of these metabolites are potent vasodilators in microcirculatory vessels (Zhang *et al.*, 2001; Morin *et al.*, 2009). Despite the knowledge of P450 metabolism of n-3 PUFAs, the contributions of individual P450s to the regulation of vascular tone and BP *in vivo* remains uninvestigated. Recently, however, we demonstrate, using CYP1A1 knockout (KO) mice, that CYP1A1 is a partial contributor to the vasodilation responses to DHA and EPA and is required for regulating BP *in vivo* as CYP1A1 KO mice exhibit significant increases in BP, particularly when active (Agbor *et al.*, unpublished data). Nonetheless, these results show that CYP1A1 is not the sole mediator of the responses to n-3 PUFAs. Since other P450s also efficiently metabolize n-3 PUFAs, we hypothesized that providing an n-3 PUFA-enriched diet to enhance substrate availability would reduce BP in CYP1A1 KO mice and this decrease would be mediated, in part, by increased NO bioavailability. We further hypothesized that providing an n-6 PUFA-enriched diet to diminish n-3 PUFA substrate bioavailability would increase BP in CYP1A1 WT mice.

C. METHODS

Chemicals

Acetylcholine (ACh), N^{ω}-nitro-L-arginine (LNNA), angiotensin (Ang) II, all ingredients of physiological saline solution (PSS) and HEPES-PSS were purchased from Sigma–Aldrich (St. Louis, MO). U46619 was purchased from Cayman Chemical (Ann Arbor, MI).

Animals

CYP1A1 KO mice, backcrossed more than eight generations onto the C57BL/6J background, were generously provided by Dr. Daniel Nebert (University of Cincinnati) and were bred at the University of New Mexico (Dalton *et al.*, 2000). Age-matched C57BL/6J mice served as wildtype (WT) controls. All animals were housed in a temperature-controlled environment. All animal protocols were approved by the University of New Mexico Animal Care and Use Committee and the investigations conform to the Guide for the Care and Use of Laboratory Animals published by the U. S. National Institutes of Health (NIH Publication No. 85-23, revised 1996). When tissues were harvested and organ weight determined, mice were anesthetized with ketamine (80 mg/kg)/xylazine (4 mg/kg). The heart was removed, atria were dissected, and the total ventricle weight measured. Kidneys and liver weights were also measured. All tissues were frozen at −80°C.

Diets

Mice were fed a standard chow rodent diet (product no. 2020XC, Teklad Diets, Harlan Laboratories, Madison WI), an n-3 PUFA-enriched diet containing 15% fish oil (wt/wt), or an n-6 PUFA-enriched diet containing 15% safflower oil/linoleic (wt/wt) (Teklad Diets, Harlan Laboratories) (Table 4.1). Both PUFA diets were equivalent in total protein, carbohydrates, fat content and all other dietary components. Diets were prepared in bulk, and packaged into individual 4 kg whirl-Pak bags (Nasco, Fort Atkinson, WI), flushed with nitrogen to minimize oxidation and stored at 4 °C. Fresh diets were fed twice weekly. Diets were weighed before and after administration to determine the amount of food consumed, and any uneaten food was discarded.

Table 4.1. Diet composition: Standard chow, n-3 PUFA enriched diet, and n-6 PUFA-enriched diet

Composition	Standard Chow (2020X) (% by weight)	n-3 PUFA diet (TD.110516) (% by weight)	n-6 PUFA diet (TD.110517) (% by weight)
Protein	24.0	18.6	18.6
Carbohydrates	60.0	52.2	52.2
Total fat	16.0	15.2	15.2
Kcal/g	3.1	4.2	4.2
Fatty acids			
n-3 PUFA	10	80	0
n-6 PUFA	90	20	100

Blood pressure analysis

Arterial BP and heart rate (HR) were measured using radiotelemetry in 4-5 month-old CYP1A1 WT and KO mice (Data Sciences International, St. Paul, MN, USA) as previously described (Lund *et al.*, 2008), using PA-C10 radiotelemeters. Mice were allowed to recover from surgery for 7 d prior to data collection. Basal BP, including systolic, diastolic, mean and pulse arterial BP, and HR were collected for 7 d before drug treatments began. BP was recorded for 10 s every 15 min during baseline measurements. After basal BP was measured, all mice were treated with LNNA in the drinking water (250 mg/L) for one week followed by one week of washout (Duling *et al.*, 2006). In addition, BP was also measured for 10 s every 1 min for 30 min, starting 5 min following an acute Ang II injection (30 µg/kg *i.p.*).

Mesenteric arteriole reactivity

Mice were administered heparin (10 µl/g of 1000 units/ml) by intraperitoneal injection for 5 min, anesthetized with ketamine (80 mg/kg)/xylazine (4 mg/kg), and euthanized by exsanguination. The intestine together with mesenteric arteries were quickly excised and placed in HEPES-PSS solution (134 mM NaCl, 6.0 mM KCl, 1 mM $MgCl_2$, 2 mM $CaCl_2$, 10 mM HEPES, 0.026 mM EDTA, 10 mM glucose, and buffered to pH 7.4 with NaOH). The tissue was then pinned to the bottom of a petri dish, and a long segment of a first-order branch of the mesenteric artery was cleared from surrounding adipose tissue and dissected. The artery was transferred to the chamber of a pressure myograph system (DMT -110 systems, Danish Myo Technology, Ann Arbor, MI) for cannulation. The chamber was filled with warm PSS at 37 ^{0}C bubbled with 21% O_2, 6%

CO_2, balanced N_2 (130 mM NaCl, 4.7 mM KCl, 1.18 mM $KH2PO_4$, 1.17 mM $MgSO_4$, 14.9 mM $NaHCO_3$, 5.5 mM glucose, 26 µM $CaNa_2EDTA$, and 1.8 mM $CaCl_2$, pH 7.4). One end of the vessel was cannulated with the outflow pipette and tied securely with 10-0 ethilon surgical silk thread. The other end of the vessel was then cannulated with the inflow pipette. The pressure was then increased by 10 mmHg increment every 5 mins to a maximum of 60 mmHg, and the artery allowed to equilibrate for 30 min. After equilibration, baseline internal was measured using edge detection software (MyoView acquisition software, DMTVAS 6.2.0.59 Danish Myo Technology, Ann Arbor, MI). Viability of arteries was tested by constriction to 60 mM KCl and vessels that failed to constrict to 30% of baseline internal diameter were discarded. After a PSS wash, the artery was allowed to return to baseline diameter and to rest for at least 15 min. Arteries were then preconstricted to 45% of internal diameter with U46619, and a dose response to ACh (0.001–100 mM) was conducted. A concentration-response to U46619 (0.01-1 µM) was also conducted. All experiments were performed without luminal flow.

Western blot

Aortas were cleaned of connective tissue and adventitial fat, and then homogenized in RIPA buffer (Santa Cruz Biotechnology, Santa Cruz, CA). The homogenate was frozen at -80 °C for 15 min, sonicated for 10 s and centrifuged at 15,000 x g 4 °C for 10 min. Protein concentration was measured using micro BCA protein assay kit (Thermo Scientific, Rockford, IL, USA). A 20 µg aliquot of protein was mixed with 6X loading buffer (100 mM pH6.8 Tris-HCl, 4% sodium dodecyl sulfate, 0.2% bromophenol blue, 20% glycerol, 200 mM dithiothreitol) and denatured at 95 °C for 10

min. Denatured samples were subjected to electrophoresis on 10 % Tris-HCL polyacrylamide gel at 150 V for 1 hour in running buffer (25 mM Tris-base, 150 mM glycine, 0.1% sodium dodecyl sulfate) and separated proteins were transferred to polyvinylidene fluoride (PVDF) membrane (Bio-Rad Laboratories) at 100 V for 1 hour in cold transfer buffer (20 mM Tris-base, 150 mM glycine, 20% methanol). The membrane was washed with Tris-buffered saline (TBST, 0.8% NaCl, 0.02% KCl, 0.3% Tris-base, 0.05% Tween-20, pH7.4) and blocked for 1 hour in 5% nonfat dry milk in TBST. The blocked membrane was incubated with mouse anti-eNOS antibody (1:2000, BD Transduction Laboratories, San Jose, CA) or mouse anti-phopho-eNOS antibody (1:2000, BD Transduction Laboratories) at 4 °C overnight, washed with TBST, and incubated with horseradish peroxidase (HRP) conjugated goat anti-mouse (Southern Biotech, Birmingham, AL) for 1 hour at room temperature. The membrane was washed with TBST and developed for 2 min with 1 mL supersignal west femto maximum sensitivity substrate (Thermo Scientific) using a KODAK Image Station 4000MM digital imaging system (Perkin-Elmer). The membrane was stripped (7 M guanidine hydrochloride, 0.75% KCl, 0.38% glycine, 50 µM EDTA, 0.14% 2-mercaptoethanol, pH10), washed with TBST, reblocked, and incubated with mouse β-actin (Santa Cruz Biotechnology) overnight, washed with TBST, incubated with HRP-conjugated goat anti-mouse IgG (Southern Biotech), washed and developed as above. Protein quantification was done using Image J software (National Institutes of Health, USA).

Lipid profile, plasma NOx, and thiobarbituric acid reactive substances (TBARS) analyses.

To analyze lipid profile prior to and following treatment with n-3 and n-6 PUFA-enriched diet, CYP1A1 WT and KO mice were fasted for 12 h overnight and using whole blood, lipid panel analysis was conducted using lipid panel screening strips, with a CardioCheck PA analyzer (Polymer Technology Systems, Inc, CardioChek, Indiana, USA). Total cholesterol, high density lipoprotein (HDL) cholesterol, and triglycerides were measured. Further, mice were anesthetized with ketamine (80 mg/kg)/xylazine (4 mg/kg) and euthanized by exsanguination. Plasma was collected from whole blood using heparinized syringes and NOx levels were measured using the Griess colorimetric assay (Cayman Chemical). Hearts were suspended in 1:10 weight:volume of saline, homogenized, and sonicated for 15 s at 40 V. TBARS was measured in heart homogenates using an assay kit (OXItek, ZeptoMetric Corp, Buffalo, NY). Triplicate samples were read on a spectrophotometer (Beckman Instruments DU Series 600), using a malondialdehyde (MDA) standard curve, and results expressed as MDA equivalents.

Statistical analysis

Diets- and genotype-related changes in organ and body weights were analyzed by two-way analysis of variance (ANOVA) with post hoc Holm-Sidak comparisons. Vasoreactivity and BP measurements following NOS inhibition and Ang II treatment were analyzed by repeated measures, two-way analysis of variance with post hoc Holm-Sidak comparisons. The eNOS and phospho-eNOS protein quantifications were analyzed using Student's t-test. *$p < 0.05$ was considered statistically significant.

D. RESULTS

Food consumption, body and organ weights, and lipid profile

We measured food intake, and compared body and organ weights of CYP1A1 WT and KO mice fed an n-3 or n-6 PUFA-enriched diet at 8 months of age. Regardless of genotype or diet, food intake was not different between treatment groups (Fig. 4.1). Body and organs weights from CYP1A1 KO mice fed an n-3 PUFA-enriched diet were not different, compared to WT mice. In contrast, CYP1A1 KO mice fed an n-6 PUFA-enriched diet exhibited significantly lower body, heart and liver weights, compared to age-matched CYP1A1 WT mice. However, when heart and liver weights were normalized to body weight, there was no difference between CYP1A1 WT and KO mice (Table 4.2). In addition, neither the n-3 nor n-6 PUFA-enriched diet had any effect on cholesterol levels, but both diets significantly reduced triglyceride levels in CYP1A1 KO and WT mice (Table 4.3).

Effects of n-3 and n-6 PUFA-enriched diets on mean 24 hr BP and HR in CYP1A1 WT and KO mice

Since n-3 PUFAs have anti-hypertensive effects due, in part, to their metabolism by P450s including CYP1A1, we sought to determine how diets enriched in n-3 PUFAs versus n-6 PUFAs would affect BP in CYP1A1 WT and KO mice. BP of CYP1A1 WT and KO mice were measured by radiotelemetry. CYP1A1 KO mice on standard chow exhibited elevated BP, compared to WT mice (mean arterial pressure (MAP) in mmHg, WT_{chow} 103 ± 1, CYP1A1 KO_{chow} 116 ± 1; $p<0.05$) (Fig. 4.2A). An n-3 PUFA-enriched diet significantly reduced MAP in CYP1A1 KO mice, compared to KO mice on standard

chow (MAP in mmHg, CYP1A1 KO_{n-3}, 107.6 ± 1.5; $p<0.05$), but had no affect on MAP in CYP1A1 WT mice (CYP1A1 WT_{n-3}: 105.0 ± 2.5), (Fig. 4.2B). In contrast, an n-6 PUFA-enriched diet significantly increased MAP in CYP1A1 WT mice, compared to WT mice on standard chow (WT_{n-6} 118.2 ± 4.1; $p<0.05$), but had no affect on MAP in CYP1A1 KO mice (CYP1A1 KO_{n-6} 115.3 ± 1.5) (Fig. 4.2C). HR increased in CYP1A1 KO mice fed an n-3 PUFA-enriched diet, but there were no other differences in HR among groups (Fig. 4.2D).

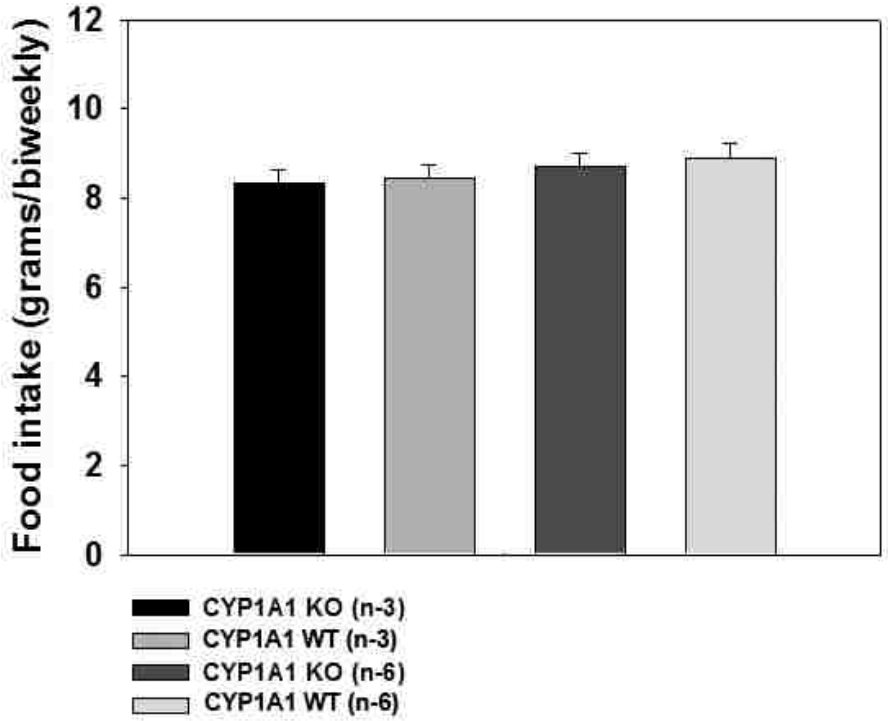

Figure 4.1. Food consumption in CYP1A1 WT and KO mice fed an n-3 PUFA-enriched diet or n-6 PUFA-enriched diet. Data represent mean ± SEM and were analyzed by student t-test (n=8/genotype/diet).

Table 4.2. Body and organ weights in 8 month-old CYP1A1 WT and KO mice on n-3 and n-6 PUFA-enriched diets

Weight	CYP1A1 WT n-3 (n=8)	CYP1A1 KO n-3 (n=8)	CYP1A1 WT n-6 (n=8)	CYP1A1 KO n-6 (n=8)
Body (g)	32.5 ± 1.1	31.2 ± 0.9	31.9 ± 0.8	28.2 ± 1.0*
Heart (mg)	128 ± 4 (0. 397 ± 0. 256)†	120 ± 4 (0. 387 ± 0. 244)	122 ± 2 (0. 386 ± 0. 179)	110 ± 0.9* (0. 394 ± 0. 160)
Liver (mg)	1661 ± 95 (5.0 ± 0. 173)	1553 ± 43 (5.0 ± 0. 190)	1382 ± 27 (4.3 ± 0. 128)	1245 ± 37* (4.4 ± 0. 064)
Kidney (mg)	403 ± 13 (1.2 ± 0. 075)	369 ± 13 (1.2 ± 0. 076)	329 ± 7 (1.0 ± 0. 046)	348 ± 9 (1.2 ± 0. 035)

Values are expressed as mean ± SEM
*$p < 0.05$ versus corresponding WT
†(Organ/body weight ratio x 100)

Table 4.3. Lipid profile measurements in CYP1A1 WT and KO mice fed standard chow, an n-3 and an n-6 PUFA-enriched diet

Parameters	CYP1A1 WT chow (n=7)	CYP1A1 KO chow (n=7)	CYP1A1 WT n-3 (n=3)	CYP1A1 KO n-3 (n=4)	CYP1A1 WT n-6 (n=4)	CYP1A1 KO n-6 (n=3)
Total cholesterol (mg/dL)	<100	<100	<100	<100	<100	<100
HDL cholesterol (mg/dL)	76 ± 5	87 ± 6	34 ± 5*	37 ± 2*	75 ± 5	84 ± 9
Triglycerides (mg/dL)	95 ± 22	83 ± 23	<50	<50	<50	<50

Values are expressed as mean ± SEM
*p < 0.05, vs chow and n-6 diet
Legend: KO, CYP1A1 KO; WT, Wildtype.

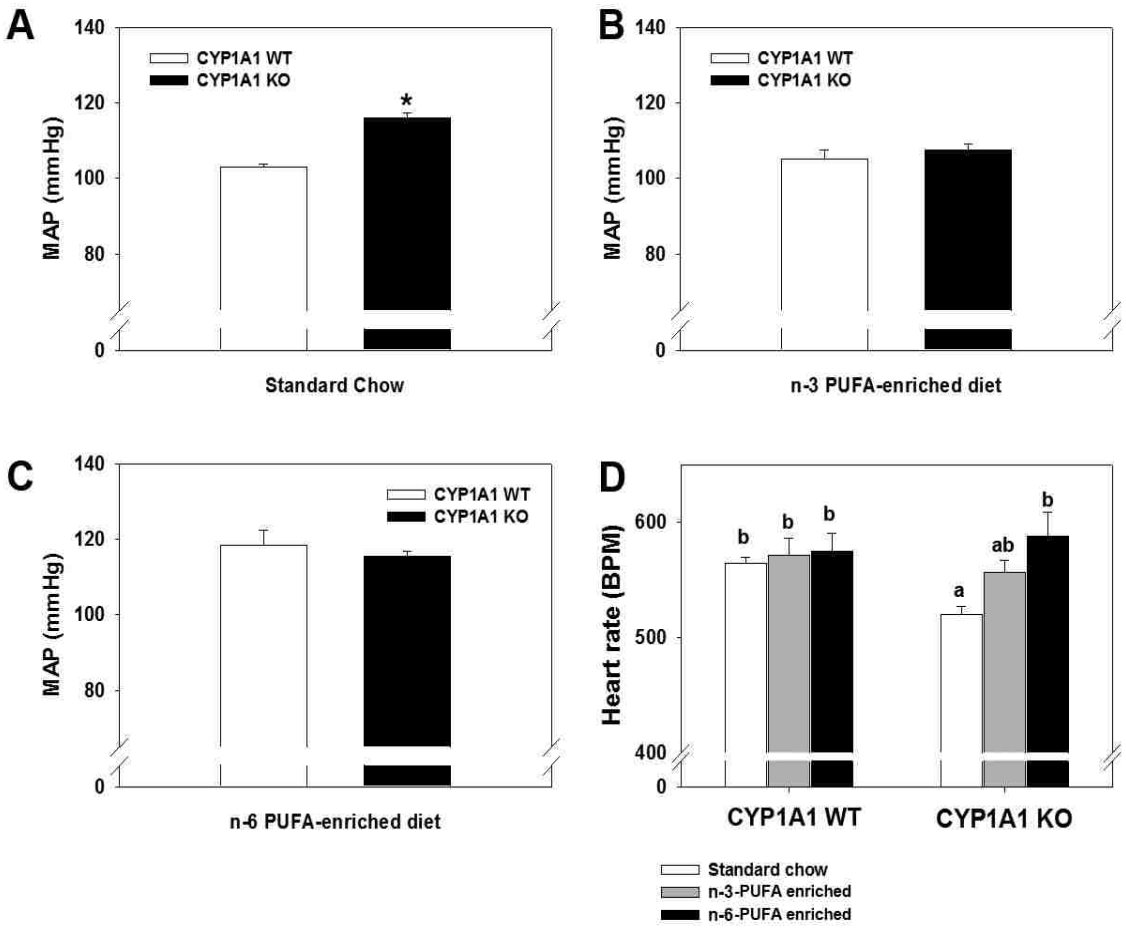

Figure 4.2. Effects of n-3 and n-6 PUFA-enriched diets on mean 24 hr BP and HR in CYP1A1 WT and KO mice. (A) MAP in CYP1A1 WT and KO mice fed standard chow, (B) an n-3 PUFA-enriched diet or (C) an n-6 PUFA-enriched diet. (D) Corresponding HR of CYP1A1 WT and KO mice fed standard chow, an n-3 PUFA-enriched diet, or an n-6 PUFA-enriched diet. Data represent mean ± SEM and were analyzed by Student's t-test. Bars with the same letters are not different from each other. *p < 0.05 (n=7/genotype/diet).

Effects of an n-3 PUFA-enriched diet ± LNNA on mean hourly BP and HR in CYP1A1 WT and KO mice.

To determine the contribution of NO to the reduction in BP in CYP1A1 KO mice fed an n-3 PUFA-enriched diet, we treated CYP1A1 WT and KO mice with the NOS inhibitor, LNNA for 1 week and continuously assessed changes in BP and HR by radiotelemetry. Hourly MAP over a 24 hr period prior to LNNA treatment was comparable between CYP1A1 WT and KO mice on an n-3 PUFA-enriched diet (Fig. 4.3A). Following NOS inhibition, hourly MAP increased in both CYP1A1 WT and KO mice, but it increased significantly less in CYP1A1 KO mice especially during nighttime periods of increased activity, although the normal circadian pattern of an increased MAP during the night wakeful period was preserved (Fig. 4.3B). Although the 24 hr mean HR was not significantly different between CYP1A1 WT and CYP1A1 KO mice fed an n-3 PUFA-enriched diet, when hourly HR was compared over a 24 hr period, CYP1A1 KO mice exhibited significantly lower HR at multiple times, particularly during peak activity after lights were turned off, compared to WT mice (Fig. 4.3C). Following NOS inhibition, HR decreased in both genotypes, but again CYP1A1 KO mice exhibited a lower HR particularly when active, compared to WT mice (Fig. 4.3D). Further, the increase in MAP following NOS inhibition was significantly greater in CYP1A1 WT mice (+16 ± 0.5 mmHg) than KO mice (+11 ± 0.6, $p<0.002$), (Fig. 4.3E). However, the decrease in HR following NOS inhibition was not different between treatment groups (Fig. 4.3F). Additionally, following NOS inhibition in CYP1A1 WT and KO mice on both standard chow and n-3 PUFA-enriched diets, BP increased significantly more in WT mice on an n-3 PUFA-enriched diet (Fig. 4.4).

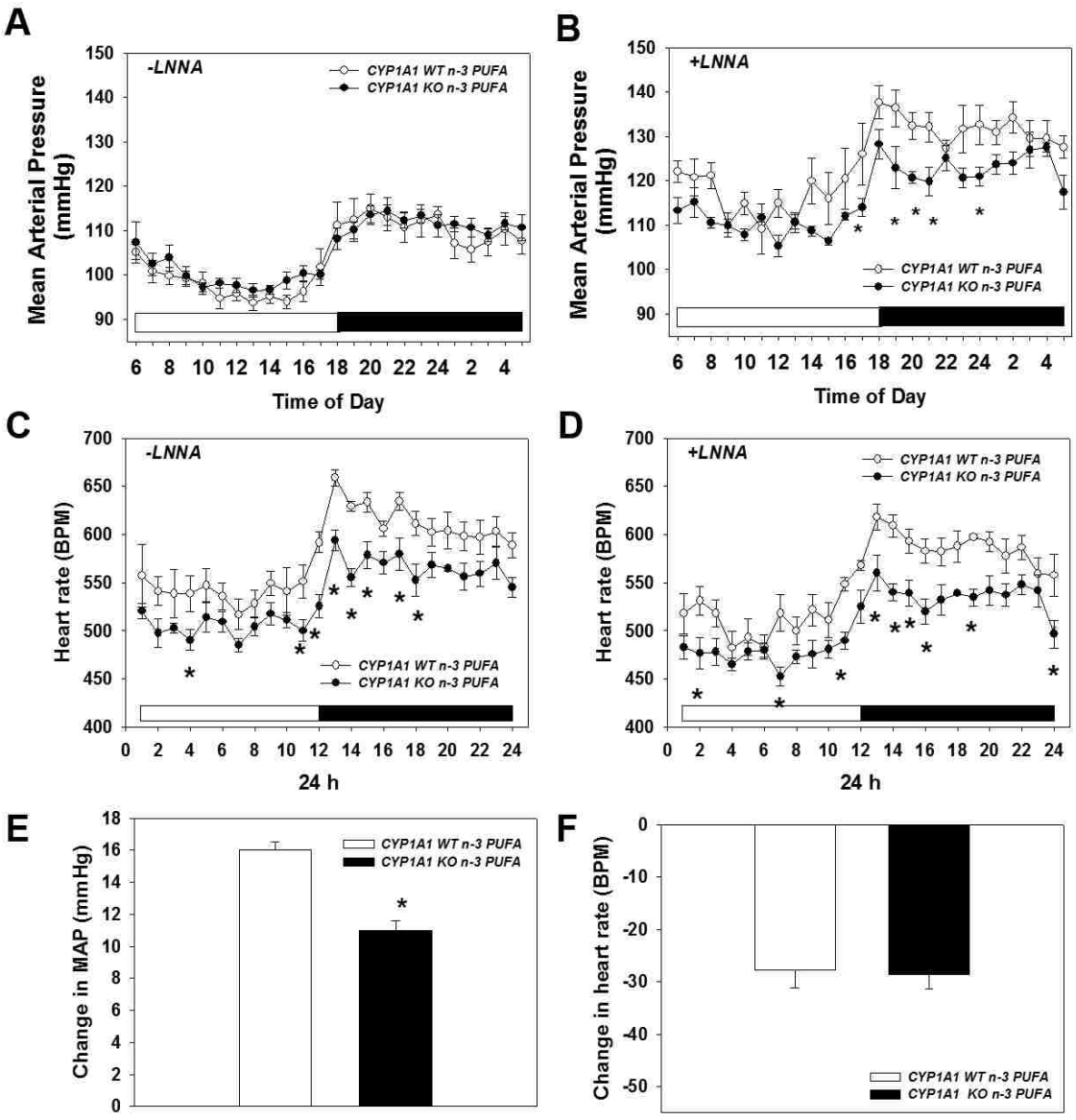

Figure 4.3. Effects of an n-3PUFA-enriched diet ± LNNA on mean hourly BP and HR in CYP1A1 WT and KO mice. (A) Hourly MAP over a 24 hr period , (B) Hourly MAP over a 24 hr period after NOS inhibition by LNNA, (C) Hourly HR and (D) Hourly HR after NOS inhibition by LNNA. (E) Change in MAP and (F) Change in HR following NOS inhibition. Data represent mean ± SEM and were analyzed by two-way, repeated measures ANOVA, using post hoc Holm-Sidak comparisons; *$p < 0.05$, compared to corresponding CYP1A1 WT (A-D), and by Student's t-test (E and F) (n=4-7/genotype).

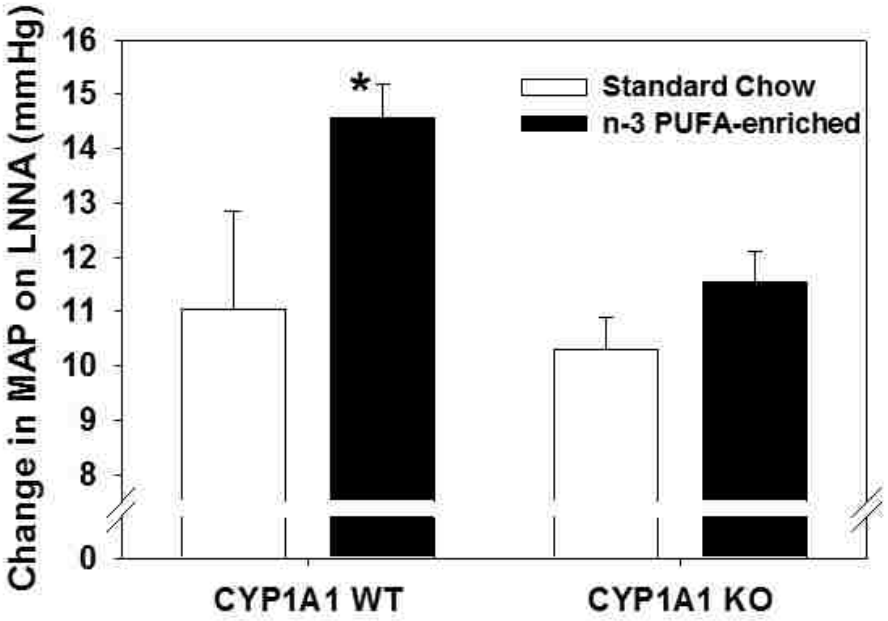

Figure 4.4. Effects of NOS inhibition on MAP in CYP1A1 WT and KO mice fed standard chow and an n-3 PUFA-enriched diet. Change in MAP following NOS inhibition by LNNA. Data represent mean ± SEM and were analyzed by two-way ANOVA, using post hoc Holm-Sidak comparisons; *$p < 0.05$ (n=4-7/genotype).

Effects of an n-6 PUFA-enriched diet ± LNNA on mean hourly BP and HR in CYP1A1 WT and KO mice

To determine if a loss of NO contributed to the increase in BP in CYP1A1 WT mice fed an n-6 PUFA-enriched diet, we treated CYP1A1 WT and KO mice with the NOS inhibitor, LNNA as described above. Hourly MAP over a 24 hr period prior to LNNA treatment was comparable between CYP1A1 WT and KO mice (Fig. 4.5A). Following NOS inhibition, hourly MAP increased, but remained similar between genotypes (Fig. 4.5B). Additionally, hourly HR over a 24 hr period was similar between genotypes both before (Fig. 4.5C) and after NOS inhibition (Fig. 4.5D). Finally, the increase in MAP (Fig. 4.5E) and decrease in HR (Fig. 4.5F) following NOS inhibition did not differ between genotypes.

Effects of n-3 PUFA-enriched diet on acute Ang II responsiveness in CYP1A1 WT and KO mice in vivo.

To determine if the CYP1A1 KO mice fed an n-3 PUFA-enriched exhibited an enhanced response to vasoconstriction, we challenged CYP1A1 WT and KO mice with a bolus dose of Ang II (30 µg/kg) and recorded BP starting 5 min after *i.p.* injection. An immediate, robust increase in BP following Ang II injection was observed in both genotypes; however, the increase in systolic BP was significantly greater in CYP1A1 KO mice, compared to WT mice, during the first 5 minutes following Ang II administration as well as from 10-15 min and 20-30 min post injection (Fig. 4.6A). Area under the curve analysis following Ang II injection showed that systolic BP was significantly increased in CYP1A1 KO mice (WT, 938 ± 90; KO, 1250 ± 51, $p<0.05$) (Fig. 4.6B).

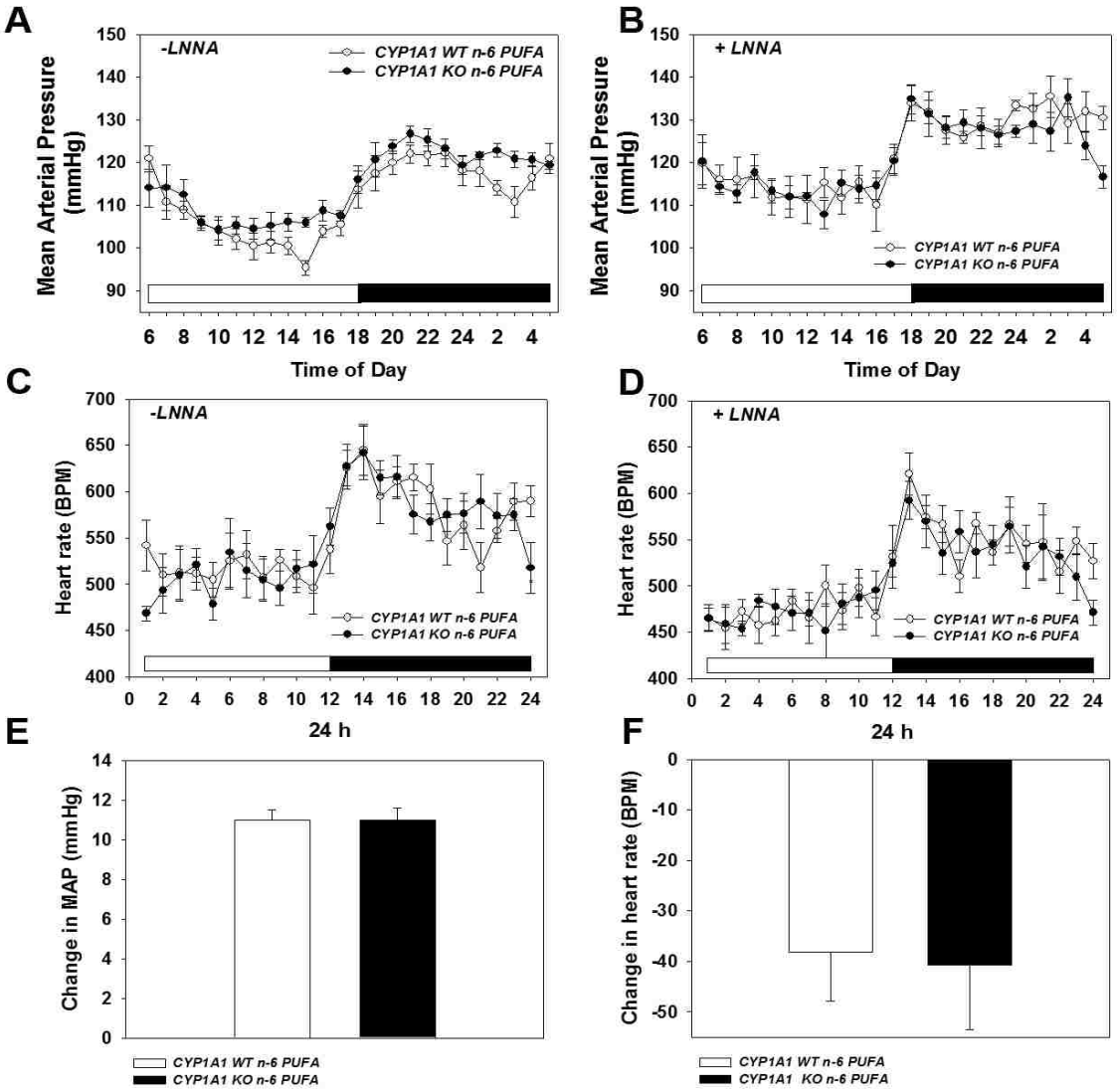

Figure 4.5. Effects of an n-6 PUFA-enriched diet ± LNNA on mean hourly BP and HR in CYP1A1 WT and KO mice. (A) Hourly MAP over a 24 hr period , (B) Hourly MAP over a 24 hr period after NOS inhibition by LNNA, (C) Hourly HR, and (D) Hourly HR after NOS inhibition by LNNA. (E) Change in MAP and (F) Change in HR following NOS inhibition. Data represent mean ± SEM and were analyzed by two-way, repeated measures ANOVA, using post hoc Holm-Sidak comparisons; *$p < 0.05$, compared to corresponding CYP1A1 WT (A-D), and by Student's t-test (E and F) (n=4-7/genotype).

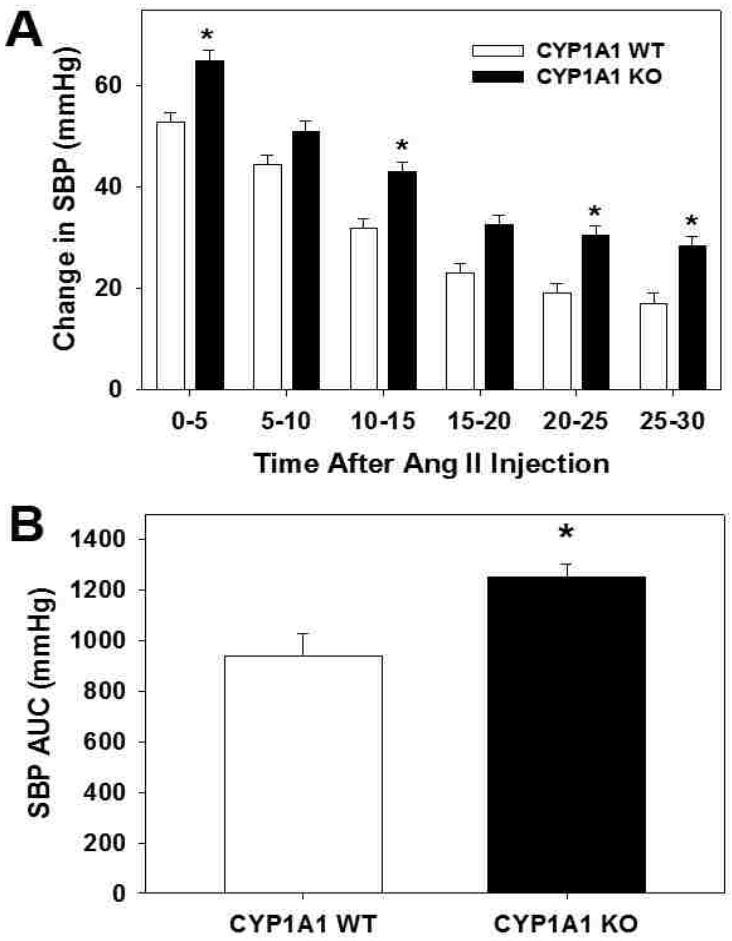

Figure 4.6. Effects of n-3 PUFA-enriched diet on acute Ang II responsiveness in CYP1A1 WT and KO mice *in vivo*. (A) Increase in systolic BP (SBP) and (B) Area under the curve analysis for 30 min following *i.p*. injection of Ang II (30 µg/kg). BP was recorded starting after 5 mins of Ang II administration. Data represent mean ± SEM and were analyzed by two-way, repeated measures ANOVA, using post hoc Holm-Sidak comparisons; *$p < 0.05$ compared to CYP1A1 WT (A). Data in (B) were analyzed by Student's t-test. (n=4/genotype).

Effects of n-3 and n-6 PUFA-enriched diets on aortic eNOS and phospho-eNOS protein expression in CYP1A1 WT and KO mice

To further elucidate the potential contribution of NOS to differences in BP, we measured protein expression of eNOS and phospho-eNOS from aortas of CYP1A1 WT and KO mice fed an n-3 or an n-6 PUFA-enriched diet. We found that eNOS protein expression in the aorta was not different between CYP1A1 WT and KO mice between diets (Fig. 4.7A-D). In contrast, phospho-eNOS protein expression was significantly reduced in CYP1A1 KO mice fed an n-3 PUFA-enriched diet, compared to WT mice (Fig. 4.8A and B). There was no difference in phospho-eNOS expression between CYP1A1 WT and KO mice fed an n-6 PUFA-enriched diet (data not shown).

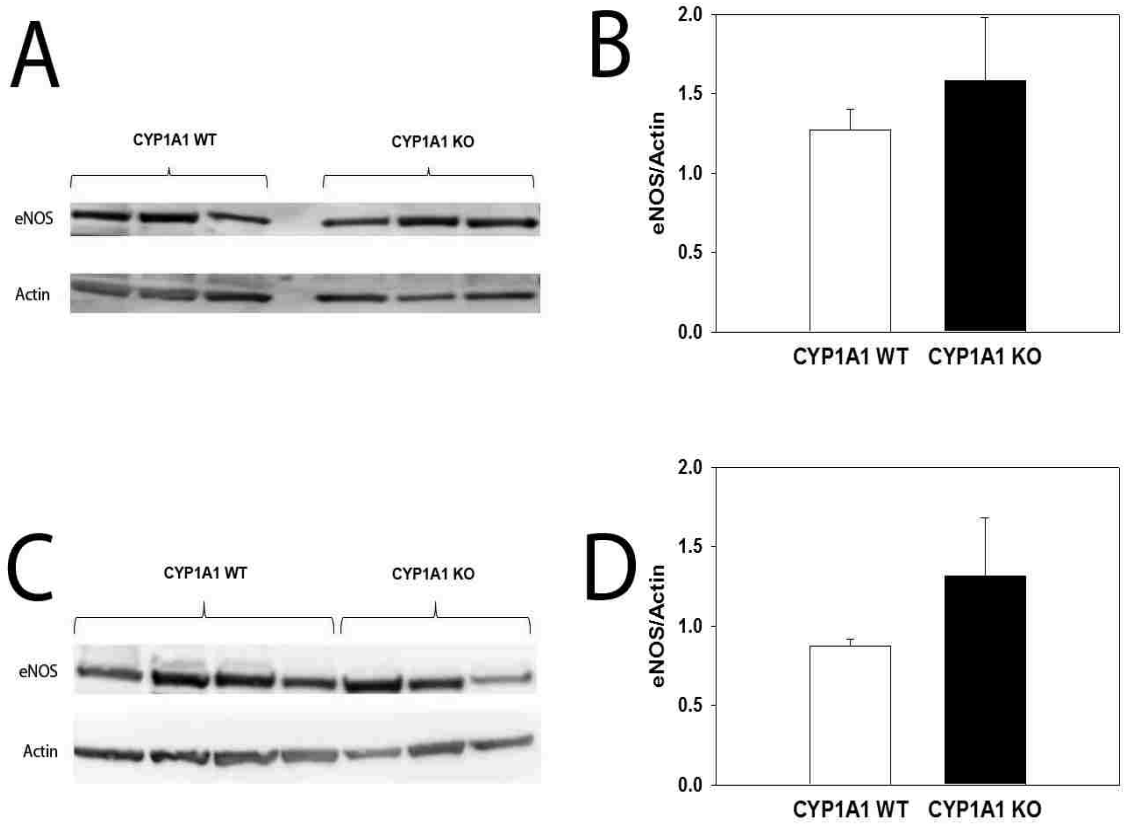

Figure 4.7. Effects of n-3 and n-6 PUFA-enriched diets on aortic eNOS protein expression in CYP1A1 WT and KO mice. Aortic eNOS protein expression and quantification relative to β-actin in CYP1A1 WT and KO mice fed an n-3 PUFA-enriched diet (A and B), or an n-6 PUFA-enriched diet (C and D). Data represent mean ± SEM and were analyzed by Student's t-test; *$p < 0.05$, compared to corresponding WT (n=3-4/genotype/diet)

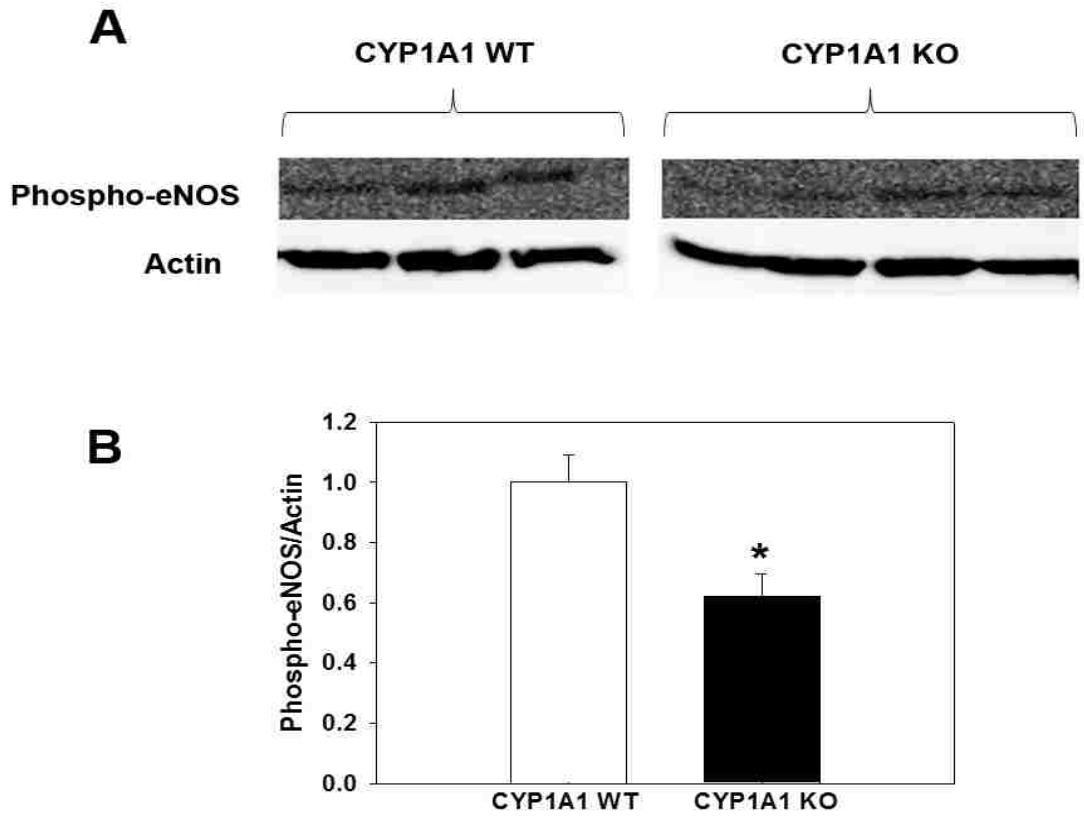

Figure 4.8. Effects of an n-3 PUFA-enriched diet on aortic phospho-eNOS protein expression in CYP1A1 WT and KO mice. (A) Aortic p-eNOS and β-actin protein expression, (B) Quantification of p-eNOS protein expression relative to β-actin in CYP1A1 WT and KO mice fed an n-3 PUFA-enriched diet. Data represent mean ± SEM and were analyzed by Student's t-test; *$p < 0.05$, compared to WT. (n=3-4/genotype)

Effects of n-3 and n-6 PUFA-enriched diets on ACh-mediated vasodilation, and U46619-dependent vasoconstriction in mesenteric arterioles of CYP1A1 KO and WT mice

To determine if vascular reactivity was altered in mice fed an n-3 or n-6 PUFA-enriched diet, we assessed mesenteric arteriolar vasodilation to ACh and vasoconstriction to U46619. We found that CYP1A1 KO mice on an n-3 PUFA-enriched diet exhibited an attenuated, dose-dependent vasodilation to ACh, compared to WT mice (Fig. 4.9A). In contrast, there was no difference in ACh-mediated vasodilation between CYP1A1 WT and KO mice on an n-6 PUFA-enriched diet (Fig. 4.9B). Further, dose-dependent vasoconstriction to U46619 did not differ between genotypes on either diet (Fig. 4.9C and D).

Effects of n-3 and n-6 PUFA-enriched diets on plasma NOx levels

To determine if CYP1A1 WT and KO mice exhibited differences in systemic levels of NO, we measured plasma NOx. We found that plasma NOx levels were not different between CYP1A1 WT and KO mice on neither an n-3 PUFA-enriched diet nor an n-6 PUFA-enriched diet (Fig. 4.10).

Effects of standard chow, n-3 and n-6 PUFA-enriched diets on cardiac TBARS levels

To determine the effects of the different diets on tissue oxidative stress levels, we measured cardiac TBARS. Levels of cardiac TBARS were significantly elevated in CYP1A1 WT and KO mice on an n-3 PUFA-enriched diet, compared to mice on standard chow or an n-6 PUFA-enriched diet (Fig. 4.11). Nonetheless, the effects of the different diets on TBARS levels were independent of genotype.

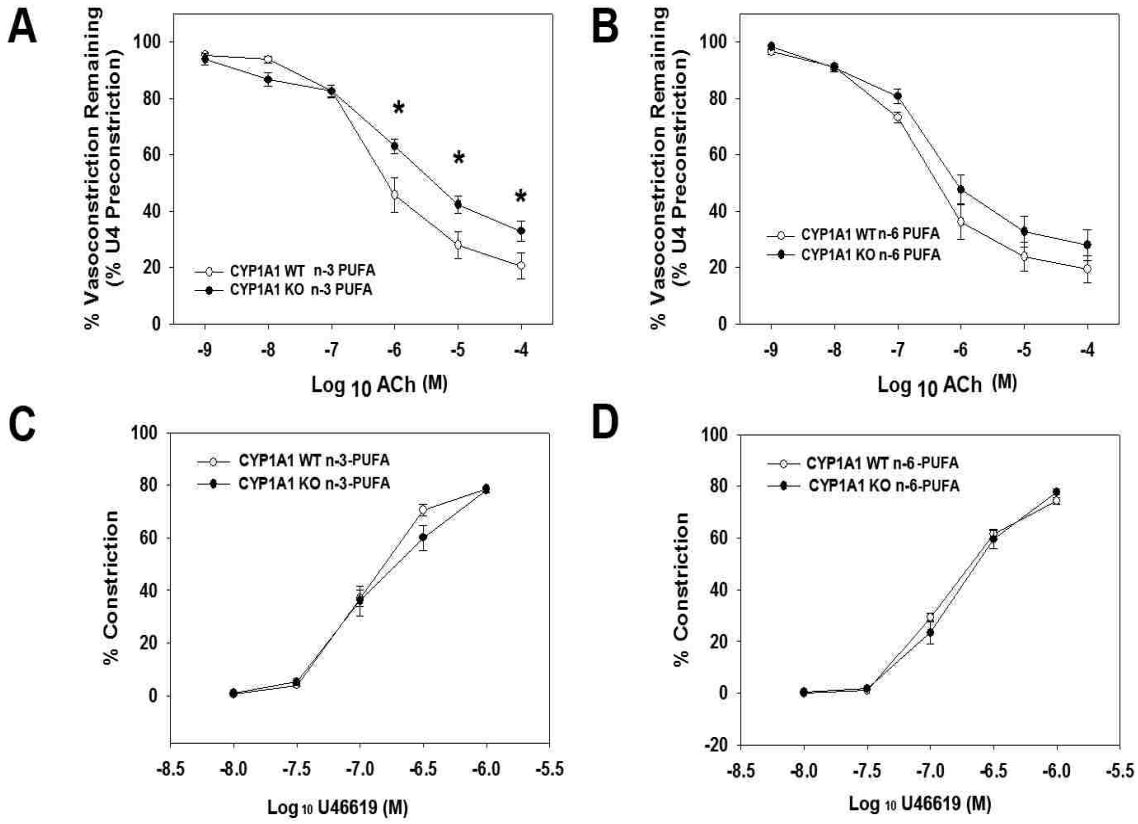

Figure 4.9. Effects of n-3 and n-6 PUFA-enriched diets on ACh-mediated vasodilation and U46619-dependent vasoconstriction in mesenteric arterioles of CYP1A1 WT and KO mice. (A) ACh-mediated relaxation in mesenteric arterioles of CYP1A1 WT and KO mice fed an n-3 PUFA-enriched diet or (B) an n-6 PUFA-enriched diet. (C) U46619-mediated vasoconstriction in mesenteric arterioles of CYP1A1 WT and KO mice fed an n-3 PUFA-enriched diet or (D) an n-6 PUFA-enriched diet. Data represent mean ± SEM and were analyzed by two-way, repeated measures ANOVA, using post hoc Holm-Sidak comparisons; *$p < 0.05$, compared to corresponding WT (n=8/genotype/diet).

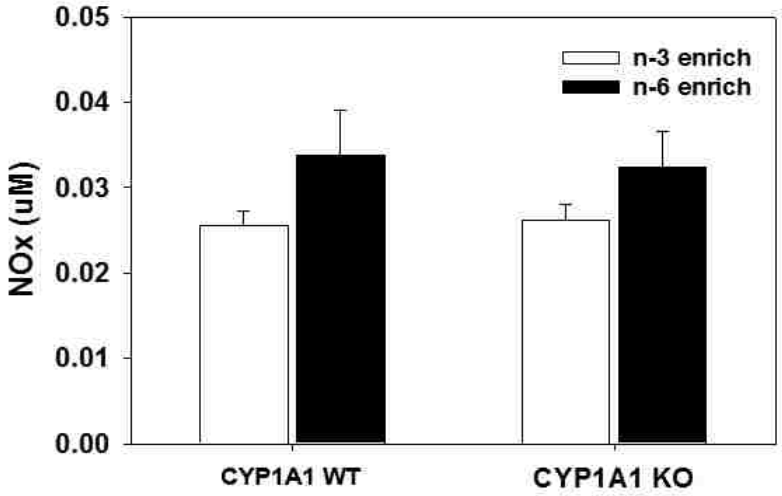

Figure 4.10. Effects of n-3 and n-6 PUFA-enriched diets on plasma NOx levels. Plasma NOx level in CYP1A1 WT and KO fed either an n-3 PUFA-enriched diet or an n-6 PUFA-enriched diet. Data represent mean ± SEM and were analyzed by Student's t-test (n=5/genotype/diet).

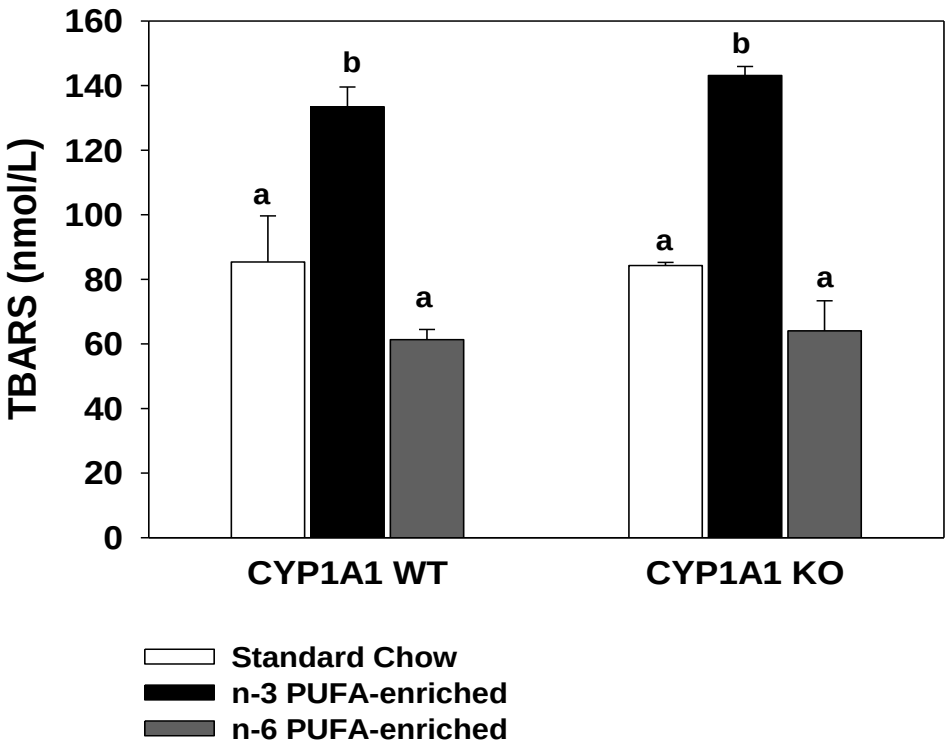

Figure 4.11. Effects of standard chow, n-3 PUFA-enriched diet, and n-6 PUFA-enriched diet on cardiac TBARS levels. Cardiac TBARS levels in CYP1A1 WT and KO mice fed standard chow, an n-3 PUFA-enriched diet and an n-6 PUFA-enriched diet. Data represent mean ± SEM and were analyzed by Student's t-test. Bars with the same letters are not different from each other. *$p < 0.05$ (n=5/genotype/diet).

E. DISCUSSION

These results show that an n-3 PUFA-enriched diet effectively reduces BP in CYP1A1 KO mice to CYP1A1 WT levels, demonstrating that CYP1A1 is not solely required to mediate the antihypertensive benefits of n-3 PUFAs. Further, our results show that the benefits of the n-3 PUFA diet on BP result, in part, by increases in NO as is illustrated by the significantly greater increase in BP when WT mice are treated with a NOS inhibitor, compared to WT mice on standard chow or an n-6 PUFA diet. Interestingly, CYP1A1 is required to mediate the n-3 PUFA-dependent increase in NO, since BP does not increase to the same extent in CYP1A1 KO mice treated with a NOS inhibitor, compared to WT mice. The contribution of CYP1A1 to n-3 PUFA-dependent increases in NO is further illustrated by the significantly reduced expression of phospho-eNOS protein and the attenuation of ACh-mediated vasodilation in CYP1A1 KO mice, compared to WT mice on the n-3 PUFA diet. Finally, our results show that BP and vascular reactivity of CYP1A1 WT and KO mice are essentially identical when fed an n-6 PUFA-enriched diet, suggesting that CYP1A1 is not necessary for n-6 PUFA-dependent regulation of BP or vascular homeostasis

Numerous studies demonstrate that an n-3 PUFA-enriched diet or n-3 PUFA supplements can lower BP in hypertensive laboratory animals and human subjects. For example, an n-3 PUFA-enriched diet fed for two months decreases BP in aged male and female spontaneously hypertensive rats (Mitasikova *et al.*, 2008; Dlugosova *et al.*, 2009). Similarly, n-3 PUFAs significantly reduce hypertension in rats infused with Ang II (Hui *et al.*, 1989). Moreover, a meta-analysis of 31 placebo-controlled trials shows that n-3 PUFAs significantly reduce BP in hypertensive humans and exhibit a dose-dependent

effect (Morris *et al.*, 1993). Our data showing that an n-3 PUFA-enriched diet fed for two months significantly reduces MAP in modestly hypertensive CYP1A1 KO mice is consistent with these previously published studies. Further, our results show that CYP1A1 is not required to mediate this decrease. In addition, we found that an n-3 PUFA-enriched diet does not reduce MAP in normotensive C57BL/6J mice. This is in contrast to a limited number of studies that show n-3 PUFAs also can reduce BP in normotensive animals and humans (Mori *et al.*, 1999; Dlugosova *et al.*, 2009; Liu *et al.*, 2011).

One mechanism by which n-3 PUFAs may regulate vascular function and BP is thought to involve an increase in NO bioavailability and signaling. In cultured HUVECs, n-3 PUFAs increase the translocation of eNOS from caveolin to the cytosol, a step required for activation (Omura *et al.*, 2001; Li *et al.*, 2007a; Li *et al.*, 2007b) and subsequently lead to increases in NO production, while in EA hy 926 endothelial cells n-3 PUFAs increase the expression of phospho-eNOS, the activated form of the enzyme (Gousset-Dupont *et al.*, 2007). Additionally, *in vivo* studies demonstrate that rats fed n-3 PUFAs exhibit increases in aortic eNOS expression (Ma *et al.*, 2004), activity (Dlugosova *et al.*, 2009), and NO production (Lopez *et al.*, 2004), as well as improvements in NO-dependent vasodilation (Matsumoto *et al.*, 2009). Finally, a meta-analysis of randomized controlled human trials shows that n-3 PUFA supplements significant improve NO-dependent brachial artery vasodilation (Wang *et al.*, 2012).

Although CYP1A1 is not required to mediate the decrease in BP by the n-3 PUFA diet, a number of lines of evidence from our study suggest that CYP1A1 does mediate increases in NO bioavailability resulting from the n-3 PUFA diet. We found that aortic

phospho-eNOS protein expression is significantly lower in CYP1A1 KO mice fed an n-3 PUFA-enriched diet, compared to WT mice. Further, ACh-mediated vasodilation is significantly attenuated in CYP1A1 KO mice fed an n-3 PUFA-enriched diet, compared to WT mice. Finally, the increase in BP resulting from NOS inhibition is significantly less in CYP1A1 KO mice fed an n-3 PUFA-enriched diet, compared to WT mice. These results suggest that CYP1A1 contributes to n-3 PUFA-dependent increases in NO. The mechanism underlying these observations remains to be elucidated; however, limited evidence supports the notion that there may be cross-talk between caveolin-1, CYP1A1, and eNOS (Lim *et al.*, 2007). Nonetheless, since eNOS knockout mice are hypertensive (Shesely *et al.*, 1996), it will be interesting to elucidate the contribution of n-3 PUFAs in reducing BP in the eNOS knockout mice, and the mechanisms involve.

One particularly surprising observation is that the n-6 PUFA-enriched diet significantly increases BP in CYP1A1 WT mice, but has no effect in CYP1A1 KO mice, compared to these same mice fed a standard chow diet. These results, however, are consistent with studies showing n-3 PUFA deficient diets lead to increases in BP. Ren-2 rats that have high levels of Ang II show significantly higher BP when maintained on an n-3 PUFA deficient diet from conception (Jayasooriya *et al.*, 2008). Similarly, rats fed n-3 PUFA deficient diets from the prenatal period through adulthood show significantly higher BP at 9 months of age (Begg *et al.*, 2012). While our n-6 PUFA-enriched diet did not contain any detectable amounts of n-3 PUFAs, we would not have expected that the two month duration of feeding was sufficiently long to deplete all endogenous n-3 PUFAs. Nonetheless, results of the tissue and blood analysis of PUFA and PUFA metabolites from

CYP1A1 WT and KO on each diet should help us to further interpret the changes in BP observed following the n-6 PUFA-enriched diet.

Lastly, we also observed fundamental differences in body and organ weights in CYP1A1 WT and KO mice fed either an n-3 PUFA or n-6 PUFA-enriched diet. We reported previously that CYP1A1 KO mice fed standard chow exhibit reduced body, heart, kidney and liver weights, compared to WT mice (Kopf *et al.*, 2010)(Agbor *at el.*, unpublish data). Notably, however, our current findings show that body and organ weights of CYP1A1 KO mice are normalized by an n-3 PUFA-enriched diet, but not an n-6 PUFA-enriched diet. Rockett *et al.*, (2010, 2012) report that high doses of n-3 PUFAs increase body weight and reduce activity of C57BL/6 mice. Similarly, mice fed an n-3 PUFA-enriched diet exhibited significant increase in body weight at 14 weeks, compared to control diet (Anderson *et al.*, 2012). Since CYP1A1 KO mice exhibit significantly lower activity on the n-3 PUFA-enriched diet (data not shown), compared to WT mice, this could account for the normalization of body and organ weights. Nonetheless, additional studies assessing metabolic activity will be needed to determine if changes in physical activity are reflected by changes in metabolism.

In summary, our study demonstrates that an n-3 PUFA-enriched diet increases the contribution of NO to vascular function and BP regulation, and this is mediated, in part, by CYP1A1. Given that CYP1A1 is constitutively expressed in the vascular endothelium and is induced by physiological levels of shear stress (Han *et al.*, 2008; Conway *et al.*, 2009), this pathway could provide some cardiovascular and BP-lowering benefits following dietary intake of foods enriched in n-3 PUFAs, in addition to regular exercise

regimens. Future studies are however, needed to investigate crosstalk between CYP1A1 and NOS signaling in contributing to the BP lowering effects of n-3 PUFAs.

V. CHAPTER 5

Conclusion and future directions

I. *Endothelial cell-specific aryl hydrocarbon receptor knockout (ECahr$^{-/-}$) mice and blood pressure (BP) regulation.*

Conclusion

Our primary objective was to develop an endothelial cell-specific aryl hydrocarbon receptor (AHR) knockout (KO) (*ECahr*$^{-/-}$) mouse to investigate the contribution of endothelial AHR to BP regulation. We successfully generated *ECahr*$^{-/-}$ mice with genetic deletion of the AHR in the endothelium using *cre-lox* recombination, and our data revealed that *ECahr*$^{-/-}$ mice are hypotensive, similar to the BP phenotype of the AHR KO mice (Zhang *et al.*, 2010). This demonstrates that endothelial-expressed AHR is a critical regulator of vascular tone and BP.

Hypotension in *ECahr*$^{-/-}$ mice was associated with altered gene expression of tissue renin angiotensin system (RAS) components, as well as decreased protein expression of aortic angiotensin 1 receptor (AT1R). In addition, the reduced BP was mediated, in part, by a reduced vasoconstriction response to Ang II, measured both *in vivo* and *ex vivo* in *ECahr*$^{-/-}$ mice, compared to *ECahr*$^{-+/+}$ mice. Vasoreactivity studies in the aorta showed a significant reduction in vasoconstriction to Ang II in the *ECahr*$^{-/-}$ mouse aorta in the presence of perivascular adipose tissue (PVAT). Additionally, renin and AT1R mRNA expression were significantly reduced in the visceral white adipose tissue. Nonetheless the specific mechanism through which the AHR regulates AT1R expression is still unclear and warrants further investigation.

Classically, the AHR modulates gene expression by binding to dioxin response elements (DRE) containing the core recognition motif 5'-TNGCGTG-3' (Denison *et al.*, 1989). Interestingly, several DRE sequences are located in the promoter region of both the mouse AT1a and AT1b genes, supporting the possibility that expression of the mouse AT1R in the vasculature could directly be modulated by the AHR. Supporting evidence for this comes from studies where activation of the AHR by TCDD was demonstrated to sensitize mice to Ang II-mediated hypertension. Taken together, this suggests that AHR expression in the endothelium is particularly important to normal vascular responsiveness to Ang II and thus, BP regulation.

Future direction

Although our findings establish an association between loss of endothelial AHR and reduced RAS signaling, it does not elucidate how the AHR regulates the AT1 receptor. Therefore, future studies should focus on determining the interaction between the AHR and the AT1 receptor. One possible way to investigate this is in cell culture studies. Using human umbilical vein endothelial cells, the AHR receptor could be knocked down by RNA interference. AT1 mRNA and protein expression profiles from both siRNA treated and untreated cells would demonstrate whether the loss of AHR contributes to the downregulation and reduced expression of the AT1 receptor mRNA and protein. If this is not the case, since the mRNA of AHR and its downstream target gene, CYP1A1, have been shown to be inducible in vsmc (Kerzee and Ramos, 2001), targeted knockdown of AHR could also be conducted in vsmc in culture.

The AHR activates its gene battery by binding to DREs in the promoters of genes to turn them on (Boutros *et al.*, 2004; Tijet *et al.*, 2006). Interestingly, the AT1 receptor gene sequence harbors several DREs in its promoter; however, their transcriptional regulation by the AHR has not been demonstrated. It is plausible therefore, that basal AHR levels could contribute to the expression of constitutive AT1 receptor by binding to DREs in its promoter region. To investigate this, we could use a luciferase reporter plasmid system containing specific nucleotide deletions of the AT1 receptor promoter, and transfect into cell lines, for example HEK29 cell lines. Following treatment with an AHR agonist such as dioxin, we could determine by luciferase activity measurements, if specific DNA regions of the AT1 receptor promoter region is regulated by the AHR.

To further elucidate how the AHR could regulate the AT1 receptor, we could conditionally delete the AHR specifically from the vsmc in mouse, to determine if AHR in vsmc alters Ang II signaling and BP *in vivo*. Notably, mice expressing *cre*-recombinase driven under a vsmc specific promoter, smooth muscle 22-alpha (SM-22α), could be bred to mice harboring exon 2 of the AHR gene flanked by lox-P sites. Through two generation of breeding, mice that are *cre*-positive or negative but harbor the floxed AHR allele could be used as conditional knockouts and wildtype controls, respectively. AT1R mRNA and protein levels in aorta and mesenteric arterioles could be determined. In addition, BP could also be measured using radiotelemetry to demonstrate whether the loss of AHR only from the vsmc is involved in BP regulation. If a significant reduction in BP is not seen, then an acute *in vivo* challenge to Ang II could be conducted to determine if a vascular deficit is present in the vasculature as a result of loss of AHR from vsmc.

In summary, the contributions of the endothelial AHR to BP regulation and the underlying mechanisms involved are not well understood. Nonetheless, the findings from this study and those from the AHR KO mice suggests that there is significant cross talk between AHR signaling and the RAS and future studies delineating this interaction would be necessary.

In conclusion, the results from the AHR KO and the *ECahr*$^{-/-}$ mice show that both models are hypotensive, suggesting that global deletion of the AHR or loss of the AHR specifically from the vascular endothelium contributes to hypotension, in part, by significantly attenuating Ang II responses. Taken into account that RAS is the primary contributor to the pathogenesis of hypertension, it is plausible that the AHR crosstalk with the RAS. The implication therefore is that specific AHR antagonists could be designed and tested as potential anti-hypertensives in the treatment of high BP in humans, in combination with other anti-hypertensive agents including Ang converting enzyme inhibitors.

II. *Cytochrome P4501A1 knockout (CYP1A1 KO) mice and BP regulation*

Conclusion

The findings reported herein show that CYP1A1 KO mice exhibit elevated BP with a reduced HR. Systolic BP was significantly elevated at nighttime periods of increased activity, while diastolic BP was significantly increased across 24 hr period, compared to WT mice. Additionally, CYP1A1 KO mice exhibited attenuated vasodilation to DHA and EPA in the aorta and mesenteric arterioles, but normal responses to NOS inhibition and aortic vasorelaxation to ACh and SNAP, suggesting that elevated BP in

CYP1A1 KO mice is not associated with loss of NO. Our data further demonstrate that putative CYP1A1 metabolites of EPA and DHA, 17,18-EEQ and 19,20-EDP, are potent and efficacious vasodilators. Lastly, inhibition of Kv channel significantly inhibited DHA-mediated vasodilation in mesenteric arterioles. Our data suggests that the limiting factor could be the amount of vasodilator metabolites produced by CYP1A1 metabolism of n-3 PUFAs. Taken together, the findings from our study show for the first time that CYP1A1 is required in maintaining normal levels of BP.

In addition, diets enriched in n-3 PUFAs contributed significantly in lowering BP in CYP1A1 KO mice. Notably, elevated BP in CYP1A1 KO mice was lowered to comparable WT levels after supplementing for 2 months with an n-3 PUFA-enriched diet, with no effects in CYP1A1 WT mice. In contrast, BP in WT mice significantly increased after supplementing with an n-6 PUFA-enriched diet, with no effect in CYP1A1 KO mice. Phospho-eNOS protein expression was significantly reduced in the aorta of CYP1A1 KO mice fed an n-3 PUFA-enriched diet, compared to CYP1A1 WT mice. Moreover, although BP was reduced in the CYP1A1 KO mice fed an n-3 PUFA-enriched diet, following NOS inhibition, BP increase was significantly less in CYP1A1 KO, compared to WT mice. Additionally, ACh-mediated vasodilation was attenuated in mesenteric arterioles from CYP1A1 KO mice fed an n-3 PUFA-enriched diet, compared to WT mice, with no difference in mice on an n-6 PUFA-enriched diets. Although we have previously reported that CYP1A1 KO mice exhibited reduced body and organ weights on standard chow (Kopf *et al.*, 2010), our data herein show that body and organ weights of CYP1A1 KO mice were normalized by an n-3 PUFA-enriched diet, but not on an n-6 PUFA-enriched diet. Consistent with studies demonstrating that n-3 PUFA supplementation

results in weight gain via reduced activity in mice (Anderson *et al.*, 2012; Rockett *et al.*, 2012), average 24 hr and nighttime activity measurements were significantly reduced in CYP1A1 KO mice, compared to CYP1A1 WT mice on an n-3 PUFA-enriched diet.

Taken together, our study suggests that the mechanism of action of n-3 and n-6 PUFAs might be different. As seen, the difference in BP phenotypes between n-3 and n-6 PUFA-enriched diets demonstrate that both diets could have opposing effects in contributing to vascular tone and BP control, and involves CYP1A1. Thus, increasing substrate availability via n-3 PUFA supplementation, changes the BP phenotype of CYP1A1 KO mice towards that of WT mice, and depleting substrate availability via n-6 PUFA supplementation changes the BP phenotype of CYP1A1 WT mice to that of CYP1A1 KO mice.

Future directions

The phenotype of the CYP1A1 KO mouse provides a good model to further elucidate the physiological role of CYP1A1 in contributing to cardiovascular homeostasis. The hypertensive phenotype strongly suggests that CYP1A1 is involved in contributing to vascular tone and BP regulation. Although CYP1A1 has been demonstrated to be induced by physiological levels of shear stress in vascular endothelial cells (Han *et al.*, 2008; Conway *et al.*, 2009), its beneficial role following shear-induction has not been elucidated. To initially investigate this, vascular endothelial cells from CYP1A1 WT and KO mice could be isolated and cultured. Following NOS inhibition with LNNA (100 µM), endothelial cells could be subjected to laminar shear stress of 15-25 dynes/cm^2, and the media collected and applied to pressurized mesenteric arterioles from C57BL/6J mice,

preconstricted to U46619. Mesenteric vasodilation can be monitored and compared to media subjected to no shear stress. Further, we could also investigate this *in vivo* using radiotelemetry to monitor BP. Notably, in CYP1A1 WT and KO mice, following NOS inhibition, MAP could be measured prior to, during, and following an exercise regimen (Harri *et al.*, 1999).

Although our studies show that CYP1A1 KO mice exhibited attenuated vasodilation to EPA and DHA in the aorta and mesenteric arterioles, these studies were carried out without any luminal flow, thereby not mimicking *in vivo* conditions that incorporate flow mediated dilation (FMD). It will be logical therefore for future studies to be conducted under varied degrees of luminal flow, since CYP1A1 has been demonstrated to be inducible by physiological levels of shear stress (Han *et al.*, 2008; Conway *et al.*, 2009). It is plausible we might expect to see even wider differences in vasodilation responses to n-3 PUFAs; EPA and DHA under flow conditions.

In addition to elucidating the contribution of CYP1A1 to shear induced vasorelaxation, it would be necessary to determine also the concentrations of n-3 PUFA metabolites from CYP1A1 metabolism of n-3 PUFAs in plasma and red blood cells, and also following treatment with diets enriched in n-3 or n-6 PUFAs. Since our data suggests that differential level of metabolites may drive the hypertension in CYP1A1 KO mice, using liquid chromatography–mass spectrometry (LC/MS/MS), we could measure these metabolites. Additionally, since diastolic BP is significantly elevated across 24 hr period in CYP1A1KO mice, this could suggest that CYP1A1 metabolism of n-3 PUFA contributes to maintaining peripheral vascular resistance. Future studies that assess cardiac output and stroke volume could be done to confirm if peripheral vascular resistance is altered in

the absence and presence of n-3 or n-6 PUFA supplementation in CYP1A1 WT and KO mice.

Furthermore, it would be very insightful to elucidate the contribution of CYP1A1 in maintaining membrane potential in vascular endothelial cells and vsmc, in the presence or absence of n-3 or n-6 PUFAs. Endothelial and vsmc could be isolated from CYP1A1 WT and KO mice and patch clamp experiments conducted to determine membrane potential prior to, and following treatment with n-3 or n-6 PUFAs. These studies could also be repeated in the presence or absence of inhibitors of BK and Kv membrane channels. This information will help determine the contribution of CYP1A1 to the hyperpolarization of the plasma membrane in general and elucidate further, alternative mechanisms of PUFA-mediated vasodilation in particular.

While the role of CYP1A1 in BP regulation and the cardiovascular system in general is not clearly understood, it is noteworthy that several polymorphisms in the CYP1A1 gene exist in the human population. For example, a common allelic variant of human CYP1A1 (*Ile462Val*) was shown to metabolize EPA in a different pattern, and the catalytic efficiency of this polymorphism for hydroxylation was five times higher, while that for epoxidation was twice higher than that of CYP1A1 WT (Schwarz *et al.*, 2005). This suggests that CYP1A1 metabolism of n-3 PUFAs could contribute to differences between individuals in the production of beneficial physiologically active PUFA metabolites in the cardiovascular system.

In summary, the nutritional benefits of n-3 PUFAs to the cardiovascular system remain not fully understood. Nonetheless, our data demonstrate a BP lowering effect of n-3 PUFAs in CYP1A1 KO mice. This suggests that n-3 PUFA-enriched diets could

contribute in lowering BP in hypertensive human subjects. Regardless of the BP lowering effects of n-3 PUFAs, our study also demonstrates that n-3 and n-6 PUFAs lower triglycerides levels, and overall, this is beneficial to cardiovascular human health. More clinical trial studies could be conducted to determine the amount and benefits of daily intake of n-3 PUFAs as supplements in humans, as a protection strategy against cardiovascular diseases.

Currently, the American Heart Association (AHA) recommends 1 g EPA+DHA/day for patients with known coronary heart disease (CHD). Additionally, for individuals with no CHD, the AHA recommends the consumption of two oily fish meals per week, which would provide 400–500 mg EPA+DHA/day (Kris-Etherton *et al.*, 2002). However, if fish meals are not desirable, fish supplements as capsules could also be taken. It is recommended that fish supplements as capsules be labeled as 'molecularly distilled' since this process removes polychlorinated biphenyls contaminants.

In summary, as show by our data herein, 17,18-EEQ and 19,20-EDP will be excellent and potential anti-hypertensive candidates. It is important therefore, for future studies to look at clinical trials of CYP1A1 metabolites of n-3 PUFAs; 17,18-EEQ and 19,20-EDP as anti-hypertensives, and the development of stable analogues of these metabolites to treat long-term resistant hypertension.

The conclusion from our study is that the AHR and its downstream target gene, CYP1A1, regulate BP through different pathways and involve the perivascular adipose tissue (PVAT). Our findings show that loss of AHR in the endothelium resulted in a hypotensive phenotype, consistent with the BP phenotype of the global AHR KO mouse, independent of NO. Additionally, the hypotension was associated with reduced Ang II

responses *ex vivo,* in the presence of PVAT. This suggests that loss of AHR in the endothelium alters paracrine signaling in the adipose tissue and supports a role for the PVAT in contributing to blood pressure regulation. Although AHR is deleted in endothelium, CYP1A1 is still expressed in the adipose tissue and could also contribute to the pro-hypotensive effects seen in the *ECahr*$^{-/-}$ mice. Our study further show that global deletion of CYP1A1, in contrast, resulted to a hypertensive phenotype associated with reduced vasorelaxation to EPA and DHA. The elevated BP was independent of NO, suggesting that CYP1A1 metabolism of n-3 PUFAs contributes to BP regulation by the production of stereospecific products that exhibit vasodilatory properties. However, our results also show that loss of CYP1A1 could be compensated by other vascular P450 epoxygenases in the presence of n-3 PUFA substrate bioavailability. Although CYP1A1 was globally deleted, n-3 PUFA supplementation was shown to normalize BP in CYP1A1 KO mice to WT levels via a NO-dependent mechanism. It is plausible that the global deletion of CYP1A1 including in the PVAT, contributes to a pro-hypertensive phenotype in the CYP1A1 KO mice. In conclusion, although AHR is deleted in endothelium, adipose CYP1A1 could contribute to the hypotension seen in the *ECahr*$^{-/-}$ mouse. In contrast, the vasodilatory benefits of CYP1A1 including contributions from the PVAT is lost, contributing to an elevated BP as seen in the CYP1A1 KO mouse.

REFERENCES:

(1999). Dietary supplementation with n-3 polyunsaturated fatty acids and vitamin E after myocardial infarction: results of the GISSI-Prevenzione trial. *Lancet* **354**, 447-455.

Adachi, J., Mori, Y., Matsui, S., Takigami, H., Fujino, J., Kitagawa, H., Miller, C. A., Kato, T., Saeki, K., and Matsuda, T. (2001). Indirubin and indigo are potent aryl hydrocarbon receptor ligands present in human Urine. *J Biol Chem* **276**, 31475-31478.

Agbor, L. N., Elased, K. M., and Walker, M. K. (2011). Endothelial cell-specific aryl hydrocarbon receptor knockout mice exhibit hypotension mediated, in part, by an attenuated angiotensin II responsiveness. *Biochem Pharmacol* **82**, 514-523.

Anderson, E. J., Thayne, K., Harris, M., Carraway, K., and Shaikh, S. R. (2012). Aldehyde stress and up-regulation of Nrf2-mediated antioxidant systems accompany functional adaptations in cardiac mitochondria from mice fed n-3 polyunsaturated fatty acids. *Biochem J* **441**, 359-366.

Annas, A., and Brittebo, E. B. (1998). Localization of cytochrome P4501A1 and covalent binding of a mutagenic heterocyclic amine in blood vessel endothelia of rodents. *Toxicology* **129**, 145-156.

Annas, A., Brunstrom, B., and Brittebo, E. B. (2000). CYP1A-dependent activation of xenobiotics in endothelial linings of the chorioallantoic membrane (CAM) in birds. *Arch Toxicol* **74**, 335-342.

Aragon, A. C., Goens, M. B., Carbett, E., and Walker, M. K. (2008). Perinatal 2,3,7,8-tetrachlorodibenzo-p-dioxin exposure sensitizes offspring to angiotensin II-induced hypertension. *Cardiovasc Toxicol* **8**, 145-154.

Athirakul, K., Bradbury, J. A., Graves, J. P., DeGraff, L. M., Ma, J., Zhao, Y., Couse, J. F., Quigley, R., Harder, D. R., Zhao, X., Imig, J. D., Pedersen, T. L., Newman, J. W., Hammock, B. D., Conley, A. J., Korach, K. S., Coffman, T. M., and Zeldin, D. C. (2008). Increased blood pressure in mice lacking cytochrome P450 2J5. *FASEB J* **22**, 4096-4108.

BÃ¸naa, K. H., Bjerve, K. S., Straume, B. r., Gram, I. T., and Thelle, D. (1990). Effect of eicosapentaenoic and docosahexaenoic acids on blood pressure in hypertension. *N Engl J Med* **322**, 795-801.

Bang, H. O., Dyerberg, J., and Sinclair, H. M. (1980). The composition of the Eskimo food in north western Greenland. *Amer J Clin Nut* **33**, 2657-2661.

Barbosa-Sicard, E., Markovic, M., Honeck, H., Christ, B., Muller, D. N., and Schunck, W.-H. (2005). Eicosapentaenoic acid metabolism by cytochrome P450 enzymes of the CYP2C subfamily. *Biochem Biophys Res Comm* **329**, 1275-1281.

Begg, D. P., Puskas, L. G., Kitajka, K., Menesi, D., Allen, A. M., Li, D., Mathai, M. L., Shi, J. R., Sinclair, A. J., and Weisinger, R. S. (2012). Hypothalamic gene expression in omega-3 PUFA-deficient male rats before, and following, development of hypertension. *Hypertens Res* **35**, 381-387.

Bernauer, U., Heinrich-Hirsch, B., Tonnies, M., Peter-Matthias, W., and Gundert-Remy, U. (2006). Characterisation of the xenobiotic-metabolizing Cytochrome P450 expression pattern in human lung tissue by immunochemical and activity determination. *Toxicol Lett* **164**, 278-288.

Billman, G. E., Hallaq, H., and Leaf, A. (1994). Prevention of ischemia-induced ventricular fibrillation by omega 3 fatty acids. *Proc Natl Acad Sci* **91**, 4427-4430.

Blanchet, C., Dewailly, E., Ayotte, P., Bruneau, S., Receveur, O., and Holub, B. J. (2000). Contribution of selected traditional and market foods to the diet of Nunavik Inuit women. *Can J Diet Pract Res* **61**, 50-59.

Boo, Y. C., Hwang, J., Sykes, M., Michell, B. J., Kemp, B. E., Lum, H., and Jo, H. (2002a). Shear stress stimulates phosphorylation of eNOS at Ser635 by a protein kinase A-dependent mechanism. *Amer J of Phys - H Circ Physio* **283**, H1819-H1828.

Boo, Y. C., Sorescu, G., Boyd, N., Shiojima, I., Walsh, K., Du, J., and Jo, H. (2002b). Shear stress stimulates phosphorylation of endothelial nitric-oxide synthase at Ser1179 by Akt-independent mechanisms. *J Biol Chem* **277**, 3388-3396.

Boutros, P. C., Moffat, I. D., Franc, M. A., Tijet, N., Tuomisto, J., Pohjanvirta, R., and Okey, A. B. (2004). Dioxin-responsive AHRE-II gene battery: identification by phylogenetic footprinting. *Biochem Biophys Res Comm* **321**, 707-715.

Braeuning, A., Kohle, C., Buchmann, A., and Schwarz, M. (2011). Coordinate regulation of Cytochrome P4501A1 expression in mouse liver by the aryl hydrocarbon receptor and the β-Catenin pathway. *Tox Sci* **122**, 16-25.

Brock, T. G., McNish, R. W., and Peters-Golden, M. (1999). Arachidonic acid is preferentially metabolized by cyclooxygenase-2 to prostacyclin and prostaglandin E2. *J Biol Chem* **274**, 11660-11666.

Bronsgeest-Schoute, H. C., van Gent, C. M., Luten, J. B., and Ruiter, A. (1981). The effect of various intakes of omega 3 fatty acids on the blood lipid composition in healthy human subjects. *Am J Clin Nutr* **34**, 1752-1757.

Burr, M. L., Fehily, A. M., Gilbert, J. F., Rogers, S., Holliday, R. M., Sweetnam, P. M., Elwood, P. C., and Deadman, N. M. (1989). Effects of changes in fat, fish, and fibre intakes on death and myocardial reinfarction: diet and reinfarction trial (DART). *Lancet* **2**, 757-761.

Busse, R., and Fleming, I. (1995). Regulation and functional consequences of endothelial nitric oxide formation. *Ann Med* **27**, 331-340.

Busse, R., and Mulsch, A. (1990). Calcium-dependent nitric oxide synthesis in endothelial cytosol is mediated by calmodulin. *FEBS letters* **265**, 133-136.

Campbell, W. B., Gebremedhin, D., Pratt, P. F., and Harder, D. R. (1996). Identification of epoxyeicosatrienoic acids as endothelium-derived hyperpolarizing factors. *Circ Res* **78**, 415-423.

Carrier, F., Owens, R. A., Nebert, D. W., and Puga, A. (1992). Dioxin-dependent activation of murine Cyp1a-1 gene transcription requires protein kinase C-dependent phosphorylation. *Mol Cell Biol* **12**, 1856-1863.

Carroll, M. A., Balazy, M., Margiotta, P., Huang, D. D., Falck, J. R., and McGiff, J. C. (1996). Cytochrome P-450-dependent HETEs: profile of biological activity and stimulation by vasoactive peptides. *Amer J Phys* **271**, R863-869.

Chang, C.-Y., and Puga, A. (1998). Constitutive activation of the aromatic hydrocarbon receptor. *Mol Cell Biol* **18**, 525-535.

Chen, H. W., Lii, C. K., Chen, W. T., Wang, M. L., and Ou, C. C. (1996). Blood pressure-lowering effect of fish oil is independent of thromboxane A2 level in spontaneously hypertensive rats. *Prostagl Leuko Ess Fatty Acids* **54**, 147-154.

Chen, Y., Joaquim, L. F., Farah, V. M., Wichi, R. B., Fazan, R., Jr., Salgado, H. C., and Morris, M. (2005). Cardiovascular autonomic control in mice lacking angiotensin AT1a receptors. *Am J Physiol Regul Integr Comp Physiol* **288**, R1071-1077.

Cherng, T. W., Campen, M. J., Knuckles, T. L., Gonzalez Bosc, L., and Kanagy, N. L. (2009). Impairment of coronary endothelial cell ET(B) receptor function after short-term inhalation exposure to whole diesel emissions. *Amer J Phys* **297**, R640-647.

Churchill, L., Chilton, F. H., Resau, J. H., Bascom, R., Hubbard, W. C., and Proud, D. (1989). Cyclooxygenase metabolism of endogenous arachidonic acid by cultured human tracheal epithelial cells. *Am Rev Respir Dis* **140**, 449-459.

Conway, D. E., Sakurai, Y., Weiss, D., Vega, J. D., Taylor, W. R., Jo, H., Eskin, S. G., Marcus, C. B., and McIntire, L. V. (2009). Expression of CYP1A1 and CYP1B1 in human endothelial cells: regulation by fluid shear stress. *Cardiovasc Res* **81**, 669-677.

Cosentino, F., Patton, S., d'Uscio, L. V., Werner, E. R., Werner-Felmayer, G., Moreau, P., Malinski, T., and Luscher, T. F. (1998). Tetrahydrobiopterin alters superoxide and nitric oxide release in prehypertensive rats. *J Clin Invest* **101**, 1530-1537.

Cunningham, K. S., and Gotlieb, A. I. (2004). The role of shear stress in the pathogenesis of atherosclerosis. *Lab Invest* **85**, 9-23.

Dalton, T. P., Dieter, M. Z., Matlib, R. S., Childs, N. L., Shertzer, H. G., Genter, M. B., and Nebert, D. W. (2000). Targeted knockout of Cyp1a1 gene does not alter hepatic constitutive expression of other genes in the mouse [Ah] battery. *Biochem Biophys Res Comm* **267**, 184-189.

Davarinos, N. A., and Pollenz, R. S. (1999). Aryl hydrocarbon receptor imported into the nucleus following ligand binding is rapidly degraded via the cytosplasmic proteasome following nuclear export. *J Biol Chem* **274**, 28708-28715.

De Caterina, R., and Madonna, R. (2009). Cytochromes CYP1A1 and CYP1B1: new pieces in the puzzle to understand the biomechanical paradigm of atherosclerosis. *Cardiovasc Res* **81**, 629-632.

Denison, M. S., Fisher, J. M., and Whitlock, J. P. (1989). Protein-DNA interactions at recognition sites for the dioxin-Ah receptor complex. *J Biol Chem* **264**, 16478-16482.

Dey, A., Jones, J. E., and Nebert, D. W. (1999). Tissue- and cell type-specific expression of cytochrome P450 1A1 and cytochrome P450 1A2 mRNA in the mouse localized in situ hybridization. *Biochem Pharmacol* **58**, 525-537.

Dimmeler, S., Fleming, I., Fisslthaler, B., Hermann, C., Busse, R., and Zeiher, A. M. (1999). Activation of nitric oxide synthase in endothelial cells by Akt-dependent phosphorylation. *Nature* **399**, 601-605.

Dlugosova, K., Okruhlicova, L., Mitasikova, M., Sotnikova, R., Bernatova, I., Weismann, P., Slezak, J., and Tribulova, N. (2009). Modulation of connexin-43 by omega-3 fatty acids in the aorta of old spontaneously hypertensive rats. *J Physiol Pharmacol* **60**, 63-69.

Dohr, O., Li, W., Donat, S., Vogel, C., and Abel, J. (1996). Aryl hydrocarbon receptor mRNA levels in different tissues of 2,3,7,8-Tetrachlorodibenzo-p-dioxin-responsive and nonresponsive mice. *Adv Exp Med Biol* **387**, 447-459.

Duling, L. C., Cherng, T. W., Griego, J. R., Perrine, M. F., and Kanagy, N. L. (2006). Loss of alpha2B-adrenoceptors increases magnitude of hypertension following nitric oxide synthase inhibition. *Amer J Phys* **291**, H2403-2408.

Engeli, S., Gorzelniak, K., Kreutz, R., Runkel, N., Distler, A., and Sharma, A. M. (1999). Co-expression of renin-angiotensin system genes in human adipose tissue. *Journal of Hypertension* **17**, 555-560.

Engeli, S., Negrel, R., and Sharma, A. M. (2000). Physiology and Pathophysiology of the Adipose Tissue Renin-Angiotensin System. *Hypertension* **35**, 1270-1277.

Engler, M. B., Engler, M. M., and Ursell, P. C. (1994). Vasorelaxant properties of n-3 polyunsaturated fatty acids in aortas from spontaneously hypertensive and normotensive Rats. *J Cardiovasc Risk* **1**, 75-80.

Engler, M. M., Engler, M. B., Goodfriend, T. L., Ball, D. L., Yu, Z., Su, P., and Kroetz, D. L. (1999). Docosahexaenoic acid is an antihypertensive nutrient that affects aldosterone production in SHR. *Proc Soc Exp Biol Med* **221**, 32-39.

Escalante, B., Sessa, W. C., Falck, J. R., Yadagiri, P., and Schwartzman, M. L. (1989). Vasoactivity of 20-hydroxyeicosatetraenoic acid is dependent on metabolism by cyclooxygenase. *J Pharmacol Exp Ther* **248**, 229-232.

Eskin, S. G., Turner, N. A., and McIntire, L. V. (2004). Endothelial Cell Cytochrome P450 1A1 and 1B1: Up-Regulation by Shear Stress. *Endothelium* **11**, 1-10.

Esther, C. R., Jr., Howard, T. E., Marino, E. M., Goddard, J. M., Capecchi, M. R., and Bernstein, K. E. (1996). Mice lacking angiotensin-converting enzyme have low blood pressure, renal pathology, and reduced male fertility. *Lab Invest* **74**, 953-965.

Fang, L., Zhao, J., Chen, Y., Ma, T., Xu, G., Tang, C., Liu, X., and Geng, B. (2009). Hydrogen sulfide derived from periadventitial adipose tissue is a vasodilator. *Journal of Hypertension* **27**, 2174-2185.

Farin, F. M., Pohlman, T. H., and Omiecinski, C. J. (1994). Expression of cytochrome P450s and microsomal epoxide hydrolase in primary cultures of human umbilical vein endothelial cells. *Toxicol Appl Pharmacol* **124**, 1-9.

Fer, M., Dreano, Y., Lucas, D., Corcos, L., Salaun, J.-P., Berthou, F., and Amet, Y. (2008). Metabolism of eicosapentaenoic and docosahexaenoic acids by recombinant human cytochromes P450. *Arch Biochem Biophys* **471**, 116-125.

Fernandez-Salguero, P., Pineau, T., Hilbert, D. M., McPhail, T., Lee, S. S., Kimura, S., Nebert, D. W., Rudikoff, S., Ward, J. M., and Gonzalez, F. J. (1995). Immune system impairment and hepatic fibrosis in mice lacking the dioxin-binding Ah receptor. *Science* **268**, 722-726.

Fernandez-Salguero, P. M., Hilbert, D. M., Rudikoff, S., Ward, J. M., and Gonzalez, F. J. (1996). Aryl-hydrocarbon receptor-deficient mice are resistant to 2,3,7,8-

tetrachlorodibenzo-p-dioxin-induced toxicity. *Toxicol Appl Pharmacol* **140**, 173-179.

Fesus, G., Dubrovska, G., Gorzelniak, K., Kluge, R., Huang, Y., Luft, F., and Gollasch, M. (2007). Adiponectin is a novel humoral vasodilator. *Cardiovasc Res* **75**, 719-727.

Fresquet, F., Pourageaud, F., Leblais, V., Brandes, R. P., Savineau, J. P., Marthan, R., and Muller, B. (2006). Role of reactive oxygen species and gp91phox in endothelial dysfunction of pulmonary arteries induced by chronic hypoxia. *Br J Pharmacol* **148**, 714-723.

Fugelseth, D., Lindemann, R., Liestol, K., Kiserud, T., and Langslet, A. (1998). Postnatal closure of ductus venosus in preterm infants < or = 32 weeks. An ultrasonographic study. *Early Hum Dev* **53**, 163-169.

Fujisawa-Sehara, A., Sogawa, K., Yamane, M., and Fujii-Kuriyama, Y. (1987). Characterization of xenobiotic responsive elements upstream from the drug-metabolizing cytochrome P-450c gene: a similarity to glucocorticoid regulatory elements. *Nucleic Acids Research* **15**, 4179-4191.

Fulton, D., Gratton, J.-P., McCabe, T. J., Fontana, J., Fujio, Y., Walsh, K., Franke, T. F., Papapetropoulos, A., and Sessa, W. C. (1999). Regulation of endothelium-derived nitric oxide production by the protein kinase Akt. *Nature* **399**, 597-601.

Gambier, N., Marteau, J. B., Batt, A. M., Marie, B., Thompson, A., Siest, G., Foernzler, D., and Visvikis-Siest, S. (2006). Interaction between CYP1A1 T3801C and AHR G1661A polymorphisms according to smoking status on blood pressure in the Stanislas cohort. *J Hypertens* **24**, 2199-2205.

Gao, Y. J., Lu, C., Su, L. Y., Sharma, A. M., and Lee, R. M. (2007). Modulation of vascular function by perivascular adipose tissue: the role of endothelium and hydrogen peroxide. *Br J Pharmacol* **151**, 323-331.

Gao, Y. J., Takemori, K., Su, L. Y., An, W. S., Lu, C., Sharma, A. M., and Lee, R. M. (2006). Perivascular adipose tissue promotes vasoconstriction: the role of superoxide anion. *Cardiovasc Res* **71**, 363-373.

Geleijnse, J. M., Giltay, E. J., Grobbee, D. E., Donders, A. R. T., and Kok, F. J. (2002). Blood pressure response to fish oil supplementation: metaregression analysis of randomized trials. *Journal of Hypertension* **20**, 1493-1499.

Giacchetti, G., Sechi, L. A., Griffin, C. A., Don, B. R., Mantero, F., and Schambelan, M. (2000). The tissue renin-angiotensin system in rats with fructose- induced hypertension: overexpression of type 1 angiotensin II receptor in adipose tissue. *Journal of Hypertension* **18**, 695-702.

Gousset-Dupont, A. L., Robert, V. R., Grynberg, A., Lacour, B., and Tardivel, S. (2007). The effect of n-3 PUFA on eNOS activity and expression in Ea hy 926 cells. *Prostagl Leuk Ess Fatty Acids* **76**, 131-139.

Granberg, A. L., Brunstrom, B., and Brandt, I. (2000). Cytochrome P450-dependent binding of 7,12-dimethylbenz[a]anthracene (DMBA) and benzo[a]pyrene (B[a]P) in murine heart, lung, and liver endothelial cells. *Arch Toxicol* **74**, 593-601.

Hahn, M. E. (1998). The aryl hydrocarbon receptor: a comparative perspective. *Comp Biochem Physiol C Pharmacol Toxicol Endocrinol* **121**, 23-53.

Hahn, M. E. (2002). Aryl hydrocarbon receptors: diversity and evolution. *Chem Biol Interact* **141**, 131-160.

Han, Z., Miwa, Y., Obikane, H., Mitsumata, M., Takahashi-Yanaga, F., Morimoto, S., and Sasaguri, T. (2008). Aryl hydrocarbon receptor mediates laminar fluid shear stress-induced CYP1A1 activation and cell cycle arrest in vascular endothelial cells. *Cardiovasc Res* **77**, 809-818.

Hankinson, O. (2005). Role of coactivators in transcriptional activation by the aryl hydrocarbon receptor. *Arch of Biochem Biophys* **433**, 379-386.

Harri, M., Lindblom, J., Malinen, H., Hyttinen, M., Lapvetelainen, T., Eskola, S., and Helminen, H. J. (1999). Effect of access to a running wheel on behavior of C57BL/6J mice. *Lab Anim Sci* **49**, 401-405.

Harrigan, J. A., McGarrigle, B. P., Sutter, T. R., and Olson, J. R. (2006). Tissue specific induction of cytochrome P450 (CYP) 1A1 and 1B1 in rat liver and lung following in vitro (tissue slice) and in vivo exposure to benzo(a)pyrene. *Toxicology in Vitro* **20**, 426-438.

Harrigan, J. A., Vezina, C. M., McGarrigle, B. P., Ersing, N., Box, H. C., Maccubbin, A. E., and Olson, J. R. (2004). DNA adduct formation in precision-cut rat liver and lung slices exposed to benzo[a]pyrene. *Toxicol Sci* **77**, 307-314.

Harris, W. S. (1997). n-3 fatty acids and serum lipoproteins: human studies. *Amer J Clin Nut* **65**, 1645S-1654S.

Hayashi, S.-i., Watanabe, J., Nakachi, K., and Kawajiri, K. (1991). Genetic linkage of lung cancer-associated MspI polymorphisms with amino acid replacement in the heme binding region of the human Cytochrome P450IA1 gene. *J Biochem* **110**, 407-411.

Hercule, H. C., Schunck, W.-H., Gross, V., Seringer, J., Leung, F. P., Weldon, S. M., da Costa Goncalves, A. C., Huang, Y., Luft, F. C., and Gollasch, M. (2009). Interaction between P450 eicosanoids and nitric oxide in the control of arterial tone in mice. *Arterio Thromb Vasc Biol* **29**, 54-60.

Holla, V. R., Adas, F., Imig, J. D., Zhao, X., Price, E., Olsen, N., Kovacs, W. J., Magnuson, M. A., Keeney, D. S., Breyer, M. D., Falck, J. R., Waterman, M. R., and Capdevila, J. H. (2001). Alterations in the regulation of androgen-sensitive Cyp 4a monooxygenases cause hypertension. *Proc Natl Acad Sci* **98**, 5211-5216.

Hudert, C. A., Weylandt, K. H., Lu, Y., Wang, J., Hong, S., Dignass, A., Serhan, C. N., and Kang, J. X. (2006). Transgenic mice rich in endogenous omega-3 fatty acids are protected from colitis. *Proc Natl Acad Sci* **103**, 11276-11281.

Hui, R., St-Louis, J., and Falardeau, P. (1989). Antihypertensive properties of linoleic acid and fish oil omega-3 fatty acids independent of the prostaglandin system. *Am J Hypertens* **2**, 610-617.

Ignarro, L. J., Buga, G. M., Wood, K. S., Byrns, R. E., and Chaudhuri, G. (1987). Endothelium-derived relaxing factor produced and released from artery and vein is nitric oxide. *Proc Natl Acad Sci* **84**, 9265-9269.

Ikuta, T., Kobayashi, Y., and Kawajiri, K. (2004). Phosphorylation of nuclear localization signal inhibits the ligand-dependent nuclear import of aryl hydrocarbon receptor. *Biochem Biophys Res Commun* **317**, 545-550.

Imig, J. D., Navar, L. G., Roman, R. J., Reddy, K. K., and Falck, J. R. (1996). Actions of epoxygenase metabolites on the preglomerular vasculature. *J Am Soc Nephrol* **7**, 2364-2370.

Iwakiri, Y., Tsai, M.-H., McCabe, T. J., Gratton, J.-P., Fulton, D., Groszmann, R. J., and Sessa, W. C. (2002). Phosphorylation of eNOS initiates excessive NO production in early phases of portal hypertension. *Amer J Phys* **282**, H2084-H2090.

Iyer, S. N., Lu, D., Katovich, M. J., and Raizada, M. K. (1996). Chronic control of high blood pressure in the spontaneously hypertensive rat by delivery of angiotensin type 1 receptor antisense. *Proc Natl Acad Sci* **93**, 9960-9965.

Jarvis, M. D., Palmer, B. R., Pilbrow, A. P., Ellis, K. L., Frampton, C. M., Skelton, L., Doughty, R. N., Whalley, G. A., Ellis, C. J., Yandle, T. G., Richards, A. M., and Cameron, V. A. (2009). CYP1A1 MSPI (T6235C) gene polymorphism is associated with mortality in acute coronary syndrome patients. *Clin Exp Pharmacol Physiol* **37**, 193-198.

Jayasooriya, A. P., Begg, D. P., Chen, N., Mathai, M. L., Sinclair, A. J., Wilkinson-Berka, J., Wark, J. D., Weisinger, H. S., and Weisinger, R. S. (2008). Omega-3 polyunsaturated fatty acid supplementation reduces hypertension in TGR(mRen-2)27 rats. *Prostagl Leuko Ess Fatty Acids* **78**, 67-72.

Jennings, B. L., Sahan-Firat, S., Estes, A. M., Das, K., Farjana, N., Fang, X. R., Gonzalez, F. J., and Malik, K. U. (2010). Cytochrome P450 1B1 contributes to angiotensin II induced hypertension and associated pathophysiology. *Hypertension* **56**, 667-674.

Jones, K. W., and Whitlock, J. P. (1990). Functional analysis of the transcriptional promoter for the CYP1A1 gene. *Mol Cell Biol* **10**, 5098-5105.

Kazlauskas, A., Sundstrom, S., Poellinger, L., and Pongratz, I. (2001). The hsp90 chaperone complex regulates intracellular localization of the dioxin receptor. *Mol Cell Biol* **21**, 2594-2607.

Kerzee, J. K., and Ramos, K. S. (2001). Constitutive and inducible expression of Cyp1a1 and Cyp1b1 in vascular smooth muscle cells: role of the Ahr bHLH/PAS transcription factor. *Circ Res* **89**, 573-582.

Kim, H. S., Krege, J. H., Kluckman, K. D., Hagaman, J. R., Hodgin, J. B., Best, C. F., Jennette, J. C., Coffman, T. M., Maeda, N., and Smithies, O. (1995). Genetic control of blood pressure and the angiotensinogen locus. *Proc Natl Acad Sci* **92**, 2735-2739.

Koni, P. A., Joshi, S. K., Temann, U. A., Olson, D., Burkly, L., and Flavell, R. A. (2001). Conditional vascular cell adhesion molecule 1 deletion in mice: impaired lymphocyte migration to bone marrow. *J Exp Med* **193**, 741-754.

Kopf, P. G., Scott, J. A., Agbor, L. N., Boberg, J. R., Elased, K. M., Huwe, J. K., and Walker, M. K. (2010). Cytochrome P4501A1 is required for vascular dysfunction and hypertension induced by 2,3,7,8-tetrachlorodibenzo-p-dioxin. *Tox Sci* **117**, 537-546.

Kris-Etherton, P. M., Harris, W. S., Appel, L. J., and Committee, f. t. N. (2002). Fish consumption, fish Oil, omega-3 fatty acids, and cardiovascular disease. *Circulation* **106**, 2747-2757.

Kromann, N., and Green, A. (1980). Epidemiological Studies in the Upernavik District, Greenland. *Acta Medica Scandinavica* **208**, 401-406.

Lahvis, G. P., Lindell, S. L., Thomas, R. S., McCuskey, R. S., Murphy, C., Glover, E., Bentz, M., Southard, J., and Bradfield, C. A. (2000). Portosystemic shunting and persistent fetal vascular structures in aryl hydrocarbon receptor-deficient mice. *Proc Natl Acad Sci* **97**, 10442-10447.

Lahvis, G. P., Pyzalski, R. W., Glover, E., Pitot, H. C., McElwee, M. K., and Bradfield, C. A. (2005). The aryl hydrocarbon receptor is required for developmental closure of the ductus venosus in the neonatal mouse. *Mol Pharmacol* **67**, 714-720.

LaPres, J. J., Glover, E., Dunham, E. E., Bunger, M. K., and Bradfield, C. A. (2000). ARA9 modifies agonist signaling through an increase in cytosolic aryl hydrocarbon receptor. *J Biol Chem* **275**, 6153-6159.

Lauterbach, B., Barbosa-Sicard, E., Wang, M.-H., Honeck, H., Kargel, E., Theuer, J., Schwartzman, M. L., Haller, H., Luft, F. C., Gollasch, M., and Schunck, W.-H. (2002). Cytochrome P450-dependent eicosapentaenoic acid metabolites are novel BK channel activators. *Hypertension* **39**, 609-613.

Li, P., Kim, S. W., Li, X., Datta, S., Pond, W. G., and Wu, G. (2008). Dietary supplementation with cholesterol and docosahexaenoic acid increases the activity of the arginine-nitric oxide pathway in tissues of young pigs. *Nitric Oxide* **19**, 259-265.

Li, Q., Zhang, Q., Wang, M., Liu, F., Zhao, S., Ma, J., Luo, N., Li, N., Li, Y., Xu, G., and Li, J. (2007a). Docosahexaenoic acid affects endothelial nitric oxide synthase in caveolae. *Arch Biochem Biophys* **466**, 250-259.

Li, Q., Zhang, Q., Wang, M., Zhao, S., Ma, J., Luo, N., Li, N., Li, Y., Xu, G., and Li, J. (2007b). Eicosapentaenoic acid modifies lipid composition in caveolae and induces translocation of endothelial nitric oxide synthase. *Biochimie* **89**, 169-177.

Lim, E. J., Smart, E. J., Toborek, M., and Hennig, B. (2007). The role of caveolin-1 in PCB77-induced eNOS phosphorylation in human-derived endothelial cells. *Amer J Phys* **293**, H3340-H3347.

Lindstedt, I., XU, C. B., Zhang, Y., and Edvinsson, L. (2009). Increased perfusion pressure enhances the expression of endothelin (ETB) and angiotensin II (AT1, AT2) receptors in rat mesenteric artery smooth muscle cells. *Blood Pressure* **18**, 78-85.

Liu, J. C., Conklin, S. M., Manuck, S. B., Yao, J. K., and Muldoon, M. F. (2011). Long-chain omega-3 fatty acids and blood pressure. *Am J Hypertens* **24**, 1121-1126.

Lohn, M., Dubrovska, G., Lauterbach, B., Luft, F. C., Gollasch, M., and Sharma, A. M. (2002). Periadventitial fat releases a vascular relaxing factor. *FASEB J* **16**, 1057-1063.

Lopez, D., Orta, X., Casos, K., Saiz, M. P., Puig-Parellada, P., Farriol, M., and Mitjavila, M. T. (2004). Upregulation of endothelial nitric oxide synthase in rat aorta after ingestion of fish oil-rich diet. *Amer J Phys* **287**, H567-H572.

Lu, D., Raizada, M. K., Iyer, S., Reaves, P., Yang, H., and Katovich, M. J. (1997). Losartan versus gene therapy: chronic control of high blood pressure in spontaneously hypertensive rats. *Hypertension* **30**, 363-370.

Lucas, D. l., Goulitquer, S., Marienhagen, J., Fer, M., Dreano, Y., Schwaneberg, U., Amet, Y., and Corcos, L. (2010). Stereoselective epoxidation of the last double

bond of polyunsaturated fatty acids by human cytochromes P450. *J Lip Res* **51**, 1125-1133.

Lund, A. K., Agbor, L. N., Zhang, N., Baker, A., Zhao, H., Fink, G. D., Kanagy, N. L., and Walker, M. K. (2008). Loss of the aryl hydrocarbon receptor induces hypoxemia, endothelin-1, and systemic hypertension at modest altitude. *Hypertension* **51**, 803-809.

Lund, A. K., Goens, M. B., Kanagy, N. L., and Walker, M. K. (2003). Cardiac hypertrophy in aryl hydrocarbon receptor (AhR) null mice is correlated with elevated angiotensin II, endothelin-1 and mean arterial blood pressure. *Toxicol Appl Pharmacol* **193**, 177-187.

Lund, A. K., Goens, M. B., Nunez, B. A., and Walker, M. K. (2006). Characterizing the role of endothelin-1 in the progression of cardiac hypertrophy in aryl hydrocarbon receptor (AhR) null mice. *Toxicol Appl Pharmacol* **212**, 127-135.

Ma, D. W. L., Seo, J., Davidson, L. A., Callaway, E. S., Fan, Y.-Y., Lupton, J. R., and Chapkin, R. S. (2004). n-3 PUFA alter caveolae lipid composition and resident protein localization in mouse colon. *FASEB J* **18**, 1040-1042.

Malek, A. M., Alper, S. L., and Izumo, S. (1999). Hemodynamic shear stress and its role in atherosclerosis. *JAMA* **282**, 2035-2042.

Marchioli, R., Barzi, F., Bomba, E., Chieffo, C., Di Gregorio, D., Di Mascio, R., Franzosi, M. G., Geraci, E., Levantesi, G., Maggioni, A. P., Mantini, L., Marfisi, R. M., Mastrogiuseppe, G., Mininni, N., Nicolosi, G. L., Santini, M., Schweiger, C., Tavazzi, L., Tognoni, G., Tucci, C., and Valagussa, F. (2002). Early protection against sudden death by n-3 polyunsaturated fatty acids after myocardial infarction: time-course analysis of the results of the Gruppo Italiano per lo Studio della Sopravvivenza nell'Infarto Miocardico (GISSI)-Prevenzione. *Circulation* **105**, 1897-1903.

Massiera, F. (2001). Adipose angiotensinogen is involved in adipose tissue growth and blood pressure regulation. *FASEB J* **15**, 2727-2729.

Matsumoto, T., Nakayama, N., Ishida, K., Kobayashi, T., and Kamata, K. (2009). Eicosapentaenoic acid improves imbalance between vasodilator and

vasoconstrictor actions of endothelium-derived factors in mesenteric arteries from rats at chronic stage of type 2 diabetes. *J Pharmacol Exp Ther* **329**, 324-334.

McMillan, B. J., and Bradfield, C. A. (2007a). The aryl hydrocarbon receptor is activated by modified low-density lipoprotein. *Proc Natl Acad Sci* **104**, 1412-1417.

McMillan, B. J., and Bradfield, C. A. (2007b). The aryl hydrocarbon receptor sans xenobiotics: endogenous function in genetic model systems. *Mol Pharmacol* **72**, 487-498.

Mehrabi, M., Steiner, G., Dellinger, C., Kofler, A., Schaufler, K., Tamaddon, F., Plesch, K., Ekmekcioglu, C., Maurer, G., Glogar, H., and Thalhammer, T. (2002). The arylhydrocarbon receptor (AhR), but not the AhR-nuclear translocator (ARNT), is increased in hearts of patients with cardiomyopathy. *Virchows Archiv* **441**, 481-489.

Menotti, A., Kromhout, D., Blackburn, H., Fidanza, F., Buzina, R., and Nissinen, A. (1999). Food intake patterns and 25-year mortality from coronary heart disease: Cross-cultural correlations in the Seven Countries Study. *Eur J Epidemiol* **15**, 507-515.

Miller, V. M., and Vanhoutte, P. M. (1985). Endothelium-dependent contractions to arachidonic acid are mediated by products of cyclooxygenase. *Am J Physiol* **248**, H432-437.

Mimura, J., and Fujii-Kuriyama, Y. (2003). Functional role of AhR in the expression of toxic effects by TCDD. *Biochim Biophys Acta* **1619**, 263-268.

Mimura, J., Yamashita, K., Nakamura, K., Morita, M., Takagi, T. N., Nakao, K., Ema, M., Sogawa, K., Yasuda, M., Katsuki, M., and Fujii-Kuriyama, Y. (1997). Loss of teratogenic response to 2,3,7,8-tetrachlorodibenzo-p-dioxin (TCDD) in mice lacking the Ah (dioxin) receptor. *Genes to Cells* **2**, 645-654.

Mitasikova, M., Smidova, S., Macsaliova, A., Knezl, V., Dlugosova, K., Okruhlicova, L., Weismann, P., and Tribulova, N. (2008). Aged male and female spontaneously hypertensive rats benefit from n-3 polyunsaturated fatty acids supplementation. *Physiol Res* **57**, 28.

Morgan, J. E., and Whitlock, J. P. (1992). Transcription-dependent and transcription-independent nucleosome disruption induced by dioxin. *Proc Natl Acad Sci* **89**, 11622-11626.

Mori, T. A., Bao, D. Q., Burke, V., Puddey, I. B., and Beilin, L. J. (1999). Docosahexaenoic acid but not eicosapentaenoic acid lowers ambulatory blood pressure and heart rate in humans. *Hypertension* **34**, 253-260.

Morin, C., Sirois, M., Echave, V., Rizcallah, E., and Rousseau, E. (2009). Relaxing effects of 17(18)-EpETE on arterial and airway smooth muscles in human lung. *Amer J Phys* **296**, L130-L139.

Morris, M., Sacks, F., and Rosner, B. (1993). Does fish oil lower blood pressure? A meta-analysis of controlled trials. *Circulation* **88**, 523-533.

Muller, D. N., Schmidt, C., Barbosa-Sicard, E., Wellner, M., Gross, V., Hercule, H., Markovic, M., Honeck, H., Luft, F. C., and Schunck, W. H. (2007). Mouse Cyp4a isoforms: enzymatic properties, gender- and strain-specific expression, and role in renal 20-hydroxyeicosatetraenoic acid formation. *Biochem J* **403**, 109-118.

Nakachi, K., Imai, K., Hayashi, S., and Kawajiri, K. (1993). Polymorphisms of the CYP1A1 and glutathione S-transferase genes associated with susceptibility to lung cancer in relation to cigarette dose in a Japanese population. *Cancer Res* **53**, 2994-2999.

Nakagawa, K., Holla, V. R., Wei, Y., Wang, W.-H., Gatica, A., Wei, S., Mei, S., Miller, C. M., Cha, D. R., Price, E., Zent, R., Pozzi, A., Breyer, M. D., Guan, Y., Falck, J. R., Waterman, M. R., and Capdevila, J. H. (2006). Salt-sensitive hypertension is associated with dysfunctional Cyp4a10 gene and kidney epithelial sodium channel. *J Clin Invest* **116**, 1696-1702.

Neuhold, L. A., Shirayoshi, Y., Ozato, K., Jones, J. E., and Nebert, D. W. (1989). Regulation of mouse CYP1A1 gene expression by dioxin: requirement of two cis-acting elements during induction. *Mol Cell Biol* **9**, 2378-2386.

Nishimura, M., Nanbu, A., Komori, T., Ohtsuka, K., Takahashi, H., and Yoshimura, M. (2000). Eicosapentaenoic acid stimulates nitric oxide production and decreases cardiac noradrenaline in diabetic rats. *Clin Exp Pharmacol Phys* **27**, 618-624.

Oesch-Bartlomowicz, B., and Oesch, F. (2009). Role of cAMP in mediating AHR signaling. *Biochem Pharmacol* **77**, 627-641.

Ohashi, Y., Kawashima, S., Hirata, K., Yamashita, T., Ishida, T., Inoue, N., Sakoda, T., Kurihara, H., Yazaki, Y., and Yokoyama, M. (1998). Hypotension and reduced nitric oxide-elicited vasorelaxation in transgenic mice overexpressing endothelial nitric oxide synthase. *J Clin Invest* **102**, 2061-2071.

Okino, S. T., Pookot, D., Li, L. C., Zhao, H., Urakami, S., Shiina, H., Igawa, M., and Dahiya, R. (2006). Epigenetic inactivation of the dioxin-responsive cytochrome P4501A1 gene in human prostate cancer. *Cancer Res* **66**, 7420-7428.

Oliw, E. H. (1991). 17R(18S)epoxyeicosatetraenoic acid, a cytochrome P-450 metabolite of 20:5n-3 in monkey seminal vesicles, is metabolized to novel prostaglandins. *Biochem Biophys Res Commun* **178**, 1444-1450.

Omura, M., Kobayashi, S., Mizukami, Y., Mogami, K., Todoroki-Ikeda, N., Miyake, T., and Matsuzaki, M. (2001). Eicosapentaenoic acid (EPA) induces Ca2+-independent activation and translocation of endothelial nitric oxide synthase and endothelium-dependent vasorelaxation. *FEBS letters* **487**, 361-366.

Palmer, R. M., Rees, D. D., Ashton, D. S., and Moncada, S. (1988). L-arginine is the physiological precursor for the formation of nitric oxide in endothelium-dependent relaxation. *Biochem Biophys Res Comm* **153**, 1251-1256.

Pavek, P., and Dvorak, Z. (2008). Xenobiotic-induced transcriptional regulation of xenobiotic metabolizing enzymes of the cytochrome P450 superfamily in human extrahepatic tissues. *Curr Drug Metab* **9**, 129-143.

Peter Guengerich, F., Martin, M. V., McCormick, W. A., Nguyen, L. P., Glover, E., and Bradfield, C. A. (2004). Aryl hydrocarbon receptor response to indigoids in vitro and in vivo. *Arch Biochem Biophys* **423**, 309-316.

Poland, A., and Glover, E. (1980). 2,3,7,8,-Tetrachlorodibenzo-p-dioxin: segregation of toxocity with the Ah locus. *Mol Pharmacol* **17**, 86-94.

Postic, C., Shiota, M., Niswender, K. D., Jetton, T. L., Chen, Y., Moates, J. M., Shelton, K. D., Lindner, J., Cherrington, A. D., and Magnuson, M. A. (1999). Dual roles

for glucokinase in glucose homeostasis as determined by liver and pancreatic beta cell-specific gene knock-outs using Cre recombinase. *J Biol Chem* **274**, 305-315.

Rees, D. D., Palmer, R. M., Hodson, H. F., and Moncada, S. (1989). A specific inhibitor of nitric oxide formation from L-arginine attenuates endothelium-dependent relaxation. *Br J Pharmacol* **96**, 418-424.

Rockett, B. D., Harris, M., and Raza Shaikh, S. (2012). High dose of an n-3 polyunsaturated fatty acid diet lowers activity of C57BL/6 mice. *Prostagl Leuko Ess Fatty Acids* **86**, 137-140.

Roger, V. r. L., Go, A. S., Lloyd-Jones, D. M., Adams, R. J., Berry, J. D., Brown, T. M., Carnethon, M. R., Dai, S., de Simone, G., Ford, E. S., Fox, C. S., Fullerton, H. J., Gillespie, C., Greenlund, K. J., Hailpern, S. M., Heit, J. A., Ho, P. M., Howard, V. J., Kissela, B. M., Kittner, S. J., Lackland, D. T., Lichtman, J. H., Lisabeth, L. D., Makuc, D. M., Marcus, G. M., Marelli, A., Matchar, D. B., McDermott, M. M., Meigs, J. B., Moy, C. S., Mozaffarian, D., Mussolino, M. E., Nichol, G., Paynter, N. P., Rosamond, W. D., Sorlie, P. D., Stafford, R. S., Turan, T. N., Turner, M. B., Wong, N. D., and Wylie-Rosett, J. (2011). Heart Disease and Stroke Statistics 2011 Update / 1. About 1. About These Statistics / 2. American Heart Association's 2020 Impact Goals / 3. Cardiovascular Diseases / 4. Subclinical Atherosclerosis / 5. Coronary Heart Disease, Acute Coronary Syndrome, and Angina Pectoris / 6. Stroke (Cerebrovascular Disease) / 7. High Blood Pressure / 8. Congenital Cardiovascular Defects / 9. Cardiomyopathy and Heart Failure / 10. Other Cardiovascular Diseases / 11. Family History and Genetics / 12. Risk Factor: Smoking/Tobacco Use / 13. Risk Factor: High Blood Cholesterol and Other Lipids / 14. Risk Factor: Physical Inactivity / 15. Risk Factor: Overweight and Obesity / 16. Risk Factor: Diabetes Mellitus / 17. End-Stage Renal Disease and Chronic Kidney Disease / 18. Metabolic Syndrome / 19. Nutrition / 20. Quality of Care / 21. Medical Procedures / 22. Economic Cost of Cardiovascular Disease / 23. At-a-Glance Summary Tables / 24. Glossary. *Circulation* **123**, e18-e209.

Roman, R. J. (2002). P-450 metabolites of arachidonic acid in the control of cardiovascular function. *Physiol Rev* **82**, 131-185.

Sahin, A. S., and Bariskaner, H. (2007). The mechanisms of vasorelaxant effect of leptin on isolated rabbit aorta. *Fundam Clin Pharmacol* **21**, 595-600.

Sanbe, A., Tanaka, Y., Fujiwara, Y., Tsumura, H., Yamauchi, J., Cotecchia, S., Koike, K., Tsujimoto, G., and Tanoue, A. (2007). Alpha1-adrenoceptors are required for normal male sexual function. *Br J Pharmacol* **152**, 332-340.

Schaldach, C. M., Riby, J., and Bjeldanes, L. F. (1999). Lipoxin A4: A new class of ligand for the Ah receptor. *Biochemistry* **38**, 7594-7600.

Schmidt, J. V., Su, G. H., Reddy, J. K., Simon, M. C., and Bradfield, C. A. (1996). Characterization of a murine Ahr null allele: involvement of the Ah receptor in hepatic growth and development. *Proc Natl Acad Sci* **93**, 6731-6736.

Schwarz, D., Kisselev, P., Chernogolov, A., Schunck, W.-H., and Roots, I. (2005). Human CYP1A1 variants lead to differential eicosapentaenoic acid metabolite patterns. *Biochem Biophys Res Comm* **336**, 779-783.

Schwarz, D., Kisselev, P., Ericksen, S. S., Szklarz, G. D., Chernogolov, A., Honeck, H., Schunck, W.-H., and Roots, I. (2004). Arachidonic and eicosapentaenoic acid metabolism by human CYP1A1: highly stereoselective formation of 17(R),18(S)-epoxyeicosatetraenoic acid. *Biochem Pharmacol* **67**, 1445-1457.

Senador, D., Kanakamedala, K., Irigoyen, M. C., Morris, M., and Elased, K. M. (2009). Cardiovascular and autonomic phenotype of db/db diabetic mice. *Exp Physiol* **94**, 648-658.

Shesely, E. G., Maeda, N., Kim, H. S., Desai, K. M., Krege, J. H., Laubach, V. E., Sherman, P. A., Sessa, W. C., and Smithies, O. (1996). Elevated blood pressures in mice lacking endothelial nitric oxide synthase. *Proc Natl Acad Sci* **93**, 13176-13181.

Shimada, T., and Fujii-Kuriyama, Y. (2004). Metabolic activation of polycyclic aromatic hydrocarbons to carcinogens by cytochromes P450 1A1 and1B1. *Cancer Science* **95**, 1-6.

Simon, P. (2003). Q-Gene: processing quantitative real-time RTPCR data. *Bioinformatics* **19**, 1439-1440.

Smith, G. B., Harper, P. A., Wong, J. M., Lam, M. S., Reid, K. R., Petsikas, D., and Massey, T. E. (2001). Human lung microsomal cytochrome P4501A1 (CYP1A1) activities: impact of smoking status and CYP1A1, aryl hydrocarbon receptor, and glutathione S-transferase M1 genetic polymorphisms. *Cancer Epidemiol Biomarkers Prev* **10**, 839-853.

Stebbins, C. L., Stice, J. P., Hart, C. M., Mbai, F. N., and Knowlton, A. A. (2008). Effects of dietary docosahexaenoic Acid (DHA) on eNOS in human coronary artery endothelial cells. *J Cardiovasc Pharmacol* **13**, 261-268.

Stegeman, J. J., Hahn, M. E., Weisbrod, R., Woodin, B. R., Joy, J. S., Najibi, S., and Cohen, R. A. (1995). Induction of cytochrome P4501A1 by aryl hydrocarbon receptor agonists in porcine aorta endothelial cells in culture and cytochrome P4501A1 activity in intact cells. *Mol Pharmacol* **47**, 296-306.

Stokes, J., 3rd, Kannel, W. B., Wolf, P. A., D'Agostino, R. B., and Cupples, L. A. (1989). Blood pressure as a risk factor for cardiovascular disease. The Framingham Study--30 years of follow-up. *Hypertension* **13**, I13-18.

Stoll, M., Steckelings, U. M., Paul, M., Bottari, S. P., Metzger, R., and Unger, T. (1995). The angiotensin AT2-receptor mediates inhibition of cell proliferation in coronary endothelial cells. *J Clin Invest* **95**, 651-657.

Swanson, H. I., Chan, W. K., and Bradfield, C. A. (1995). DNA binding specificities and pairing rules of the Ah receptor, ARNT, and SIM proteins. *J Biol Chem* **270**, 26292-26302.

Swanson, H. I., and Yang, J.-H. (1998). The aryl hydrocarbon receptor interacts with transcription factor IIB. *Mol Pharmacol* **54**, 671-677.

Tagawa, H., Shimokawa, H., Tagawa, T., Kuroiwa-Matsumoto, M., Hirooka, Y., and Takeshita, A. (1999). Long-term treatment with eicosapentaenoic acid augments both nitric oxide-mediated and non-nitric oxide-mediated endothelium-dependent forearm vasodilatation in patients with coronary artery disease. *J Cardiovasc Pharmacol* **33**, 633-640.

Takemori, K., Gao, Y. J., Ding, L., Lu, C., Su, L. Y., An, W. S., Vinson, C., and Lee, R. M. (2007). Elevated blood pressure in transgenic lipoatrophic mice and altered vascular function. *Hypertension* **49**, 365-372.

Tang, M. S., Vulimiri, S. V., Viaje, A., Chen, J. X., Bilolikar, D. S., Morris, R. J., Harvey, R. G., Slaga, T. J., and DiGiovanni, J. (2000). Both syn- and anti-7,12-dimethylbenz[a]anthracene-3,4-diol-1,2-epoxides initiate tumors in mouse skin that possess -CAA- to -CTA- mutations at codon 61 of c-H-ras. *Cancer Res* **60**, 5688-5695.

Thackaberry, E. A., Gabaldon, D. M., Walker, M. K., and Smith, S. M. (2002). Aryl hydrocarbon receptor null mice develop cardiac hypertrophy and increased hypoxia-inducible factor-1alpha in the absence of cardiac hypoxia. *Cardiovasc Toxicol* **2**, 263-274.

Tijet, N., Boutros, P. C., Moffat, I. D., Okey, A. B., Tuomisto, J., and Pohjanvirta, R. (2006). Aryl hydrocarbon receptor regulates distinct dioxin-dependent and dioxin-independent gene batteries. *Mol Pharmacol* **69**, 140-153.

Traub, O., and Berk, B. C. (1998). Laminar shear stress: mechanisms by which endothelial cells transduce an atheroprotective force. *Arterioscler Thromb Vasc Biol* **18**, 677-685.

Tsuchida, S., Matsusaka, T., Chen, X., Okubo, S., Niimura, F., Nishimura, H., Fogo, A., Utsunomiya, H., Inagami, T., and Ichikawa, I. (1998). Murine double nullizygotes of the angiotensin type 1A and 1B receptor genes duplicate severe abnormal phenotypes of angiotensinogen nullizygotes. *J Clin Invest* **101**, 755-760.

van Haperen, R., de Waard, M., van Deel, E., Mees, B., Kutryk, M., van Aken, T., Hamming, J., Grosveld, F., Duncker, D. J., and de Crom, R. (2002). Reduction of blood pressure, plasma cholesterol, and atherosclerosis by elevated endothelial nitric oxide. *J Biol Chem* **277**, 48803-48807.

Vasquez, A., Atallah-Yunes, N., Smith, F. C., You, X., Chase, S. E., Silverstone, A. E., and Vikstrom, K. L. (2003). A role for the aryl hydrocarbon receptor in cardiac physiology and function as demonstrated by AhR knockout mice. *Cardiovasc Toxicol* **3**, 153-163.

Vaughan, D. E., Lazos, S. A., and Tong, K. (1995). Angiotensin II regulates the expression of plasminogen activator inhibitor-1 in cultured endothelial cells. A potential link between the renin-angiotensin system and thrombosis. *J Clin Invest* **95**, 995-1001.

Verlohren, S., Dubrovska, G., Tsang, S. Y., Essin, K., Luft, F. C., Huang, Y., and Gollasch, M. (2004). Visceral periadventitial adipose tissue regulates arterial tone of mesenteric arteries. *Hypertension* **44**, 271-276.

Von Schacky, C., Angerer, P., Kothny, W., Theisen, K., and Mudra, H. (1999). The effect of dietary omega-3 fatty acids on coronary atherosclerosis. A randomized, double-blind, placebo-controlled trial. *Ann Intern Med* **130**, 554-562.

Walisser, J. A., Bunger, M. K., Glover, E., Harstad, E. B., and Bradfield, C. A. (2004). Patent ductus venosus and dioxin resistance in mice harboring a hypomorphic Arnt allele. *J Biol Chem* **279**, 16326-16331.

Walisser, J. A., Glover, E., Pande, K., Liss, A. L., and Bradfield, C. A. (2005). Aryl hydrocarbon receptor-dependent liver development and hepatotoxicity are mediated by different cell types. *Proc Natl Acad Sci* **102**, 17858-17863.

Walker, M. K., and Catron, T. F. (2000). Characterization of cardiotoxicity induced by 2,3,7, 8-tetrachlorodibenzo-p-dioxin and related chemicals during early chick embryo development. *Toxicol Appl Pharmacol* **167**, 210-221.

Wang, Q., Liang, X., Wang, L., Lu, X., Huang, J., Cao, J., Li, H., and Gu, D. (2012). Effect of omega-3 fatty acids supplementation on endothelial function: a meta-analysis of randomized controlled trials. *Atherosclerosis* **221**, 536-543.

Wang, R.-x., Chai, Q., Lu, T., and Lee, H.-C. (2011). Activation of vascular BK channels by docosahexaenoic acid is dependent on cytochrome P450 epoxygenase activity. *Cardiovasc Res* **90**, 344-352.

Wang, X. L., Greco, M., Sim, A. S., Duarte, N., Wang, J., and Wilcken, D. E. L. (2002). Effect of CYP1A1 MspI polymorphism on cigarette smoking related coronary artery disease and diabetes. *Atherosclerosis* **162**, 391-397.

Wen, Z.-Y., and Chen, F. (2003). Heterotrophic production of eicosapentaenoic acid by microalgae. *Biotechnology Advances* **21**, 273-294.

Westphal, C., Konkel, A., and Schunck, W. H. (2011). CYP-eicosanoids--a new link between omega-3 fatty acids and cardiac disease? *Prostagl Lip Med* **96**, 99-108.

Wilson, J. Y., Wells, R., Aguilar, A., Borrell, A., Tornero, V., Reijnders, P., Moore, M., and Stegeman, J. J. (2007). Correlates of Cytochrome P4501A1 expression in bottlenose dolphin (Tursiops truncatus) integument biopsies. *Tox Sci* **97**, 111-119.

Yamawaki, H., Tsubaki, N., Mukohda, M., Okada, M., and Hara, Y. (2010). Omentin, a novel adipokine, induces vasodilation in rat isolated blood vessels. *Biochem Biophys Res Commun* **393**, 668-672.

Yanagida, A., Sogawa, K., Yasumoto, K. I., and Fujii-Kuriyama, Y. (1990). A novel cis-acting DNA element required for a high level of inducible expression of the rat P-450c gene. *Mol Cell Biol* **10**, 1470-1475.

Yang, G., Wu, L., Jiang, B., Yang, W., Qi, J., Cao, K., Meng, Q., Mustafa, A. K., Mu, W., Zhang, S., Snyder, S. H., and Wang, R. (2008). H2S as a physiologic vasorelaxant: hypertension in mice with deletion of cystathionine gamma-lyase. *Science* **322**, 587-590.

Yang, X. P., Liu, Y. H., Shesely, E. G., Bulagannawar, M., Liu, F., and Carretero, O. A. (1999). Endothelial nitric oxide gene knockout mice: cardiac phenotypes and the effect of angiotensin-converting enzyme inhibitor on myocardial ischemia/reperfusion injury. *Hypertension* **34**, 24-30.

Yang, Y., Lu, N., Chen, D., Meng, L., Zheng, Y., and Hui, R. (2012). Effects of n-3 PUFA supplementation on plasma soluble adhesion molecules: a meta-analysis of randomized controlled trials. *Amer J Clin Nut*.

Yazawa, K. (1996). Production of eicosapentaenoic acid from marine bacteria. *Lipids* **31**, S297-S300.

Ye, D., Zhang, D., Oltman, C., Dellsperger, K., Lee, H.-C., and VanRollins, M. (2002). Cytochrome P-450 epoxygenase metabolites of docosahexaenoate potently dilate coronary arterioles by activating large-conductance calcium-activated potassium channels. *J Pharmacol Exp Ther* **303**, 768-776.

Yeh, C. C., Sung, F. C., Kuo, L. T., Hsu, W. P., and Chu, H. Y. (2009). Polymorphisms of cytochrome P450 1A1, cigarette smoking and risk of coronary artery disease. *Mutat Res* **667**, 77-81.

Yokoyama, M., Origasa, H., Matsuzaki, M., Matsuzawa, Y., Saito, Y., Ishikawa, Y., Oikawa, S., Sasaki, J., Hishida, H., Itakura, H., Kita, T., Kitabatake, A., Nakaya, N., Sakata, T., Shimada, K., and Shirato, K. (2007). Effects of eicosapentaenoic acid on major coronary events in hypercholesterolaemic patients (JELIS): a randomised open-label, blinded endpoint analysis. *The Lancet* **369**, 1090-1098.

Zhang, N., Agbor, L. N., Scott, J. A., Zalobowski, T., Elased, K. M., Trujillo, A., Duke, M. S., Wolf, V., Walsh, M. T., Born, J. L., Felton, L. A., Wang, J., Wang, W., Kanagy, N. L., and Walker, M. K. (2010). An activated renin angiotensin system maintains normal blood pressure in aryl hydrocarbon receptor heterozygous mice but not in null mice. *Biochem Pharmacol* **80**, 197-204.

Zhang, Y., Oltman, C. L., Lu, T., Lee, H.-C., Dellsperger, K. C., and VanRollins, M. (2001). EET homologs potently dilate coronary microvessels and activate BKCa channels. *Amer J Phys* **280**, H2430-H2440.